OFF-GRID PV SYSTEM AS A RESOURCE IN TELECOMMUNICATIONS, FARMING AND HUMANITARIAN AID

By

SIZWE MBADULI

Thesis Submitted in partial fulfilment of the requirements for the degree

Master of Engineering in Energy

Faculty of Engineering and Built Environment

Cape Peninsula University of Technology

Supervisor: Prof. MTE Khan

Bellville Campus

April 2023

CPUT copyright information

DECLARATION

I, **SIZWE MBADULI**, declare that the contents of this dissertation/thesis represent my own unaided work, and that the thesis has not previously been submitted for academic examination towards any qualification. Furthermore, it represents my own opinions and not necessarily those of the Cape Peninsula University of Technology.

April 2023

Signed **Date**

ABSTRACT

It has become more obvious how using fossil fuel as a source of energy has contributed to both global warming and general environmental pollution in the past decade. Consequently, it is necessary to operate an electrical grid network that is more sustainably powered by renewable resources including wind, solar PV, hydroelectricity, biofuel, and biomass. Solar photovoltaic energy is a dependable source of power to address the energy issue and the associated environmental degradation especially in off-grid mode such as farming communities, telecommunication base stations and humanitarian aid facilities. The development of technology and the decline in price of solar PV panels has largely informed the choice of solar PV application in off-grid applications. However, due to the intermittent nature of solar PV supply, the power supply and subsequent power output from an off-grid network with high solar-PV penetration are typically unstable. Thus, a lithium-ion battery system is required as the preferred energy storage solution.

This study established a control mechanism for an off-grid hybrid system that uses solar PV and lithium-ion battery to give a remote farming community, humanitarian aid facility and telecommunication base station affordable, dependable, adaptable, and sustainable energy. The developed off-grid system is made up of a lithium-ion battery system and a 50 kWp solar PV system as distributed energy resources (ESS). In the MATLAB/Simulink environment, an energy management system (EMS) was developed and implemented utilizing a PI controller (PIC). The off-grid system's stability is increased by using a lithium-ion battery system, which also serves as a backup power source. According to the available power and the battery SOC, a load shedding scheme is a component of the system that supports the supply by automatically disconnecting or reconnecting the secondary loads (farming community, and telecommunication base station). This ensures dependability and continuous power supply to the primary load (humanitarian aid facility) and secondary loads. Connecting the solar PV to the rest of the network used a DC-DC boost converter, which improves the quality of the power generated and permits power flow in the system. The research design performance analysis considered the solar PV system's intermittent power supply and the load demand's adaptability to varied conditions and times of day.

To assess the system's performance, the study developed various scenarios using the energy management system algorithm. The results demonstrated that the chosen EMS guaranteed system stability, enhanced reliability, expanded system flexibility, and provided efficient power distribution. Additionally, the developed algorithm maintained the charging and discharging of the battery within acceptable SOC and provided proper power distribution between the solar PV and the lithium-ion battery. Based on the three scenarios that were developed, the results

also demonstrated that the battery increased the system's power storage. The developed energy management system additionally offered the chance to redesign and modify the off-grid system parameters. The results showed that the EMS was successful in meeting the load requirement and could be compared to other similar off-grid systems and implemented for farming community, humanitarian aid facility and telecommunication base station.

Key words: Energy storage system (ESS), Lithium-ion battery, MATLAB/Simulink, Off-grid system, Renewable energy, Photovoltaic(PV), State of charge(SOC), EMS, DC-DC boost converter, Humanitarian aid facility, Farming community and Telecommunication base station

ACKNOWLEDGEMENTS

I wish to thank:

- GOD our all mighty for giving me strength and opportunity to complete my dissertation successfully. I believe it is not by me it is by his power.
- The financial assistance from NRF, LTSA and CPUT postgraduate bursary
- My parents for giving me an opportunity to study and motivation from them that everything is possible through hardworking. Their constant motivation on how important education is for my personal growth and their constant prayers for my wellbeing and focus.
- Friends, thank you very much for making this year fun and enjoyable even in hard times you were always with me. Thank you for your valuable insights and motivation as well as your company during late nights of work. Your help did not go unnoticed.
- Prof MTE Kahn for his technical project wide guidance, constant encouragement throughout the whole project.

DEDICATION

I dedicate this dissertation warmly to the following people:

Late grandmother: Nonayisana Sophie Mbaduli,

Mother: Nandipha Mbaduli,

Brother: Simamkele Mbaduli,

Sister: Siyamthanda Mbaduli

Cousins: Ayabonga Mbaduli, Tunu Mbaduli, Sandiswa Mbaduli and the list goes on….

Lastly, I would like I dedicate this dissertation to all electrical engineering students at the Cape Peninsula University of technology for their friendship and support.

TABLE OF CONTENTS

TABLE OF FIGURES

LIST OF TABLES

LIST OF ACRONYMS AND ABREVIATIONS

A	Ampere
AC	Alternating current
CSI	Current source inverter
Cu	Copper
DC	Direct current
DOD	Depth of Discharge
EMS	Energy management system
ESS	Energy storage system
GHG	Greenhouse gases
GHI	Global horizontal irradiation
IRENA	Renewable energy agency
KCL	Kirchhoff current law
LTSA	Liquid telecommunication South Africa
MOx	Metal-oxide
MPP	Maximum power point
NRF	National research foundation
P&O	Perturb and observe
PV	Photovoltaic
RAN	Radio access network
RES	Renewable energy system
SANS	South African national standard
SEI	Solid Electrolyte Interphase

SOC	State of charge
STC	Standard test condition
UPS	Uninterrupted power supply
VSI	Voltage source inverter

CHAPTER 1: INTRODUCTION

1.1 Background

Ideally every household in the globe should, in theory, have access to reliable and sufficient source of energy. While this might be conceivable in developed countries where utility grid was established over decades, the situation in developing countries is not the same particularly in remote areas with low population density. Apart from the fact that connecting remote areas to the grid is expensive, individuals in developing countries use so little electricity that 80 percent of African power suppliers lose money every time they connect to a rural customer (Klepacka, 2019). Off-grid PV technologies have the potential of supplying electricity to remote at a cheaper cost.

This study is a design of an off-grid PV system for application in rural areas and highlight the lack of energy where the is no reliable electrical supply for key technologies of the fourth industrial revolution(4IR), namely telecommunication and food security due to robust farming industry. The concept of implementing off-grid PV system for application in such areas is not something new, many project from world bank have been developed and more than 320 100 base stations have been rolled out across South Asia, Sub-Saharan Africa, East Asia. The majority of mobile tele-communication towers rely on diesel generators for power, but with diesel prices rising daily, telecommunication companies are losing money due to financial issues. On the other hand, burning diesel releases carbon dioxide into the atmosphere, which reduces the ozone layer, which protects the world from ultraviolet UV rays, resulting in a variety of events such as acid rain, air pollution and land excavation. Implementing solar PV will be significant in cutting the operation and maintenance (O&M) cost and expand network coverage to rural areas as to make enough revenue. Furthermore, the key significance of deploying such systems is cost effectiveness, sustainability, reliability and reduction in greenhouse gases emission (Alsharif et al., 2015; Alsharif & Kim, 2016).

More than 1.4 billion people live in rural areas around the world, and off-grid installations are being investigated to improve power to dispersed locations (Aris & Shabani, 2015). Such systems are considered because they do not rely on the grid to turn on, and many countries have begun to construct off-grid PV systems to help businesses reduce their energy expenses. The installation of a PV system has demonstrated economic benefits and increased productivity, particularly for enterprises that rely on electricity to operate (Feron, 2016). The acceleration of off-grid PV system for remote areas is triggered by the depletion of fossil resources such as coal, oil and natural gas (Moumouni & Gdeisat, 2018). Solar PV systems have a variety of applications in farming as indicated in several studies (Showers, 2019). They

are utilized in two ways: firstly, in small applications as solar Pico systems to replace kerosene lamps and secondly, in mid-scale applications as solar homer systems (SHS) (Franklin, 2018a).

South Africa's overall energy supply is shown in Figure 1.1. As can be observed, the country relies largely on coal for power generation which accounts for 69%, followed by crude oil (14%) and renewable energy sources such as wind, solar and biomass which accounts for 11%. Nuclear and natural gas are not very prominent energy sources as it accounts for only 3% of total energy supply. South Africa is one of the countries in the African continent with the highest record of environmental pollution. This is because, non-renewable energy sources accounts for 80% of the total energy generation in the country. A reduction in non-renewable energy sources dependency is required to meet the country's goals of reaching net zero emissions by 2050 (Irena, 2016).

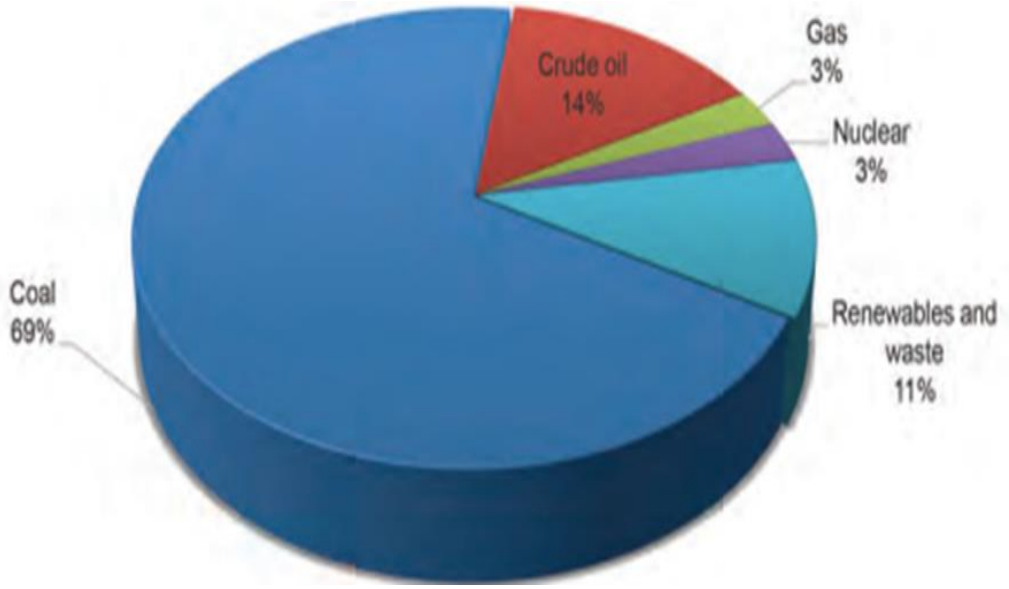

Figure 1.1: Total primary energy in South Africa (DOE, 2020)

The amount of greenhouse gas (GHG) emissions by several industries in South Africa with carbon dioxide accounting for 85% of total emissions is shown in Figure 1.2. Carbon dioxide emissions are high as a result of burning coal for power generation thereby making South Africa rank amongst the top 20 global carbon dioxide emitters (DOE, 2020). The need to install solar PV is critical because South Africa has a large solar energy potential and several sites have been found to deploy more solar photovoltaic (PV) systems in rural regions (van der Merwe & Brent, 2020). The country has an estimated 887 GW of potential and according to the South African integrated resource plan of 2010, renewable energy sources should account for 21% of the country's energy output of 17800 MW (Van der Merwe & Brent, 2020). This

study is a design of an off-grid PV system for Van Wykslvei farm in Northern Cape. It comprises of PV arrays, charger controller, DC-DC converter, DC-AC converter and battery for storage purposes. The project is simulated under MATLAB/Simulink environment.

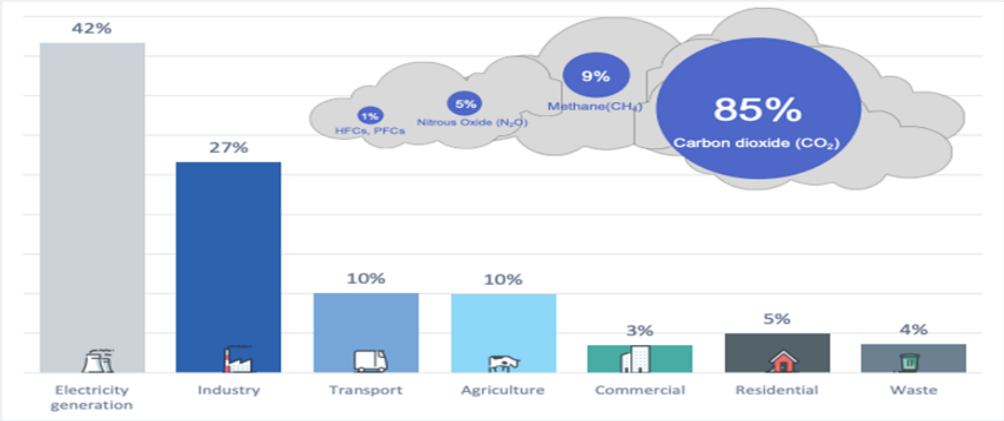

Figure 1.2: South Africa gross national GHG emissions by different sectors (IRENA, 2019a)

Off-grid PV system is not connected to the electricity grid hence, it is operated in islanded mode. In its simplest form, it consists of solar PV arrays directly connected to the load being powered as shown in Figure 1.3. Such system is used in various applications as it is primarily used to power batteries, ventilation fan, water pumping system with a single solar PV source connected. Since there is no storage on the system, power is operated at the same time for example ventilation fan that needs to operate during the day when the sun is present will use off-grid system without a battery and also a DC submersible pump in a garden can be powered by the solar module only (Franklin, 2018a).

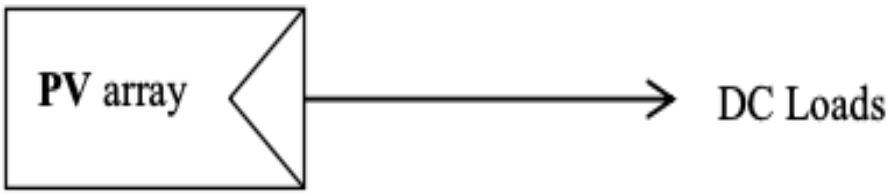

Figure 1.3: Off-grid PV DC system without battery (Franklin, 2018a)

The addition of an inverter is illustrated as shown in Figure 1.4. This is to enable off-grid PV system to adequately power AC appliances such as lights, refrigerators and AC water pumping system. The load of the system is AC, all the loads in the system are connected to the AC inverter and it is essential as it converts DC power from PV arrays to 230V AC.

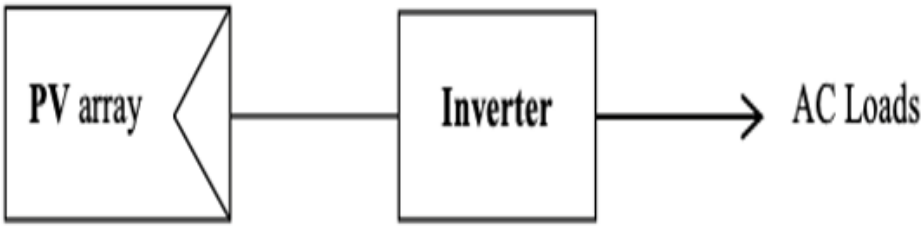

Figure 1.4: Off-grid PV AC system with inverter (Franklin, 2018b)

Figure 1.5 illustrates an off-grid PV system with charger controller, battery and DC loads. Such systems are used in telecommunications where a pure 48 VDC is required to run the base station components such as:

- Radio equipment
- Transmission equipment
- Switching equipment
- Digital multiplexer
- Air mux

The system is also used in navigation aids, traffic control signs and cathodic protection where continuous DC is required. The battery is used to store excess energy where it would be used during the night when the solar PV is not producing enough power or there is no solar irradiation. The capacity of this type of system ranges from 100 W to 1 kW of solar modules with exceptional cases having smaller or larger capacities. The design principle such as sizing of the battery and charger controller selection is the same and they are installed in rural areas residence (Aris & Shabani, 2015). The main advantage of this type of system is the availability of power in the 24 hours of the day. In rural areas where critical load must be energised this system is ideal however, there are limitations such as initial cost, load calculation, maintenance and taking care of the battery life expectancy. The loads are DC and if AC is required then small inverter with 12 V can be plugged in directly to the battery and the inverters are available in different wattages ranging between 125W to 6 kW.

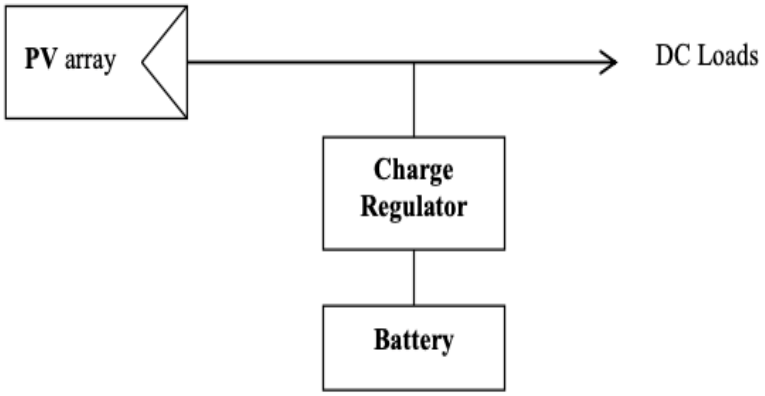

Figure 1.5: Off-grid PV DC system with battery (Franklin, 2018b)

The combination of off-grid PV system shown in Figures 1.3 and 1.5 normally result in a complete system as shown in Figure 1.6. The system consists of a 230 AC load and a DC load used in remote areas to power electrical appliances for basic needs such as lighting and cooking (Issi & Kaplan, 2018).

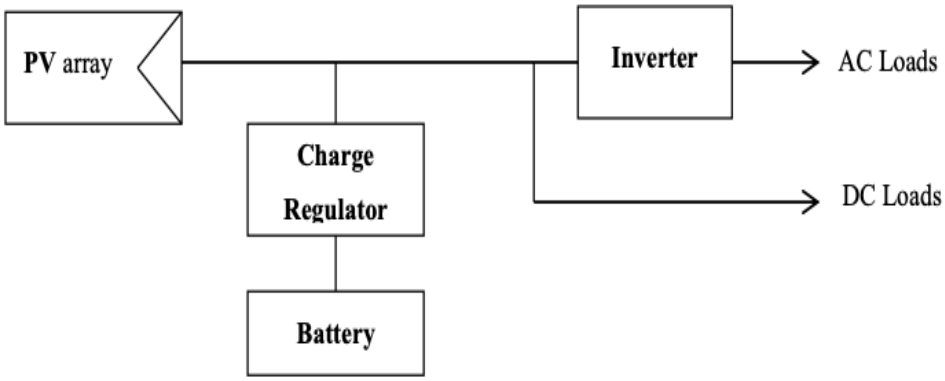

Figure 1.6: Off-grid PV system AC/DC load with battery storage (Issi & Kaplan, 2018)

1.2 Problem statement

In rural areas, the demand for electricity for cooking, lighting, farming as well as communication is increasing daily as a result of the interest in off-grid renewable energy sources. This specific interest has been favourable to solar PV as it is seen as the prime choice amongst the renewable energy sources (Mulaudzi & Bull, 2016). South Africa is one of the countries that has implemented off-grid energy sources for application in dispersed areas and the decision to include such systems was triggered by lack of energy and sharing information via mobile cellular phones. Off-grid renewable energy sources are widely used in rural applications. However, there are different factors to be considered when designing the

system because such systems are complex and may require proper design as to mitigate the chances of failure once the system is up and running. Vital factors such as technical standards and economic analysis must be taken into consideration during the design phase. This will assist in understanding the different costs associated with the project from start to completion including maintenance. In 2010 South Africa issued an IRP2010 which opened up the use of solar PV to solve the issue of depending on coal for power generating and use of diesel to power remote base stations. A reduction in coal usage will have a direct positive impact on the environment as well as stimulating economic growth thus moving the country into sustainable energy development is seen as the best and most viable option. Therefore, this study will model an off-grid solar PV system in the MATLAB/Simulink environment to better comprehend and evaluate the technical viability of the project.

1.3 Aim and objectives of the research

The primary aim of this research is to design and model an off-grid PV system that is robust and cost efficient for Van Wykslvei farm in the Northern Cape. In order to accomplish the aforementioned aim and provide anticipated solution, the research needs to realize the following objectives:

- Carry out a literature review on standalone Solar PV systems.
- Develop load profile for Van Wykslvei farm using MATLAB/Simulink
- Calculate number of PV modules to be connected in parallel and series.
- Size the system; PV array, inverter and charger controller.
- Model a solar PV system in the MATLAB/Simulink environment.
- Model a control system that will regulate the intermittent solar power supply and the variable load demand.
- Provide results, conclusion and recommendation on the use of solar PV in telecommunication, farming and humanitarian aid.

1.4 Significance of the research

- The proposed model is a smart and effective system that will provide a comprehensive result that will assist independent power producers to better comprehend the performance of Solar PV system in islanded mode.

- The outcome of this study will improve the use of Solar PV in farming communities and telecommunication stations hence, reducing over reliance on fossil fuel-based grid network.
- Achieving the anticipated results will position solar PV as the perfect option in farming communities which will assist the Government achieve its policy on the provision of sustainable and eco-friendly electrical energy to rural communities.
- Lastly, the results of this study will provide researchers and Government agencies saddled with the responsibility of providing clean electricity a reliable model of an off-grid system.

1.5 Research Design

This research uses an AC mechanism for an islanded solar PV system. The system is made up of different components such as solar PV which serves as the primary source of energy, a battery system which serves as an energy storage system for back purposes and the variable load which comprises of essential and non-essential loads determined by its usage. The aforementioned components are connected across a boost converter and a control system for the bidirectional flow of both active and reactive power. This will be implemented using appropriate control tools in the MATLAB/Simulink environment. Although, the actual design of the solar PV and the quantity of power it can provide relies on the solar irradiation and other climatic conditions on the chosen site.

Basically, the solar PV is designed to provide sufficient power to the load and the extra power is used to charge the battery for later use. The size and capacity of the battery depends on the load demand and the solar PV capacity as power wastage is eliminated in the design. The controller is designed to operate smartly in disconnecting or connecting non-essential loads whenever the power supply is less than the load demand. Hence, this system is an intelligent system that regulates available power and load demand including battery state of charge (SOC). The load curve for a typical solar PV system with its fundamental characteristics is shown in Figure 1.7.

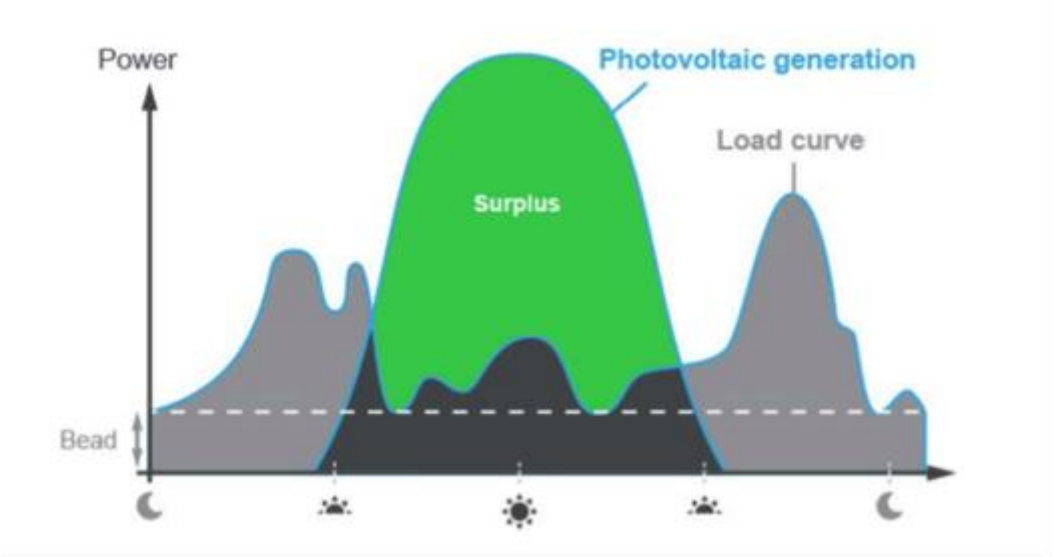

Figure 1.7: A typical solar PV power supply curve (Swe, 2018)

The model is executed in the MATLAB/Simulink environment to validate the practicability of it using different sets of data and parameters derived from a couple of sources under unique conditions. This is to ensure consistency, flexibility and predictability of the model under different times and climatic conditions.

1.6 Research Methodology

To achieve the anticipated results, the research is conducted as follows:

- Several thesis, articles and conference papers were reviewed to have a comprehensive knowledge of solar PV system, off-grid systems, system modelling and energy storage systems.
- The study is executed in the MATLAB/Simulink environment using variable loads and power supply scenarios. This includes solar PV systems, control algorithms, boost converters, MPPT, energy storage systems and other load demand parameters.
- An evaluation of different off-grid solar PV control systems is conducted to provide information on the most suitable control system for this model using consistency as the primary factor.
- The final model and simulation results were analysed, evaluated and compared with other similar studies to understand the effectiveness of the chosen control system and algorithm.

1.7 Delineation of the research

Currently, there are several control systems used in off-grid solar PV systems and load distribution.

- This research focused only on the management of active power flow in solar PV and battery off-grid hybrid system and not grid-connected system.
- The research was implemented in the MATLAB/Simulink environment only. No other software was used in this research.
- Battery was the only energy storage system used in this research.

1.8 The contribution of the Research

The outcome of this research will provide useful information on the management of power flow in off-grid solar PV system mostly in rural farming communities and telecommunication base stations. Most rural farming communities are not connected to the national electricity grid due to high cost of connection. Hence, implementing the results of this study which shows the viability of solar PV-battery hybrid system, farming communities, humanitarian aids and telecommunication industries that want to operate in rural areas will be adequately supplied with affordable electricity thereby improving the economy of that area.

- The result of this study will provide a low-cost control system, provide affordable power to the abovementioned communities and ensure effective power distribution.
- The outcome will further highlight the environmental and economic benefits of solar PV system and position it as the most affordable source of power in such areas.
- Based on the obtained results using reliable parameters and values, a thesis will be compiled and a conference paper generated as a unique contribution to the body of knowledge.

1.9 Thesis outline

Chapter 1 introduces the thesis by providing a short background of solar PV system in islanded mode. Followed by the statement of research problem, aims and objective, significance of the research, research design and methodology, delineation of the research and some contributions that the research outcome will provide.

Chapter 2 presents literature review on off-grid PV/battery hybrid system. This includes literature on solar PV systems, energy storage systems such as battery (lithium-ion) system and different types of converters.

Chapter 3 presents the system design and methodology. This includes solar PV model design, lithium-ion battery system, control systems, converters, MPPT and variable loads.

Chapter 4 presents the energy management algorithm, flowchart and MATLAB/Simulink model used.

Chapter 5 presents the simulation results of a solar PV/battery hybrid off-grid AC system with adequate controllers and a detailed discussion of the results comparing it with previous studies.

Chapter 6 concludes the research and highlights some areas that requires further research.

CHAPTER 2: LITERATURE REVIEW

2.1. Introduction

Most existing electricity grid systems around the world are centralised with large power generation plants that transmits electricity from the generation plants to consumers through long transmission lines (Feron, 2016; Utility, 2015). Off-grid systems are intending to compliment or replace these existing power systems due to the several advantages it provides. Off-grid systems are more sustainable, environmentally friendly and cost effective in areas were connecting to the grid is challenging. This is an integral part of operating a more sustainable grid system that will meet future electricity demands and address anticipated complexities. Furthermore, it is achievable to generate tens of megawatts electricity from renewable energy sources such as solar PV and wind but synchronisation with grid characteristics is a main challenge hence, they are usually connected at medium or low voltage points (Benavente et al., 2019). Again, integrating intermittent renewable energy sources to the current grid is challenging but an off-grid system is the most suitable for farming, telecommunication and humanitarian aid facilities due to the above-mentioned reasons. Therefore, to solve this problem, there is the need to operate an off-grid systems in areas were connecting to the existing grid is not economical. Hence, chapter 2 presents literature review on off-grid PV/battery hybrid system. This includes literature on solar PV systems, components of off-grid solar PV system, energy storage systems such as battery (lithium-ion) system, global off-grid solar PV applications and solar PV potential in South Africa.

(Pougoue Tchintchui & Raji, 2019) designed a system that evaluated the techno-economic feasibility of a residence using off-grid PV system as generating source. The system was modelled using Homer-Pro for cost analysis and optimisation. The study used a wide range of data such as load estimation, solar irradiance and cost of components to arrive at its technical and economic results. AC and DC load were listed in order to select and size PV arrays, battery banks and system converter. The result of the study showed that off-grid electricity is used worldwide and regarded as one of the most reliable and efficient option of expanding electrification to remote areas where it is expensive to connect to the grid. Even thou the study focused primarily on the feasibility of solar PV system the gap in the actual study did not include protection devices in case there is under or over voltage in the system. When designing off-grid PV it is imperative to define South African standards (SANS) as well as making sure that the system is protected (Ntshiba & Krishnamurthy, 2022)

(Rebeka et al., 2019), conducted research on the optimization of off-grid systems for power supply in rural areas using renewable energy. According to the study, diesel and gasoline are

still used as power sources in rural areas, but renewable energy is considered to reduce greenhouse gas emissions. The purpose of the study was to find a system with a lower net present cost (NPC). To reach the actual purpose Homer pro software was used as the simulation software and two scenarios were considered. The first scenario optimizes micro scale consumers such as residences, while the second situation optimises tiny villages or dispersed places were connecting to the grid is expensive.

(Li et al., 2014), conducted research on the viability of off-grid solar PV systems in remote areas application. The result of the study showed that selecting appropriate power electronics devices is the most important and technical aspect in the design of off-grid PV system because it is responsible for power conversions from solar PV to tangible electrical energy. The power electronics part of the entire solar PV system is responsible for reliable and efficient power conversion and as a result, various power converters have been developed and commercialised widely.

2.2. Off grid solar PV system application in farming communities

(Feron, 2016), examined different off-grid applications in rural electrification and claimed that deploying an off-grid solar PV system will assist the country (South Africa) to perform many activities in farming such as water pumping, maximise crop production, food and energy output. Querikiol & Taboada, (2018), in their study supported the above article that agricultural sector plays an important role in human existence. According to Cho et al., (2020), 843 000 people are employed in the agricultural sector which has positioned the sector as a strategic and essential sector in both developed and developing economies around the world. Globally, the agricultural sector is ranked as the third highest source of income that employs several people with differs skills and experiences. Again, there have been several studies conducted on the suitability and economic viability of solar PV application in off grid mode using Homer pro in the last decade due to the search for a more sustainable source of power in farming communities (Querikiol & Taboada, 2018).

A study conducted by Jain & Jain, (2017), showed a significant increase in off grid solar PV installations in the past decade due to the high cost of integrating solar PV to the national electricity grid network. Currently, 43.81 MW of solar PV have been installed and operating in the form of roof tops units in the country. In rural areas many projects are carried out including Solar Homer Systems (SHS) programme which plays an important role in rural areas and provides households with basic electricity needs such as lighting, cooking and charging mobile phones. The programme started early in 2001 and currently more than 96 000 SHS has been deployed according to the study.

2.3. Off-grid solar PV system application in telecommunication

The advent of mobile telecommunication in most parts of the world has given rise to the demand for a cost effective and sustainable sources of power for its operation (Samuels, 2017). Again, the energy management for these new power systems installed in various telecommunication base stations generating electricity from renewable energy sources such as solar PV with the capacity to provide end-users with the certainty that it requires is a critical aspect of its adoption. These stations must be supplied with power that is both environmentally friendly and cost-effective. The use of cell phone base stations is expanding significantly around the world, with the majority of the growth occurring in areas where people lack access to the power grid, hence, forcing mobile operators and users alike to rely on diesel generators to power off-grid base stations. The usage of diesel generators as a source of power has a number of drawbacks, including high running costs, environmental pollution and regular maintenance. Many mobile operators are presently grappling with the difficulty of lowering total operating costs and cutting high levels of diesel fuel, which is predominantly utilized by generators to power base stations. Solar PV systems are considered as the prime option in powering of most rural base stations around the world. Algeria in a study conducted by Mougay et al., (2021), has an average solar radiation of 4.6 kWh/m^2/day while South Africa is between 4.5 and 6.5 kWh/m^2/day. This means that most areas in South Africa have an average of more than 2 500 hours of sunshine per year which is suitable for the powering of telecommunication base stations if properly harnessed (Van der Merwe & Brent, 2020).

The study on solar PV deployment in telecommunication base stations by Alsharif et al., (2015), supports the above statement that mobile operators are looking at cutting the operating cost as well as expanding network coverage to rural areas to increase their revenue base. Unfortunately, rural areas have demonstrated unique economic and geographic challenges because power is not always available all through the day and night due to the area sparsely populated and has no access to the grid. Such challenges have forced operators to use diesel generators (DG) as the powering method of base stations. However, using diesel generators is not a good option as mentioned above that they are associated with high operation and maintenance (O&M) cost of the base station. In most cases, it will require more than 100 trucks to supply enough fuel to these base stations and will also require full time technicians to be onsite for service outage and this leads to many factors such as economic loss where a company would spend more than 5 million USD to purchase fuel for different base stations. The study further supports the position that, renewable energy sources such as solar PV system are reliable energy sources with the capacity to supply power to rural areas. Also implementing renewable energy for off grid base stations would be a great benefit to mobile

operators and implementation is not something new as more than 320100 base stations was rolled out in 2014 across south Asia, Sub-Saharan Africa, east Asia with the number of base stations expected to be rolled out in the future. With the current progress in the deployment of renewable energy systems in the telecommunication sector, the key significance of these power sources are cost effectiveness, sustainability, reliability and reduction in greenhouse gases emission. A typical configuration of a solar PV system application in the telecommunication sector is shown in Figure 2.1.

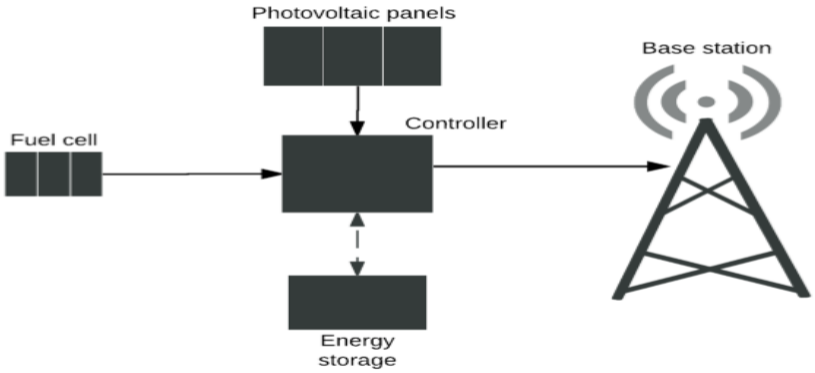

Figure 2.1: Rural base stations configuration (Aris & Shabani, 2015)

2.4. Overview of Off grid solar PV application in humanitarian activities

The study by Franceschi et al., (2014), reviewed the use of off-grid solar PV systems for humanitarian purposes such as refugee camps and disaster aid. The study examined several humanitarian operations for which solar PV remains a viable solution, including emergency assistance communications, household lighting, schools and camp security activities. Access to reliable and affordable power in the health sector is critical in achieving universal healthcare and sustainable development goals. Many healthcare facilities, especially those in rural areas, lack reliable and affordable electricity to operate basic energy services like lights, communications and other medical devices (Mikul et al., 2018). Furthermore, the study indicated that the cost of implementing renewable energy in the health sector is critical since renewable energy sources are more economical than diesel generators, which are commonly used as a power source in rural hospitals.

In the last ten years, solar PV has grown significantly in healthcare facilities. Its expansion is due to a number of government initiatives and improvements in solar PV technology. This number has grown significantly from 2010 to reach a capacity above 10 MW in 2018 as shown in Figure 2.2. The study further supports the position of IRENA where it stated that access to affordable and reliable energy in the healthcare sector plays a major role in the functionality

of hospitals in rural areas. Currently, more than 1 billion people in the world are served by health facilities without reliable electricity supply and closer to 255 million reside in sub-Saharan Africa. The results of the study showed that lack of reliable source of power in health centers results in many challenges such as maternal death due to insufficient maternal care. According to world health organization, there has been a decrease in vaccine spoilage ever since off-grid solar PV systems were deployed in rural hospitals (Mikul et al., 2018) (IRENA, 2018b).

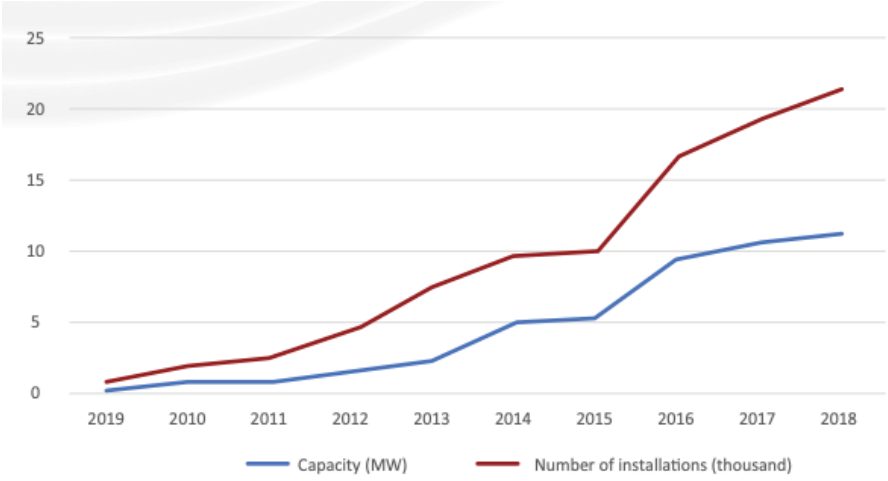

Figure 2.2: Solar PV growth in the healthcare sector (IRENA, 2018b)

2.5. Off grid solar PV system components

The concept of solar PV system was first developed by Becquerel with the primary purpose of investigating the impact of light on electrolytic cells (Hossam-Eldin et al., 2015).The term photovoltaic is derived from the words "photo" (light) and "voltaic" (voltage). Solar PV systems are similar to other electrical power generation systems, but the equipment used is not the same as that used in traditional electromechanical generation systems. However, the operating principles and interfacing with other electrical systems remain unchanged, governed by a well-established body of electrical codes and standards. Although a solar PV array generates power when exposed to sunlight, it also necessitates the use of a number of other components in order to properly conduct, control, convert, distribute, and store the energy generated by the array. (Khamisani Advisors et al., 2018). Solar PV systems are made up of various components, each of which plays an important role in the system's operation. Various components are used in various PV systems, and the components used are determined by the system to be designed and its primary purpose. A direct simple PV system, for example, consists of only solar modules connected in series or parallel with a load device (Van der Merwe & Brent, 2020). Most common load that uses direct PV systems are water pumps which

are primarily used in farming for water pumping and ventilation fans. An off-grid system will use more or less the same components, but it will have energy storage system and different power electronics converters are used to convert DC to AC depending on the type of load (Franklin, 2018a). DC is a current that flows in one direction and used to power up electronic devices and AC is a real current that changes direction every second. The basic components of a solar PV system such as solar panels, inverter, charge controller and energy storage system (battery) including its connection as it can be seen on the Figure 2.3 below (Naqvi et al., 2021)**.** The aforementioned components play an important role in power generation. PV panels are the generating plant of the system that interface with the sun by absorbing solar irradiation and generating DC power. The generated DC power can then be stepped up using a boost converter or stepped down using a buck converter. Different types of converters and other system components are discussed in detail in Chapter 3 of the dissertation.

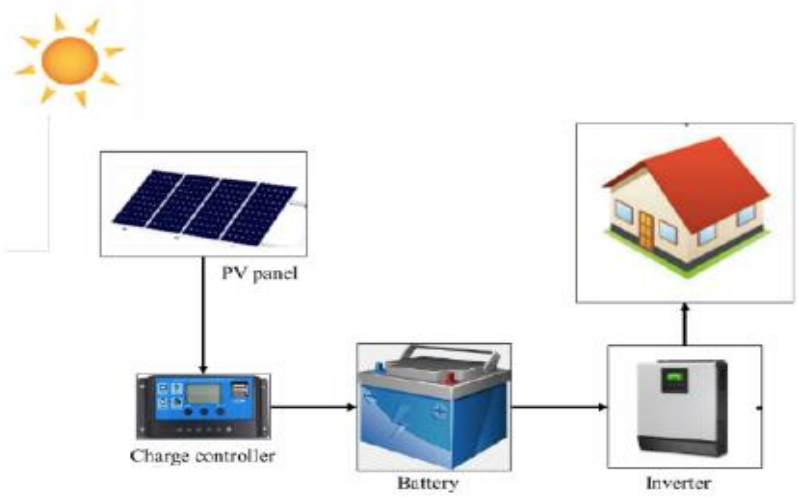

Figure 2.3: Off-grid solar PV system components (Naqvi et al., 2021)

2.5.1 Solar panels

Photovoltaic panels are another name for solar panels (IRENA, 2018a). Solar cells are famous because they induce energy from the sun through a process called photovoltaic effect. The process allows semi-conductive materials to absorb photons of light and release electrons. They are made from conductive elements such as silicon, which is the second most abundant element in the earth's crust and has the potential to convert sunlight into useable energy. One of the reasons for its popularity is that it can readily vary its conductivity by familiarizing impurities with the capacity the use solar irradiation to generate voltages between 0.5 and 0.6 volts at currents between 2 and 4 Amperes.

There are types of solar cells available today but monocrystalline and polycrystalline are the two most common types used in the industries. Monocrystalline solar cells are homogeneous solar cells with high efficiency ranging from 0 to 20% with a considerable market share. These cells are the oldest, yet they are still one of the most reliable energy sources, having been around for almost 50 years. Polycrystalline on the other hand, are made up of non-uniform solar cells with a low efficiency of 10-15% and are much cheaper than monocrystalline. However, the main disadvantage of polycrystalline is its large size, but its output power is the same as monocrystalline. Hence, it is unnecessary to install polycrystalline in large areas. Polycrystalline and monocrystalline solar cells are shown in Figure 2.4 (a) and (b) respectively (Hossam-Eldin et al., 2015).

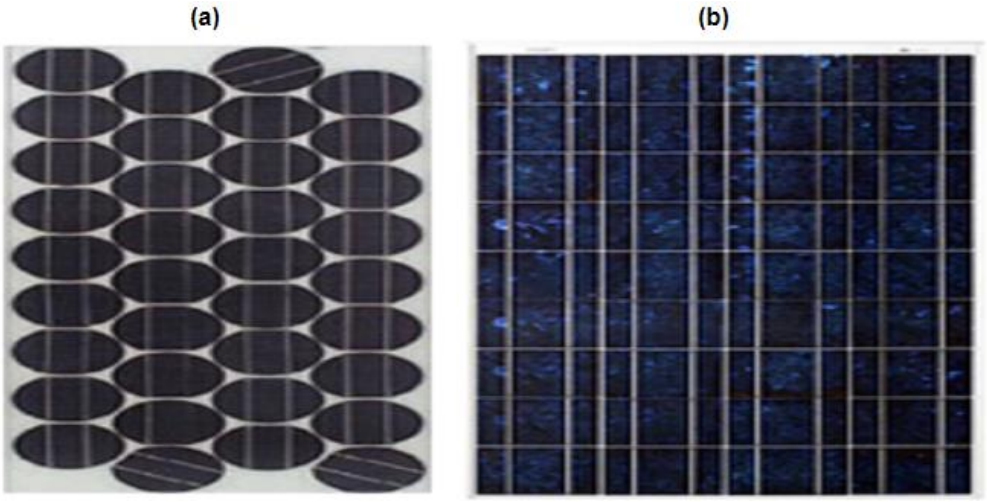

Figure 2.4: Types of solar cells (a): Polycrystalline, (b): Monocrystalline (Hossam-Eldin et al., 2015)

In a complete PV system, solar cells are basic components connected in a frame to form solar module and modules are combined to form solar array as shown in Figure 2.5. Since solar modules are derived from solar cells, solar modules are in most cases made up of silicon crystalline material (Moumouni & Gdeisat, 2018). PV panels are used to generate electricity in both residential and commercial applications, and they are responsible for directly converting the energy from solar radiation into direct current (DC) electricity.

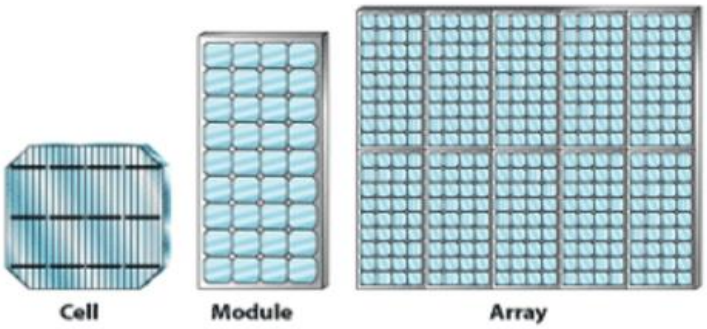

Figure 2.5: Solar cell, module and array (Hossam-Eldin et al., 2015)

For any PV array to be approved for installation, it must be tested under a solar standard test condition (STC) at a standard temperature of 25℃ with a solar irradiance of 1000 W/m^2 and air mass of 1.5 spectrum distribution. Where, irradiance is the amount of solar power measured per unit area falling on the surface of the solar panel and mathematically expressed as the sum of the direct radiation from the sun while diffused radiation, is the radiation that is scatted by the atmosphere and reflected radiation is the reflect on the solar arrays (Querikiol & Taboada, 2018). When installing PV arrays, it is imperative to optimise the slope so that it can receive most of the available irradiance at a specific location. The output power of solar panels depends on its efficiency and the efficiency depends on the material and manufacturing method used. On the other hand, the performance of STC must range between 85% to 95% rating since the above conditions are not typical and they are done to check PV cell conversion efficiency (van der Merwe & Brent, 2020).

Furthermore, solar panels are divided into three generations: first generation, second generation and third generation. As shown in the Table 2.1, monocrystalline and polycrystalline solar cells are examples of first generation solar panels, while amorphous silicon and thin-film solar cells are examples of second generation solar panels. Third generation solar panels include biohybrid, concentrated PV, and cadmium telluride solar cells.

Table 2.1: Classification of solar panels according to generation (Hossam-Eldin et al., 2015)

First generation	Second generation	Third generation
Monocrystalline solar panels	Amorphous Silicon Solar Cell	Biohybrid Solar Cell
Polycrystalline Solar Panels	Thin-Film Solar Cells	Concentrated PV Cell (CVP and HCVP)
		Cadmium Telluride Solar Cell

2.5.1.1 PV cell working principle

PV cells are composed of semiconductor materials that when exposed to sunlight generate electrical energy electromagnetically and this process is called photovoltaic effect as mentioned above (Samuels, 2017). It consists of four valence electrons to stimulate the conductivity. Solar PV cells have two sides, one of which contains silicon impurities doped with phosphorus atoms and is used to donate electrons to the silicon material (n-donor), resulting in an excess negative charge carrier. To absorb electrons, boron atoms with five valence electrons (p-donor) with a higher affinity than silicon are used. When a P-type silicon comes into contact with an n-type silicon, a p-n junction is formed, and electrons diffuse from the region of high electron concentration to the region of low electron concentration. When these electrons diffuse, they recombine with holes on the p-type side, creating an electric field due to the charge imbalance on the other side of the p-n junction. This created electric field allows current to flow in only one direction. Crystalline silicon and amorphous silicon are the two most common semiconductor materials used in commercial PV cells (Luo et al., 2017). The fundamental operation of a PV cell is shown in Figure 2.6.

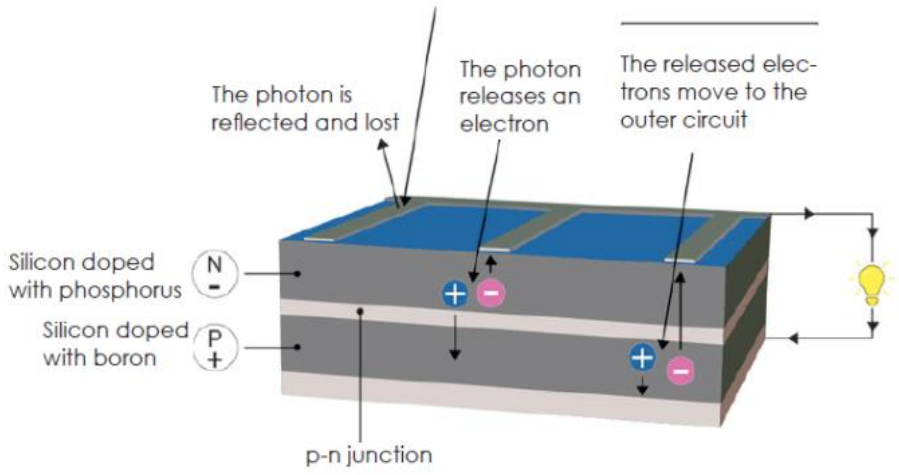

Figure 2.6: PV cell working principle (Luo et al., 2017)

2.5.1.2 Equivalent circuit of solar cells

The equivalent circuit of a solar cell is shown in figure 2.7 and it is made up of I_L; the current that is generated by light in the cell, I_D; the current that flows through the diode, R_s; a series resistance encountered when electrons travel along thin top sheet of n- or p-type doped material R_{Sh}; a parallel resistance also called shunt which represents the effect of p-n junction interface of the diode. Again, it is imperative in the design that the value of the shunt resistor remain high compared to the resistor in series, $\mathrm{I_{Sh}}$, the shunt current I; and the load voltage V; generated by the PV solar cell. The equations to calculate the current flowing across the series resistance and current across the diode of the equivalent circuit solar circuit can be obtained using Kirchhoff current law as shown below (Tamrakar et al., 2015);

$$I = I_L - I_D - I_{sh} \tag{2.1}$$

$$I_D = I_o \left[exp\left(\frac{V + R_s}{nV_T}\right) - 1 \right] \tag{2.2}$$

$$V_T = \frac{KT_c}{q} \tag{2.3}$$

$$I_M = I_L - I_o \left[exp\left(\frac{Vm + I_M NsRs}{nNsV_T}\right) - 1 \right] - \frac{Vm + I_M NsRs}{NsR_{sh}} \tag{2.4}$$

$$a = \frac{nNsKTs}{q} \tag{2.5}$$

Where;

a- Terminal voltage of the module

I_o - Saturation current of the diode

n - Ideal factor of the diode

k - Boltzmann constant equal to $1.38 \times 10^{-23}\mathrm{J/K}$

q - Absolute value of an electron equal to 1.602×10^{-19}

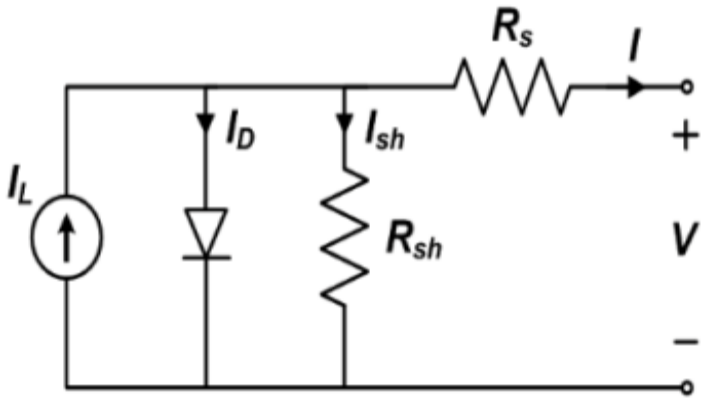

Figure 2.7: Equivalent circuit of solar cell called one diode model (Tamrakar et al., 2015)

2.5.1.3 Current-Voltage characteristics

The I-V characteristics curve of a solar cell is an integral parameter in ascertaining its power rating as shown in Figure 2.8. Mathematically, the power generated by a single solar cell is obtained by multiplying voltage and current using the equation 2.6.

$$P = V \times I \tag{2.6}$$

The power value from equation above can be determined at any point on the curve by combining the voltage and current in various short and open circuits. As shown in Figure 2.7, only one diode model is used in this study. There will be zero current across the cells when there is no load or when the sun is not hitting solar cells, resulting in maximum voltage. R_s determines the I-V curve's slope, where steep slopes result from high R_s values. A single diode model is used to generate the voltage-current characteristic curve, and a straightforward power formula is used to calculate power-voltage. Because it indicates the maximum power point (MPP) of a solar PV system, the current-voltage curve is an essential component in its

design and operation (Kyari et al., 2020). Again, it is beneficial and recommended to operate solar PV system at the maximum power point in order to extract the maximum power from the solar PV. When the sun shines on PV modules, a short circuit current is created meaning the positive and negative leads are connected together which results in current flow across the load resistance. But when the voltage is zero, the current flowing across the load is equal to the short circuit current (I_L= I_{LSC}). If the voltage increases or adjusted slightly, the junction current effectively becomes zero and the slope of the current-voltage depends on the parallel resistance. If the shunt resistance is infinite, then the curve would be horizontal across that region (Mohanty et al., 2016; Khamisani Advisors et al., 2018).

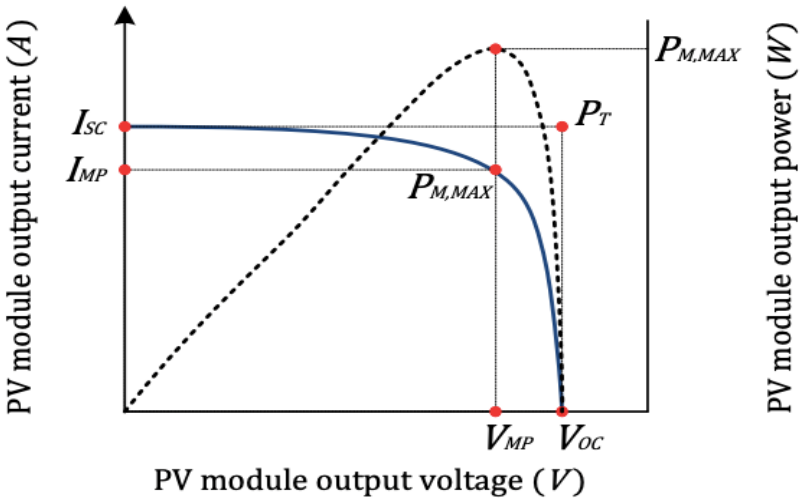

Figure 2.8: V-I characteristics curve of a solar cell (Kyari et al., 2020)

2.5.1.4 Efficiency and fill factor of a solar cell

The efficiency of a solar cell is used to distinguish the performance of various solar cells. It is the output power of the actual solar cell to the input power dissipated by the cell from the sun. The performance of solar cells depends on the spectrum and the intensity of the light received therefore, the formula to calculate the efficiency of the solar cell is as follows (Alemshet, 2010):

$$n = \frac{P_{out}}{P_{in}} \tag{2.7}$$

$$n = \frac{P_{max}}{P_{in}} \tag{2.8}$$

$$n = \frac{V_{oc} I_{sc}}{P_{in}} FF \tag{2.9}$$

Where:

P_{out} = Power output of the cell

P_{in} = Power input of the cell

FF = Fill factor

V_{oc} = Open circuit voltage

I_{sc} = Short circuit current

The fill factor is the ratio of the theoretical maximum power, which cannot be achieved, to the actual rated maximum power, P_max. It is the most important metric used to evaluate a solar panel's performance. Grade B solar panels have fill factors between 0.4 and 0.7, while typical commercial panels have fill factors greater than 0.70. Due to the series and parallel resistance in the cells themselves, a solar panel with a high fill factor has fewer losses. The fill factor is calculated using equation 2.10 as:

$$FF = \frac{V_{mp} I_{mp}}{V_{oc} I_{sc}} \tag{2.10}$$

Where:

I_{mp} = Current at maximum power point

V_{mp} = Voltage at maximum power point

2.5.2 Inverter

(Tan et al., 2020) MATLAB/Simulink simulation software was used to model a single phase off-grid inverter for use in remote areas. The system included a high frequency DC-DC converter and a full bridge PI voltage source inverter with SPWM modulation to generate sine wave voltage. The study found that this type of system can be used in many small commercial off-grid inverters capable of producing a pure 230 Vac sine wave with less than 1% total harmonic distortion (THD). The system also included a lead acid battery, which was used to store excess power and discharge it when the solar PV power was less than the load demand.

In a study conducted by Soman Chithra, (2014), the result indicated that most popular inverters in power electronics for off-grid applications systems are voltage source inverters (VSI). VSI converts voltage by means of power electronics proper communication within switches. The comparison is done by a comparator with an input carrier waveform and reference waveform to give an output that is close and/or open to switches depending on the

configuration. VSI and CSI uses gate turn-off thyristor (GTO) switch or insulated gate bipolar transistor (IGBT) are examples of this type of switch but prone to power losses. A standard VSI and CSI inverter can be designed in two ways either as half bridge or full bridge configuration. In such system, all the single phases are joined to form three phase or multiphase topologies. Inverters are widely applied across several industries for adjustable ac drivers, induction heating, uninterrupted power supply (UPS), etc. The schematic of a half bridge PWM inverter is shown in Figure 2.9 (Algaddafi et al., 2016).

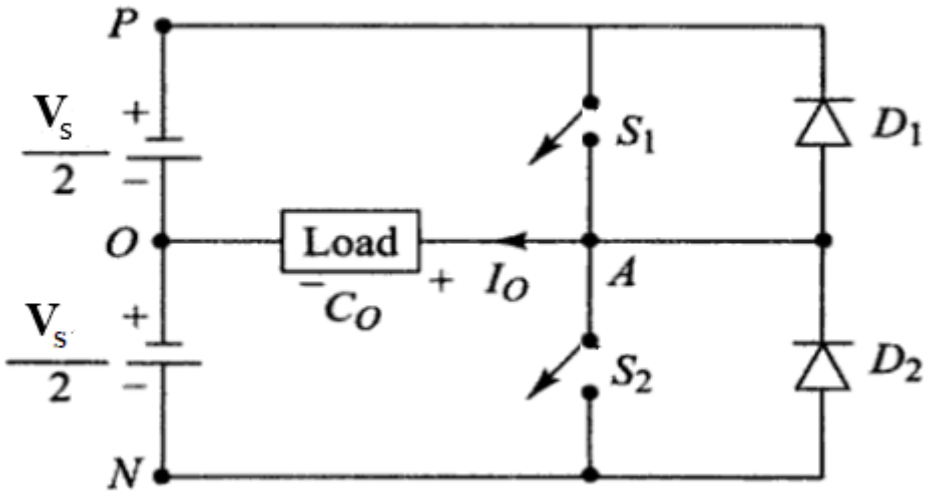

Figure 2.9: Schematic of a half bridge PWM inverter (Algaddafi et al., 2016)

VSI inverters are used to change incoming DC voltage from the solar PV to a corresponding AC voltage and it is widely used in high applications for providing power to the grid. However, the major problem is to design a cost effective VSI inverter with less harmonics. These types of inverters have been widely used in power electronics for DC-AC conversion with the help of PWM technique. In the past decade there have been an improvement in power electronics technology which has enhanced the adoption of this type of converter in power conversion applications. Carrier-based PWM technique was the first technique established and the earliest for modulation signals using sinusoidal (SPWM). The SPWM method compares carrier signal and a pure sinusoidal wave modulation to establish the optimal point of operation (Algaddafi et al., 2016).

2.5.3 Charge controller

Charge controllers are essential in solar PV systems and essential in standalone systems as they serve vital functions due to the presence of batteries whose function is the storage of excess power that will be deployed whenever it is needed. The main function of charge controller is to monitor the charging and discharging of the battery to avoid deep discharge

due to over current which can decrease the life expectancy of a battery. Furthermore, charge controller is a system used to prevent reverse current from flowing back to the PV system with two basic types in the market presently. They both ensure adequate monitoring of the battery charge and discharge in conjunction with the solar PV power output (Khamisani Advisors et al., 2018).

2.5.3.1 PWM charge controller

This controller is called pulse width modulation and used to match the input power of the battery regardless of the power generated by PV modules. The main disadvantage of this type of charge controller it is that power get lost easily hence, it is not widely used. The study reviews different PWM configuration techniques and how the quality of power can be improved with all the configurations based on THD and FFT (Patel et al., 2009). Nevertheless, it is one of the charge controllers that is utilized the most frequently for the storage of energy from the solar panel to the battery system. A switching circuit is designed to allow the input solar energy to be stored in the backup battery. An oscillator is in charge of this switching circuit. The oscillator's pulse width changes depending on how much energy is stored in the battery system. Figure 2.10 depicts a solar PWM charge controller block diagram.(Acharya & Aithal, 2020).

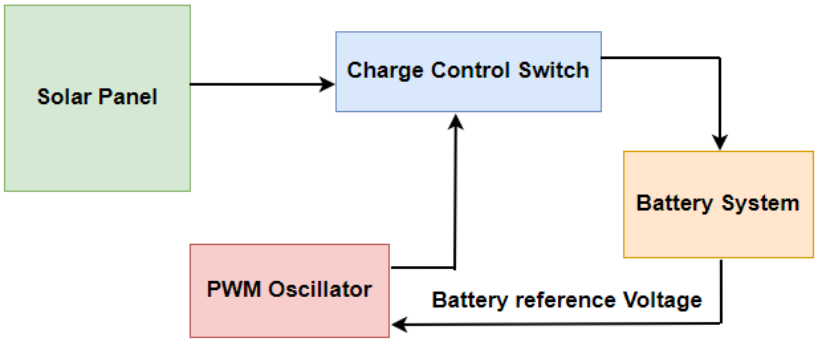

Figure 2.10: Conceptual model of solar PWM charge controller (Acharya & Aithal,2020)

In addition, the pulse width of the low state will only experience a single spike if the battery system's energy is less than that of the high state. In order to regulate the charging and discharging of the battery, a switching circuit is always connected to the PWM oscillator's output. Throughout the entire pulse cycle, the switch is mostly in the "ON" position, and the battery system stores the solar energy. However, the "ON" state of the pulse width will decrease and the "OFF" state of the pulse width will increase when the battery system SOC is greater than 90%. In a similar vein, the PWM oscillator's pulse width varies in such a way

that the majority of the time, the pulse will only be in the low state, with a spike in the high state when the battery SOC is close to 100% (Acharya & Aithal, 2020).

2.5.3.2 Maximum power point tracker (MPPT) charge controller

This controller is used to track and maintain power from solar PV at the maximum point. MPPT enable better efficiency and provide maximum power compared to PWM hence, it is the most widely used technique in standalone systems (Luo et al., 2017). Currently, there are various techniques that have been developed by engineers on maximum power point tracker (MPPT). Globally, there is significant interest in developing more efficient and appropriative MPPT control methods to ensure PV cells trap as much power as possible to supply the load for any given temperature and solar irradiance in a particular area (Essefi et al., 2014). Maximum power point tracker is very imperative on off-grid or standalone systems as it relate to the DC part of the system. Maximum power point tracker in off-grid PV system is used to control the output power of solar modules. The output current and voltage across solar modules varies due to different weather conditions and irradiance of the climate and maximum power point tracker plays an important role in ensuring that during such condition, current and voltage across solar cell remains at its maximum. The system is configured in such a way that solar modules operate at maximum point regardless of change in temperature.

Salehi & Solyali, (2018), reviewed different maximum power point tracking systems and arrived at more suitable algorithms that can be used to monitor, control and manipulate voltage and current across solar modules to operate at MPP. The algorithms are fuzzy logic control (FLC), incremental conductance and perturb and observe (P&O). Again, Belkaid et al., (2017) conducted a study on off-grid PV system as resource in telecommunication , farming and humanitarian aid where it used P&O algorithm as shown in figure 2.11. From the Figure, the algorithm sense voltage V(k) and current I(k) at Kth sample and instantaneous power P(k) can be calculated by multiplying current and voltage. This method compares the present power sample P(k) with the previous power sample P(k-1), and if the two are different then it compares the previous voltage (k-1) and that enables the system to generate maximum power at all times through comparison.

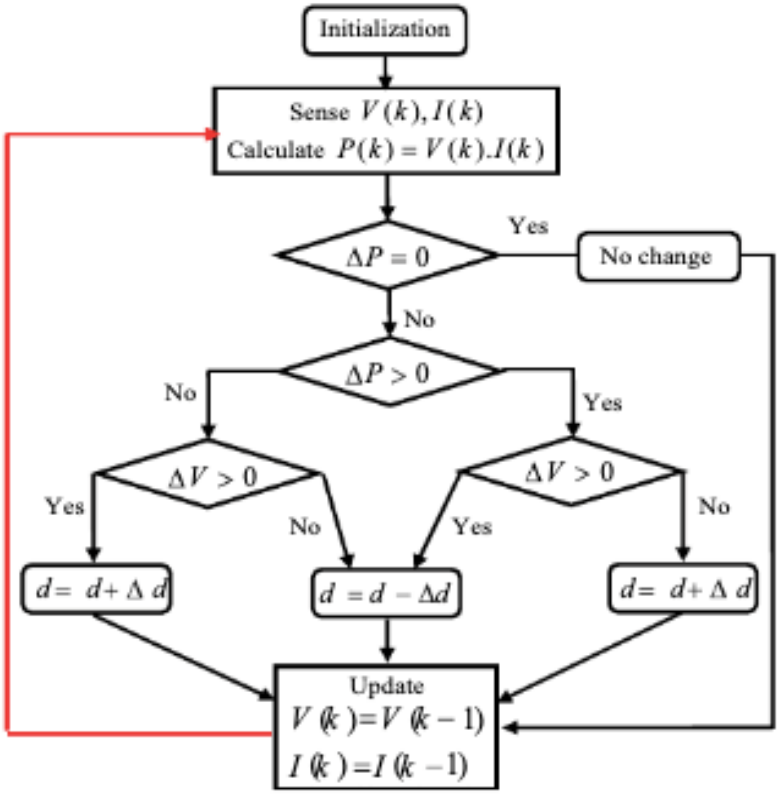

Figure 2.11: P&O algorithm (Belkaid et al., 2017)

2.5.4 Solar battery energy storage systems

The results of studies focused on the design of off-grid photovoltaic system with battery storage system shows that battery storage system is an integral component in an off-grid application but, the major problem with it is selecting an adequate size (Naqvi et al., 2021). A study on off-grid PV system application in telecommunication, farming and humanitarian aid, batteries are used to supply power to the load when the solar PV is not producing which is mostly at night and during cloudy days. This is to ensure system stability by supplying enough power to meet the essential load demands in the system (Kamran et al., 2020). The energy conversion process of battery system from chemical to electrical and vice versa is shown in Figure 2.12.

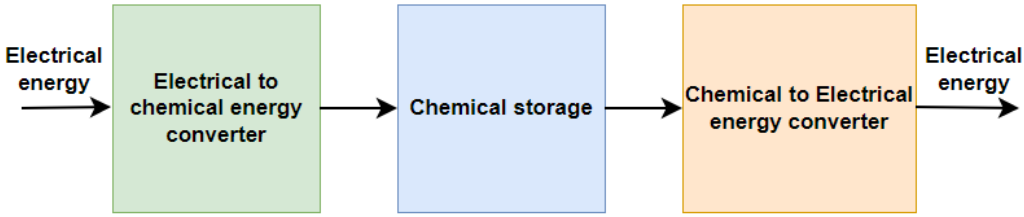

Figure 2.12: Principle of batteries operation (Naqvi et al., 2021)

Furthermore, having an off-grid Photovoltaic (PV) system along with a battery storage system is an effective solution for rural and remote electrification. However, battery capacity selection is the most challenging task in such a system because batteries are electrochemical cells used to store energy in chemical bonds and later converted to electrical energy to provide power to existing loads demands (Moumouni & Gdeisat, 2018). Batteries are vital in RES both on and off-grid interconnection and serve two basic functions; firstly, they are used as voltage current stabilization to provide stable current and voltage, secondly, they are used to store excess current during charging period and released when the need arises. Generally, batteries are divided into two categories, primary and secondary. Primary batteries are batteries that cannot be recharged and secondary batteries are rechargeable batteries which are mostly used in solar PV. The following are examples of rechargeable batteries with advance technology that makes it suitable of RES in off-grid applications (Samuels, 2017);

- Nickel cadmium
- Sodium Sulphur
- Lithium-Ion
- Lead acid

In off-grid systems, power generated by solar PV panels is used to charge the energy storage systems which in most cases is battery. Different types of batteries may be used as listed above based on the type of design and the purpose that the system needs to serve. Lead acid batteries are most popular and matured technology due to their advantages of having little discharging tolerance, ability to be noticeable when they are discharging, easily transportable, suitable for off-grid application due to less maintenance and no need to add water (Rousis et al., 2018). Presently, the life expectancy of most batteries is up to 20 years or 5000 cycles. Equation 2.11 can be used to calculate battery size with the assumption that the maintenance of the solar PV and rechargeable annual activities are set at 1.5 per the speculative cost (Naqvi et al., 2021).

$$\text{Battery capacity} = \frac{\text{Total Watt} - \text{hours/day used by appliances} \times \text{Days of automy}}{0.85 \times 0.6 \times \text{nominal battery voltage}} \qquad (2.11)$$

Again, Nickel cadmium is popular due to technology advancement hence, used in many applications. However, the main disadvantage with it is that it's not environmentally friendly due to the harmful elements that it disposes during and after use hence, making it less attractive. By construction a battery is made up of individual cells with each cell having an

ability to produce a voltage of up to 2V. Mathematically, a battery of 12V needs 6 cells to produce the nominal voltage. To properly design a battery, it is imperative that the designer have a better comprehension of the following factors (Querikiol & Taboada, 2018):

- Design features
- Performance characteristics
- Operational requirements

In addition, when designing a battery for solar PV application, the designer should ensure that the following characteristics are met (Naqvi et al., 2021):

- Low cost
- Long life expectancy
- Less discharge
- Good reliability
- Wide operating temperature
- Low maintenance

2.5.4.1 Lithium-ion batteries

As previously stated, lithium batteries are most suitable type of battery for solar PV system applications. These types of batteries can be 6V or 12V and can either be flooded or sealed gel type. Flooded types are mostly used in renewable energy systems and the electrodes are submerged in an electrolyte. During charging, hydrogen and oxygen obtained from water by a certain chemical reaction passes through the vents of the battery at negative and positive charges. This process allows the battery SOC to be maintained at a level close to the maximum point (100%) and determines the duration taken for the water to migrate fully to the battery system. Furthermore, sealed/gel type have immobilised form of electrolyte and during charging, oxygen and hydrogen gas recombine to form water at the negative and positive terminals (Li et al., 2014).

2.5.4.1.1 Working principle of lithium-ion batteries

The performance of Li-ion battery depends on the electrode properties, cycling stability, cost and energy density. Lithium-ion (Li-ion) cell consists of two materials namely; Carbon graphite

(C) at the anode and metal-oxide (MOx) at the cathode (Naqvi et al., 2021). The Li-ion cell formation depends on the reversible inclusion of graphite anode and metal oxide cathode through an organic liquid electrolyte. Anode consists of aluminium (Al) electrodes and cathode consists of copper (Cu) electrodes with both serving as current collector at the electrodes which demonstrates the desired stability and oxidation potentials. The electrode material of interface of organic electrolytes is thermodynamically unstable because, when the first charge-discharge cycle occurs, the Solid Electrolyte Interphase (SEI) is formed particularly on the graphite anode side. SEI layer protects the anode from direct electrolyte contact because it is not conductive neither is it an ideal insulator (Hesse et al., 2017). A lithium-ion battery internal configuration that shows the anode and cathode is shown in Figure 2.13.

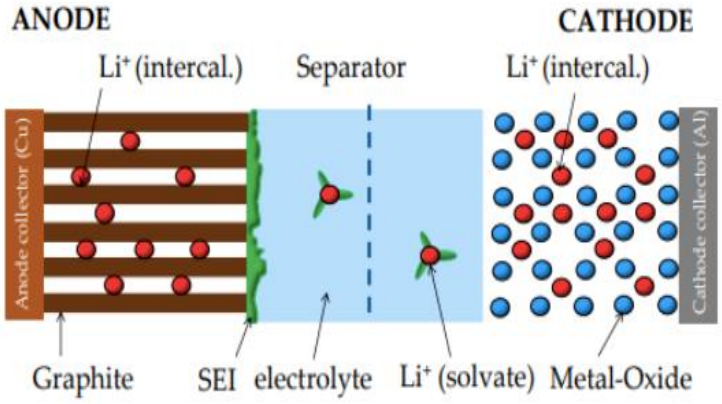

Figure 2.13: Lithium-ion battery (Hesse et al., 2017)

2.5.5 Battery sizing

When selecting a battery energy storage system for any application, there important parameters that must be considered, these are the battery State of Charge (SOC) and Depth of Discharge (DOD) including the battery capacity (AH) which is a measure of the total number of cycle depths of discharge it can permit without dropping into deep discharge. Other important factors to be considered is the ability of the battery to charge and discharge power regularly without encountering technical difficulties. The battery bank capacitor must be designed and calculated based on the energy that will delivered in order to prevent battery SOC to reach a point below the minimum values of the battery. The total energy of the battery must be greater than the energy desired by the load to compensate for the loss factor and the anatomy of the system. The battery capacity is determined by diving the total energy needed to supply the load over the battery voltage (Hesse et al., 2017).

2.5.6 Battery modelling

Mathematically, battery modelling focusses mainly on the voltage and current to achieve the desired power output. The current is determined by the flow of electrons from positive terminal to negative terminal and the voltage is determined using the open circuit voltage between the positive and negative terminals of the battery. Hence, when designing a battery, the following equations that determines the capacity of the battery at a given point *t* must be taken into consideration (Bokanga et al., 2014):

$$C_t = C_{(t-1)} + \frac{N_b(P_{Bt})\Delta t}{Vbus} \quad (2.12)$$

Where:

C_t = accessible battery capacitor (Ah) at hour t

$C_{(t-1)}$ = accessible battery capacitor (Ah) at hour t-1

N_b = 80% state of charge of the battery

P_{Bt} = battery output/input power

$Vbus$ = required voltage by the DC bus

Δt = simulation time step

The size of the battery system is determined as follows (Zakaria et al, 2008):

$$BatteryStorage = 2 * AD * TDWU \quad (2.13)$$

Where:

AD = autonomous day (1< AD >5)

TDWU = total hours used daily

The controller size is determined using equation (2.14) as follows:

$$I = I_{SC} * F_{SAFE} \quad (2.14)$$

Where:

I = controlled current

I_{SC} = short-circuit on PV

F_{SAFE} = safe factor

2.6. Global Off-grid Solar PV applications

International renewable energy agency (IRENA) defines off-grid solar PV system as a system that is not connected to the grid. These are system having solar PV systems with energy storage system/s that might either be a battery, supercapacitor or any other energy storage system but not connected to the grid (IRENA, 2018a). An off-grid system is also known as a standalone or Minigrid (MG) system due to its ability to generate and distribute power without connection to the grid. In this type of system, electricity is generated at the same place where it is consumed without distribution and transmission lines needed. The generated electricity can either power a DC or AC load depending on the type of electrical appliances and purpose of installation. Off-grid solar PV with DC load are applicable in dispersed telecommunication base stations applications where, the output from the solar panels or charge controller is directly connected to base station equipment as they require 48V DC to operate (IRENA, 2019b). Off-grid solar PV systems have gained popularity over the years due to its ability to supply power to remote areas and are widely used in countries where significant number of the citizens have little or no access to electricity because of affordability, population increase and high cost of connection to the grid. In this system power is generated through solar panels and the generated power is stored or saved in an energy storage system (ESS). The energy is stored due to various reasons ranging from, power supply higher than load demand and saving it for future use (IRENA, 2018b). The use of solar PV for different applications is shown if Figure 2.14.

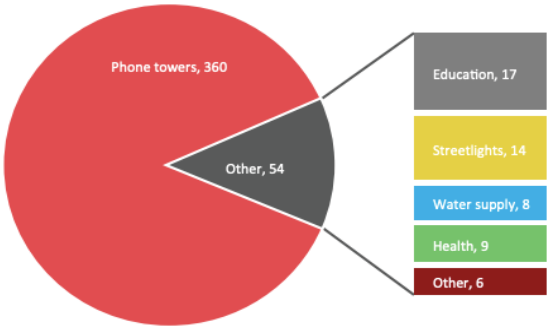

Figure 2.14: Solar PV system application according to sectors (IRENA, 2018b)

Furthermore, global research was conducted by international renewable energy agency (IRENA) to analyse and identify the potential of off-grid solar PV system applications in remote areas as well as existing global power capacity in off-grid. The result of the study indicated a significant growth from 0.21 GW to 2.94 GW over a period of ten years (decade) as shown in Table 2.3. This significant growth of off-grid solar PV application has been partially triggered by rapid decrease in the cost of solar PV, improved technology and government policies regarding the provision of access to electricity to citizens in remote areas. The prices of solar module and battery systems have reduced drastically over the past decade to approximately 80% (Showers, 2019). The decrease in the price has triggered innovation in the delivery and financing models to ensure that the technology is accessible and affordable for a longer period. Off-grid solar PV system offers various advantages such as reliability, reduced cost, rapid installation, sustainable energy development and provides solution in the quest for energy accessibility (IRENA, 2018b).

Table 2.2: Global power capacity for off-grid (IRENA, 2018b)

Year	Global annual capacity (GW)
2008	0.21
2009	0.31
2010	0.39
2011	0.51
2012	0.67
2013	0.90
2014	1.19
2015	1.52
2016	1.98
2017	2.56
2018	2.94

Because of the aforementioned factors, solar photovoltaic (PV) systems have been regarded as one of the renewable energy technologies with accelerating growth over the past ten years. The total installed capacity of solar PV reached 760 GW worldwide in 2020 with a projection of reaching 8050 GW by 2050 as shown in figure 2.15 (IEA, 2020).

Different sectors such as healthcare, agriculture, residential and farming communities use standalone solar PV system for water pumping. Boutelhig & Bakelli, (2012), conducted research on PV system as a solution to water pumping and the result showed that, deploying such system will help to provide water in areas where the department of water affairs might not be able to provide such due to lack of access to the grid. The result further showed that that in such communities, the system will help people in various domestic chores such as drinking, bathing, house cleaning, cooking, laundry, small garden irrigation and livestock for drinking purposes. The application of off-grid PV system for the above purposes is popular in most communities that do not have access to the grid with the most application in water pumping as shown in Table 2.4.

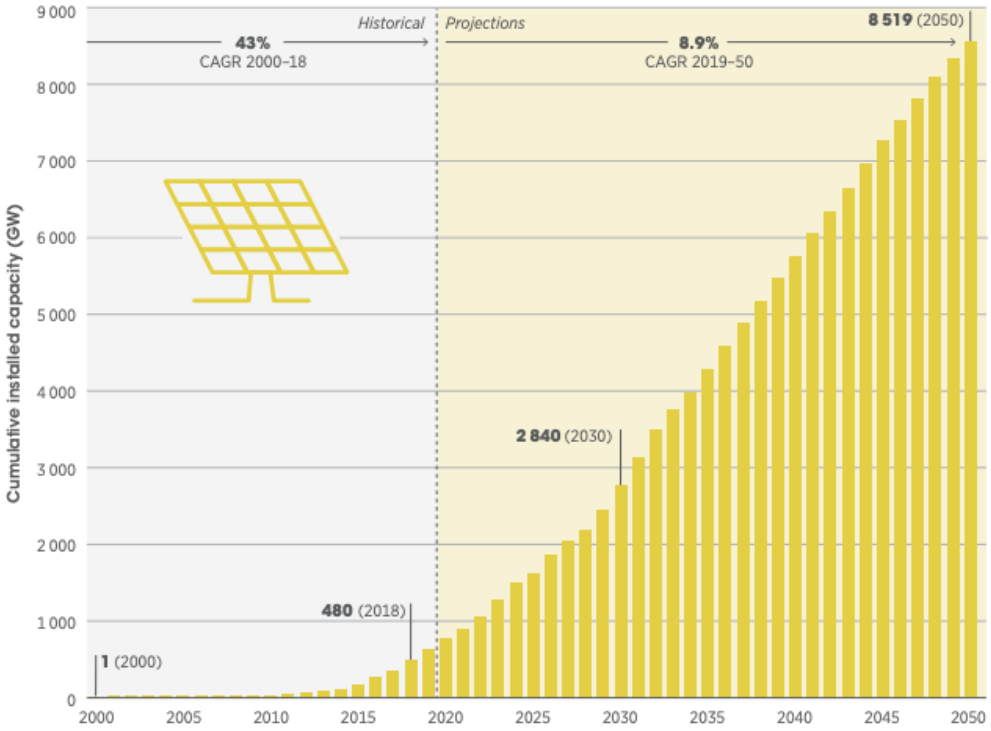

Figure 2.15: Estimated installation of solar PV (IEA, 2020)

Table 2.3: Standalone solar PV system applications

Sector	Application
Health care	• Water pumping • Used in communications ranging from telephone and radio communication systems
Agriculture	• Used in irrigation • Water pumping
Community	• To provide lighting in schools • Used as standalone to provide lighting in public parks • Refrigeration for medicines/vaccines • Water pumping • lighting of wards
Domestic	• Used in televisions, radio equipment
Farming	• Water pumping • Supplying power to people residing in a farm
Small enterprise	• Lighting in business • Power to small equipment's such as computers and other electronics devices • Provide lighting in stores and other facilities

2.7. Solar energy potential in South Africa

Mulaudzi & Bull, (2016), assessed the potential of solar energy as means of power generation in South Africa and the result showed that South Africa is characterised with large solar energy resource. The solar radiation is above $2.150\ \mathrm{KWh/m^2}$ per year of global horizontal irradiation (GHI). The most suitable province for deploying solar PV system is the Northern cape and as

a result, various studies have been conducted to support that claim (Van der Merwe & Brent, 2020). The annual global horizontal irradiation (GHI) across South Africa is shown in Figure 2.16. The GHI includes the diffuse radiation i.e., the light that has been dissipated by the clouds as well as the sunshine that reaches the ground without any interference from the clouds.

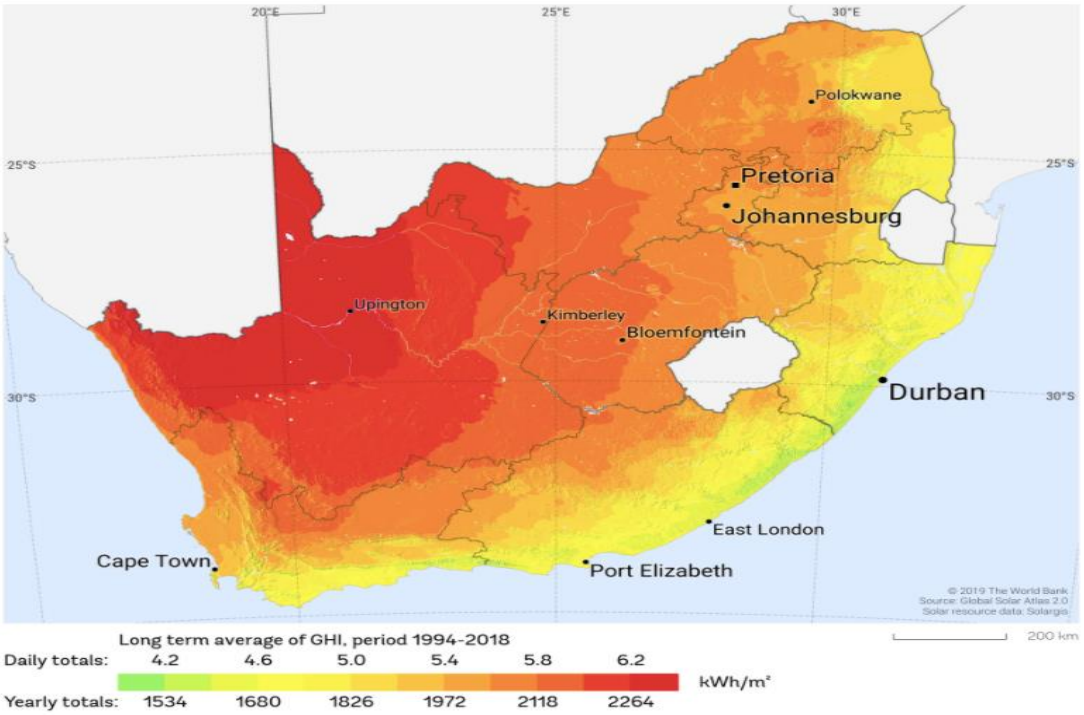

Figure 2.16: Solar irradiation in South Africa (Van der Merwe & Brent, 2020)

2.8 Summary

This chapter presented literature review on off-grid solar PV system including the different components that make up the system. This includes an overview of solar PV application in farming communities, telecommunication base station and humanitarian facilities. The different components of solar PV system, solar panels composition, working principles, equivalent circuit of solar cells, current-voltage characteristics and fill factor of a solar cell were presented. In addition, the types of converters applicable in this study, lithium-ion battery and its working principle were also considered. Lastly, a brief review on the global off-grid solar PV applications and solar energy potential in South Africa were presented in detail.

CHAPTER 3: SYSTEM DESIGN AND METHODOLOGY

3.1 Introduction

An off-grid power system is composed of different components as shown in the preceding chapter. These are categorised according to the type of energy source/s, energy storage system and type of load (AC or DC). In this study, the primary source of power is a photovoltaic (PV) system, the energy storage system is a battery (Lithium-ion) and the load is AC load. Therefore, this chapter presents the modelling of an off-grid solar PV system with lithium-ion battery as a resource for telecommunications, farming and humanitarian aid application in the MATLAB/Simulink environment. The design, modelling and selection of correct values for the various components/sections of the system is critical to ensure effective power distribution, control and operation of the system. Thus, this chapter presents the method of modelling the solar PV system, the DC-DC boost converter, DC-DC bi-directional converter, inverter (DC-AC), energy storage system (lithium-ion battery), variable loads and the control system. The modelling of the solar PV system and the control mode including calculations and power rating is presented in section 3.2. In section 3.3 is the design process of the various converters (DC-DC boost converter, bidirectional converter and inverter) showing all applicable formulae and calculations. The energy storage system (lithium-ion battery) is presented in section 3.4, the variable load profile in section 3.5 and the summary in section 3.6. The controller ensures adequate power distribution between the solar PV system and the lithium-ion battery to meet the load demand. This is because, effective power distribution is very crucial in off-grid system with intermittent power supply based on the solar PV power output, battery SOC and the load demand at any particular point.

3.2 Solar PV system modelling

The inner performance of the solar PV system, which is determined by the cell temperature in degrees Celsius (°C) and the solar irradiance in W/m^2, may be thoroughly understood by properly modelling the system in the MATLAB/Simulink environment. Therefore, these two variables must be carefully chosen because they affect the photovoltaic system's power production. Additionally, with the aid of the maximum power point tracker, PVs are designed to function at their maximum power point determined by the voltage and current.

3.2.1. Ideal PV module

The output characteristics of a perfect photovoltaic array are determined by the cell temperature, the amount of solar radiation available, and the output voltage of the solar array. Therefore, precise parameter selection is essential to ensuring that the PV produces the

maximum amount of power. This is supported once more by the facts that the PV's short circuit current is linearly controlled by the ambient radiation and that a rise in solar irradiance corresponds to an increase in the PV's open circuit voltage.

The photovoltaic (PV) array block that is offered in the MATLAB/Simulink environment is made up of a number of carefully organized PV modules. Each module in this PV array is connected in series and is placed in series, however they are all connected in parallel. In order to characterize the temperature-dependent features and solar irradiance I-V characteristics of the modules, each PV array block includes a diode, current source Iph (light-generated current), series resistor (Rs), and shunt resistor (Rsh) as illustrated in Figure 3.1.

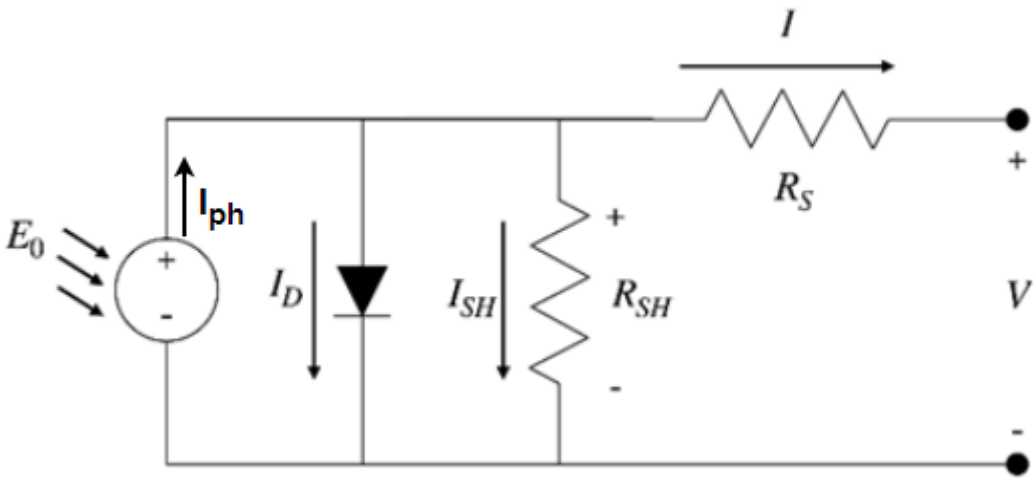

Figure 3.1: Equivalent circuit model of a PV Cell

The ambient cell temperature has a major impact on the short circuit current because it causes an increase in the short circuit current but a drop in the open circuit voltage when the cell temperature rises. Thus, a rise in cell temperature results in a decrease in power production and cell efficiency. The electrical circuit of the solar cell is depicted in Figure 3.1 using a photocurrent, although it is characterized by a continuous current source connected in parallel to a diode and a shunt resistor. This demonstrates the internal resistance to current flow and is indicative of the leakage current that is connected in series with the series resistance.

Equation 3.1 represents the voltage-current characteristics of the solar cell from Figure 3.1:

$$\mathrm{I} = \mathrm{I_{ph}} - \mathrm{I_{SH}}\left(\exp\frac{\mathrm{e(V + IR_s)}}{\mathrm{mkT_c}} - \frac{\mathrm{(V + IR_s)}}{\mathrm{R_{sh}}}\right) \tag{3.1}$$

Where:

- $\mathrm{I_{ph}} = \text{Photocurrent generated by the solar irradiance (A)}$

- I_D = Current flowing through the diode (A)
- I_{sh} = Current flowing through the parallel resistance (A)
- I = Output current of the solar cell (A)
- V = Output voltage of the solar cell (V)
- R_s = Junction resistance(Ω)
- R_{sh} = Loss of dissipative effect of the solar cell (Ω)
- k = Boltzman's constant, $1.3810^{-23}\,\frac{J}{K}$
- T_c = cell temperature (℃)

Again, as shown in equation 3.2, the photocurrent I_{ph} is greatly influenced by the solar cell's operating temperature and radiation.

$$I_{ph} = \frac{\left(I_{SC} + ki(T_c - T_{ref})\right)\lambda}{1000} \tag{3.2}$$

Equation 3.3 can be used to express the cell saturation current, which was already demonstrated to be considerably temperature dependent:

$$I_s = I_{RS}\left(\frac{T_C}{T_{Ref}}\right)\exp\left(\frac{qE\left(\frac{1}{T_{Ref}} - \frac{1}{T_C}\right)}{KA}\right) \tag{3.3}$$

Where; q = electron charge; 1.610^{-19} C

and

$$I = I_{ph} - I_D \tag{3.4}$$

Furthermore, figure 3.1 depicts a perfect equivalent photovoltaic system with various components, such as series and shunt resistors coupled in parallel with diodes, but inversely proportional to shunt leakage current. However, as the PV array is unaffected by a change in the value of the shunt resistor, its corresponding leakage resistance will rise dramatically even if the leakage current is not linked to ground. The power output of the PV array, however, will be significantly affected by a little change in the series resistor's value (Showers, 2019).

Equation 3.5 shows the ideal model of a solar cell with all of its complexities as:

$$I = I_{ph} - I_0\left(\exp\frac{q(V + IR_S)}{mkT_C} - 1\right) \tag{3.5}$$

The following parameters are used to describe the solar cell:

- Short circuit current is the maximum current generated by the solar cell when the voltage is equal to zero (V = 0)
- Open circuit voltage, V_{oc} is the maximum voltage of the solar cell when, $I_D = I_{ph}$ while the generalised current is generally assumed to be zero.
- Mathematically, the cell voltage without light is expressed as:

$$V_{OC} = \frac{mkT_C}{e} \ln\left(\frac{I_{ph}}{I_O}\right) = V_t \ln\left(\frac{I_{ph}}{I_O}\right) \tag{3.6}$$

Where:

$T_C = \text{absolute cell temperature}$

$V_t = \frac{mkT_C}{e} = \text{thermal voltage}$

- The maximum power to incident light power ratio, or solar cell efficiency, is expressed as:

$$\text{Efficiency } (\eta) = \frac{P_{max}}{P_{in}} = \frac{I_{max} V_{max}}{A G_a} \tag{3.7}$$

Where:

$G_a = \text{local irradiance on the solar cell surface}$

$A = \text{cell area}$

- The maximum power point (MPP) on the I-V characteristic curve is the point where the product of the voltage and current is highest, i.e., the point where the curve records the highest power.

3.2.2. Solar PV design in MATLAB/Simulink

Different types of solar panels are available in the MATLAB/Simulink environment, and each has unique parameters for maximum current, maximum voltage and power rating. In order to accurately represent the local weather, the temperature and solar radiation were carefully chosen. In this study, the maximum power point was tracked using the incremental conductance approach under the South African meteorological conditions. Therefore, the details of the selected solar PV system used in this study is shown in Figure 3.2.

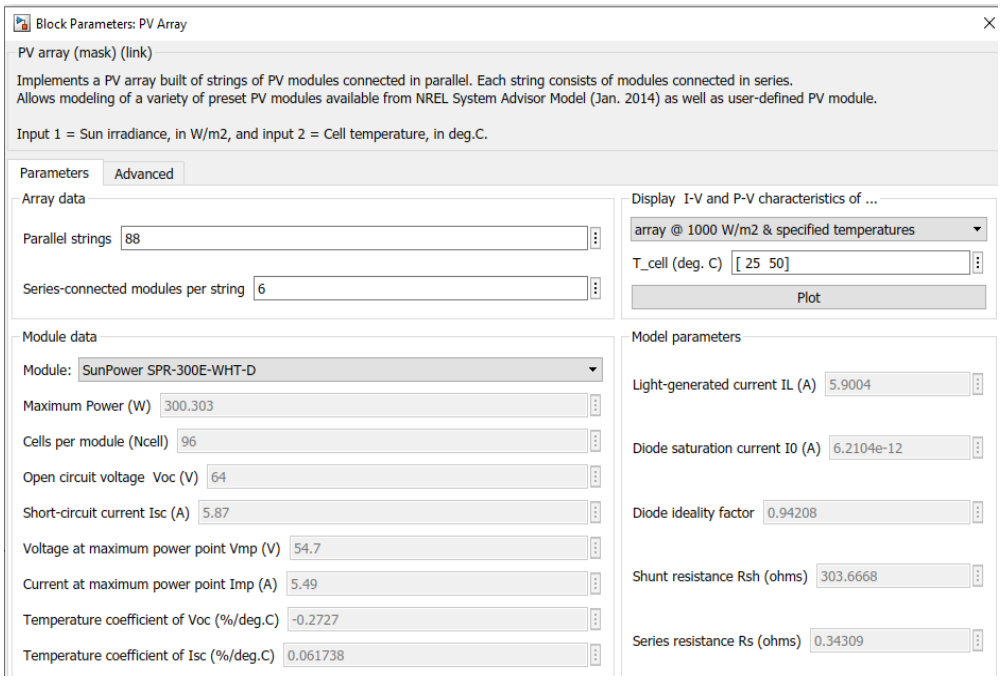

Figure 3.2: The simulated values of the 50 kW PV array

Calculations on how many modules would need to be installed both in series and parallel to produce 50 kW of electricity in total.

Total number of panels in series = $\frac{V_{dcmax}}{V_{mp}} = \frac{300}{37.86} = 7.924$

It is not practical to have fractional panel of 0.924, hence, the total number of panels needed in series is rounded up to 8 panels.

$\therefore$ the total number of panels needed in series $= 8$ panels

Therefore, the actual output voltage from the PV system: $8 \times 37.86 = 302.88\ V_{dc}$

The output current generated by the PV system $(I_{out}) = \frac{P_{out}}{V_{out}} = \frac{50\ kW}{302.88} = 165.082\ A$

The number of panels connected in parallel $(N_p) = \frac{I_{PV}}{I_{mp}} = \frac{165.082}{8.32} = 19.842$

Because it is not feasible to have 0.842 panels, the number of panels needed in parallel is rounded up to 20 panels.

The active power is then calculated as:

Active power = (No. of panels in parallel $\times I_{mp}$) $\times$ (No. of panels in series $\times V_{mp}$)

Hence, the active power (P_O)= $(20 \times 8.32) \times (8 \times 37.86)$

$$\therefore P_O = 50.399 \text{ kW}$$

Furthermore, the solar irradiance and associated temperature indicating the actual current against the voltage is shown in Figure 3.3 (a) and the actual power against voltage is shown in Figure 3.3 (b) respectively. The actual value of the solar PV power output is 50.339 kW, the actual current is 167.21 A and the output voltage is 302.88 V respectively. It is obvious and clearly shown from both Figures that the output current and solar irradiance have a substantial impact on the solar PV system's power output.

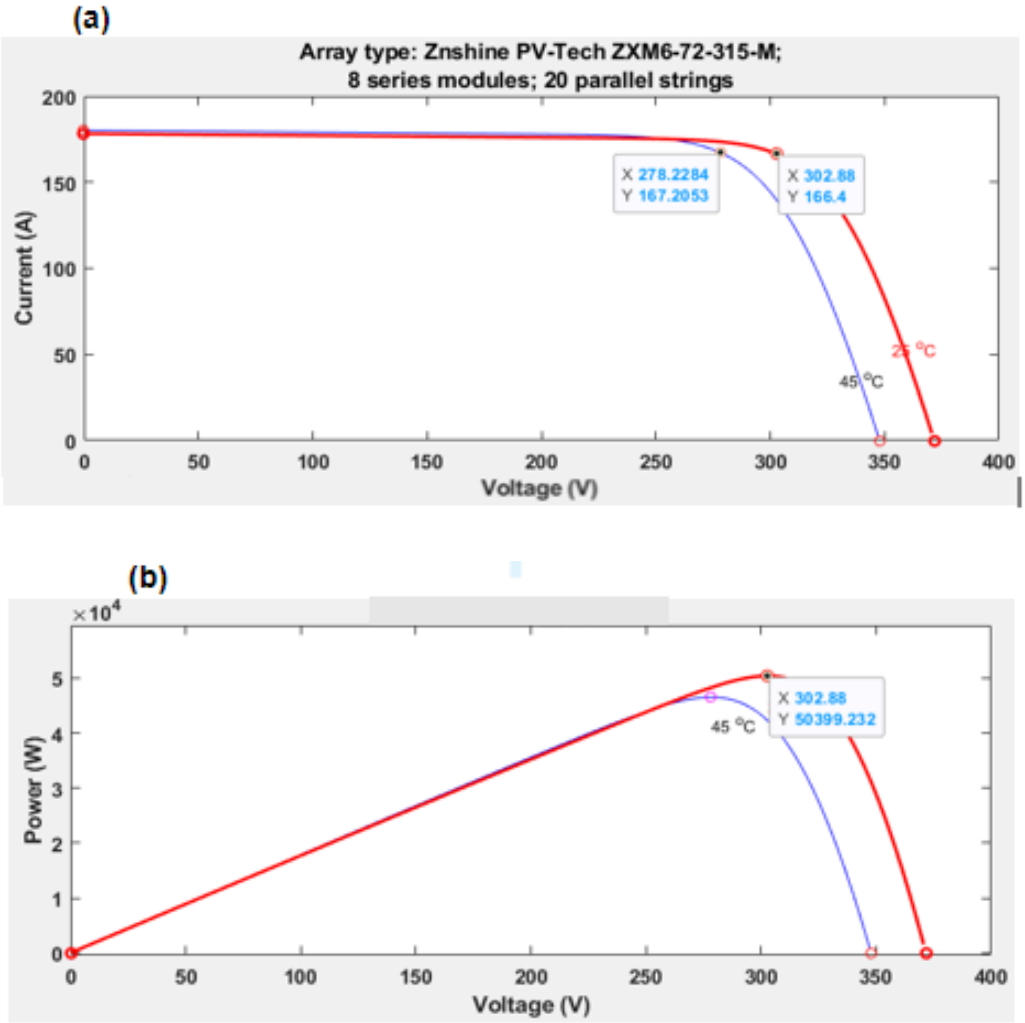

Figure 3.3: Solar PV characteristics (a) Current Vs Voltage; (b) Power Vs Voltage

Again, to reduce the ripple voltage across the solar PV terminals, a capacitor is connected at the output and calculated using equation 3.8 as (Showers, 2019):

$$C_{DCLink} = \frac{V_{PV} D}{4 \Delta V_{PV} f_s^2 L_{boost}} \quad (3.8)$$

Where:

$C_{DCLink} = \text{Capacitor value}$

$V_{PV} = \text{Solar PV output voltage}$

$D = \text{Duty cycle}$

$\Delta V_{PV} = \text{Ripple voltage}$

$f_s^2 = \text{Switching frequency}$

$L_{boost} = \text{Inductor value}$

$$\therefore C_{DCLink} = \frac{302.88 \times 0.596}{4 \times 90.864 \times 364.5 \times 10^{-6} \times (10 \times 10^3)^2} = 13.625\ \mu H$$

3.3 Power converters

Power electronics converters have the responsibility of managing the power flow from generation to a load such that the load is supplied with an appropriate current, voltage, and/or frequency. This is accomplished by minimizing power losses as much as possible to increase conversion efficiency. Depending on the type of conversion, many types of power electronic converters are classified. Conversions can be made from DC to AC, AC to DC, DC to AC, or even AC to AC (Luta, 2019).

Inductors, capacitors and semiconductor switches are frequently used in the construction of power electronic converters. These switches can either be fully regulated, like thyristors, or fully uncontrolled, like diodes (BJTs, MOSFETs, IGBTs, GTOs, etc.). Semiconductor devices that are controlled are line commutated, whereas uncontrolled semiconductor devices are driven by circuits employing control signals (Khamisani Advisors et al., 2018).

The modelling of the DC-to-DC and DC-to-AC converters employed in this thesis is the focus of this section where three power converters were employed. The solar photovoltaic array voltage is boosted from 300 V to 750 V to meet the DC link voltage. A DC-DC bidirectional converter is used to change the DC voltage from 750 V to match the voltage of the battery bank of 200 V in order to charge the lithium-ion battery. Similarly, a three-phase DC-to-AC inverter is used to convert the 750 DC V from the DC link to an AC voltage to supply the AC

load at 350 Volts. The control of the solar PV DC-DC boost converter was accomplished using a maximum power tracking technique (algorithm) and the bidirectional converter used a single loop voltage mode control.

3.3.1 Boost Converter design

A DC-DC boost converter is used to step-up the voltage in order to provide an output voltage greater than the voltage from the solar PV system. This basically amplifies the input voltage from the solar PV. A semi-conductor switch, an inductor, a diode, and a pulse width modulator make up the DC-DC boost converter.

For the photovoltaic system in this study, a two-stage architecture is chosen. The obvious justification for choosing this specific topology is because two stage topology permits further extension. It makes the system adaptable, allowing it to be changed into a multi-string system to increase its capacity in the future, with each string having a different MPPT and DC-DC converter. Again, since a solar cell is a current source, a capacitor must be connected in parallel across the solar PV output in order for the DC-DC boost converter to see it as a voltage source.

The fundamental model of a boost converter is presented in Figure 3.4 where the semiconductor devices Q and D are presumed to be ideal. The states of the inductor current determine the boost converter operating modes. If the inductor current does not reach zero, the converter is said to be operating in continuous conduction mode (CCM), otherwise it is operating in discontinuous conduction mode (DCM). When the converter is operating at steady state, the input voltage V_{in} charges the inductor L and the capacitor powers the load R when the semiconductor device Q is turned on. The inductor releases its stored energy to the load through the diode when Q is in the off state.

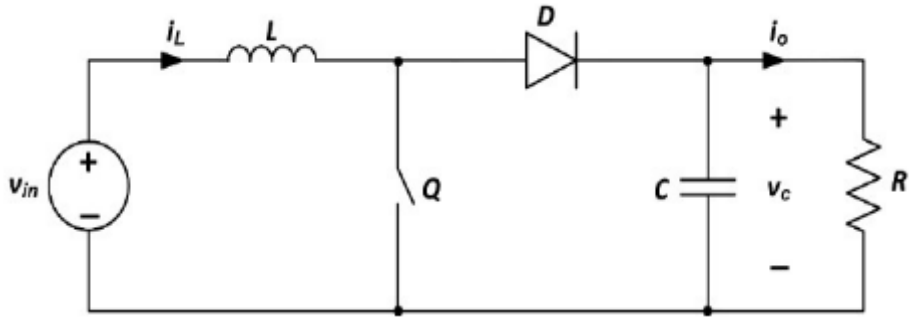

Figure 3.4: Ideal boost converter

As seen in Figure 3.5, the duty cycle time on (DT) inductor charges and the current I_L rises linearly as the switch is turned on, while the capacitor discharges as the load discharges the capacitor.

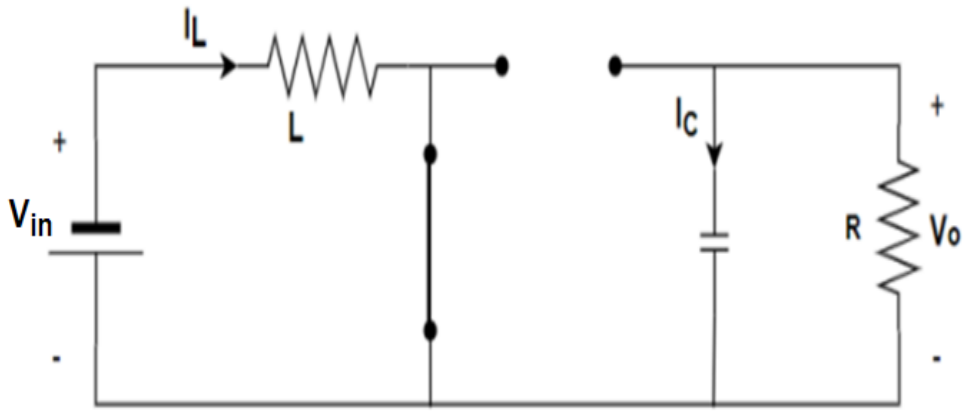

Figure 3.5: Boost converter schematic when switch is in the "ON" position

In addition, when the switch is turned "OFF", the magnetic field's stored energy is released, forcing I_L through the diode while the inductor simultaneously powers the load and charges the capacitor as shown in Figure 3.6.

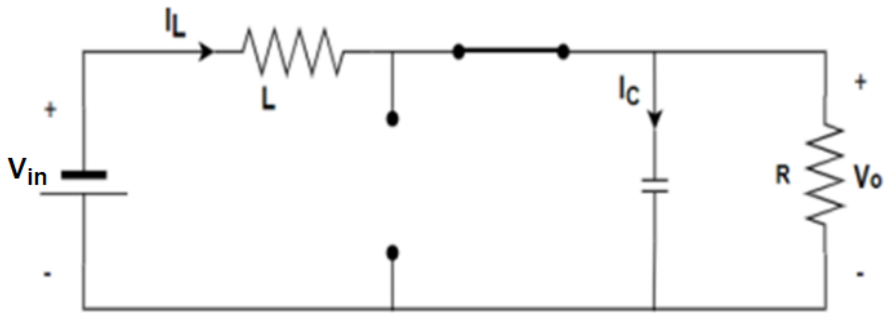

Figure 3.6: Boost converter schematic when switch is in the "OFF" position.

Furthermore, the steady state voltage and inductor current waveforms are presented in Figure 3.7 (a) and (b) respectively.

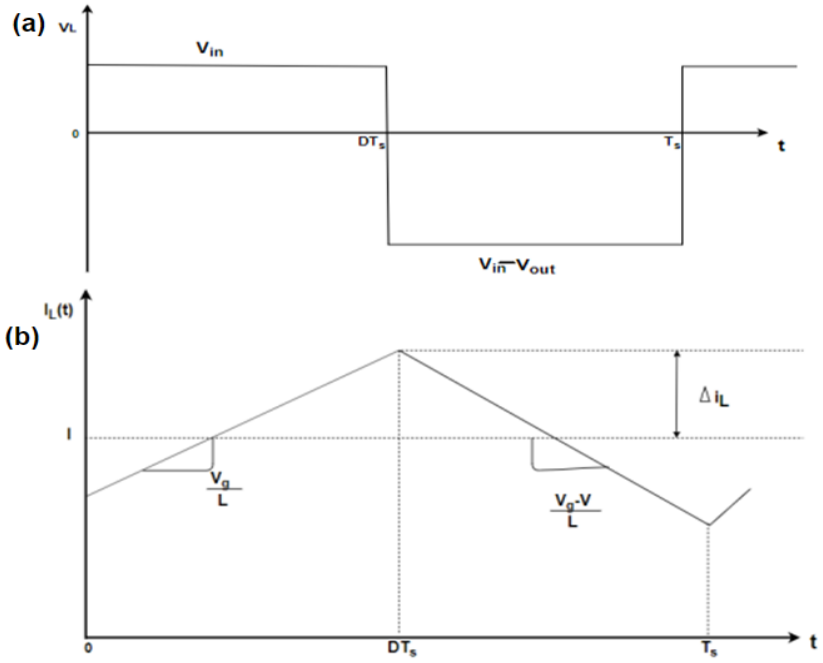

Figure 3.7: (a) Inductor voltage (b) Inductor current (Gebreab, 2013)

$$\Delta i_L = \frac{V_i}{L} DT = -\frac{V_i - V_o}{L}(1 - D)T$$

$$V_i D = (-V_i + V_o)(1 - D)$$

$$D = 1 - \frac{V_{in}}{V_{out}} \tag{3.9}$$

$$\therefore D = 1 - \frac{302.88}{750} = 0.596$$

Again, if the ripple current and the associated value of the inductor's peak current are known, equation 3.10 can be used to determine the suitable value of the inductor L as:

$$L = \frac{V_i D}{\Delta I_i f_s} \tag{3.10}$$

Where:

ΔI_i = inductor ripple current (30% of I_L)

I_L = load current

D = duty cycle

V_i = solar PV voltage

$f_s = \text{switching frequency}$

$$I_L = \frac{P_{in}}{V_{in}} = \frac{50 \times 10^3}{302.88} = 165.082 \text{ A}$$

$$\Delta I_i = 0.3 \times 165.082 = 49.525 \text{ A}$$

$$L = \frac{302.88 \times 0.596}{49.525 \times 10 \times 10^3} = 364.5 \text{ µH}$$

Furthermore, the value of the capacitor can be calculated using equation 3.11 as (Gebreab, 2013):

$$C_{DC} = \frac{I_O D}{\Delta V_O f_s} \tag{3.11}$$

Where:

$I_O = \text{output current}$

$\Delta V_O = \text{ripple voltage (1\% of boosted voltage)}$

$$I_O = \frac{P_O}{V_O} = \frac{50.399 \times 10^3}{750} = 67.199 \text{ A}$$

$$\therefore C_{DC} = \frac{67.199 \times 0.596}{7.5 \times 10 \times 10^3} = 534 \text{ µF}$$

However, when there is more power available in the system, this capacitor stores extra energy and releases it when there is not enough to maintain the capacitor's power flow.

3.3.2 DC-DC Bi-directional Converter

The DC-DC bidirectional converter regulates current flow in both directions, enables bidirectional current flow, requires little in the way of storage components and simplifies battery charging and discharging. Figure 3.8 shows a few common and in-use non-isolated topologies of DC-DC bidirectional converters. They are broadly divided into core topologies like Cúk converters, SEPIC converters and half-bridge converters as well as subsequently derived topologies like interleaved half-bridge converters and cascaded half-bridge converters as shown in Figure 3.9.

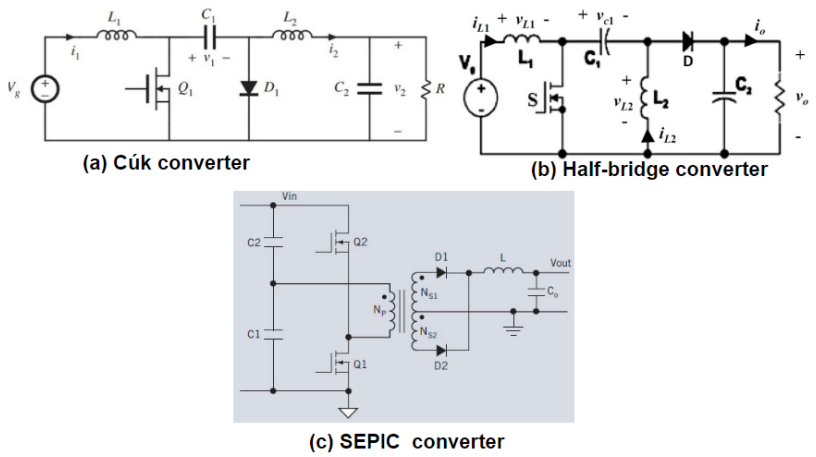

Figure 3.8: Basic non-isolated DC-DC converter topologies (Showers, 2019)

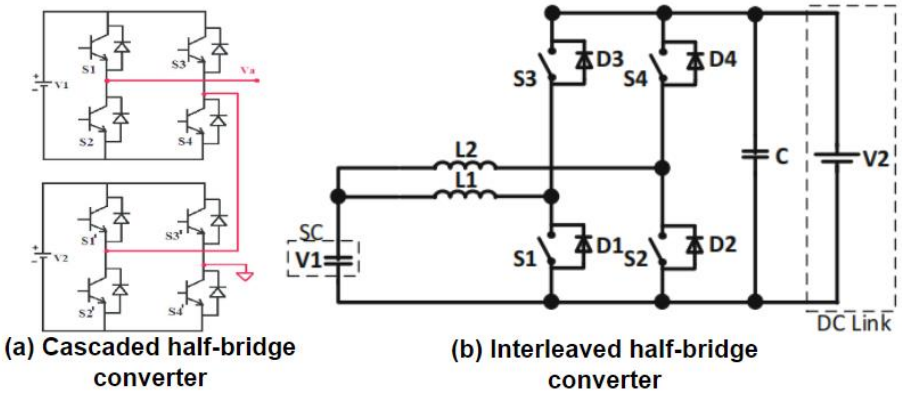

Figure 3.9: Derived non-isolated DC-DC converter topologies

Using two main switches, the Cúk and SEPIC converters convert electricity in both directions. The half-bridge converter is chosen in this study because it is mostly used in DC-DC bi-directional converter and its simplicity in operation. The fundamental half-bridge is where the interleaved and cascaded half-bridge converters are derived from, therefore their features can be evaluated in relation to those of the fundamental half-bridge converter.

The main drawback of utilizing a half-bridge converter is that when running in boost mode, the output capacitor's capacity and the discontinuous output current are greatly impacted. The main benefit is that the architecture only utilizes two switches and a modest amount of storage. This is because it has lower switching and conduction losses on active parts, as well as less inductor conduction. As a result, it is more affordable and capable of handling higher efficiencies than Cúk and SEPIC converters. Due to lower stresses and higher efficiency, the derived interleaved half-bridge converter would have been the optimum option for this study. But because of its light weight, straightforward design and need to cut costs, the half-bridge converter was chosen.

The half-bridge non-isolated DC-DC bi-directional converter that is used in this study is shown in Figure 3.10. The battery is connected on the low voltage side (200 Vdc) while the high voltage side (750 V) is connected immediately after the DC-DC boost converter. Depending on the load demand, solar PV power output and the battery state of charge (SOC), this architecture can operate in the buck or boost mode.

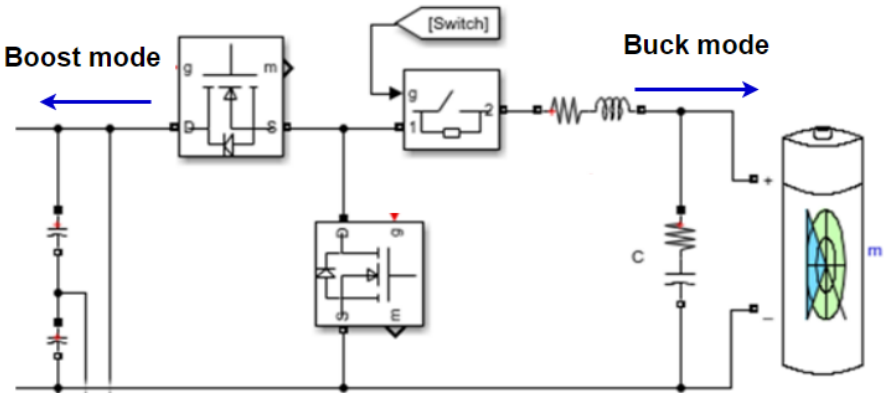

Figure 3.10: Bi-directional converter used in the study

The value of the inductor used in the DC-DC bi-directional converter is obtained using equation 3.12 as (Showers, 2019):

$$L_{min} = \frac{(1-D)^2 V H^2}{2 P_C f_s} \tag{3.12}$$

Where:

$L_{min} = \text{minimum inductor value}$

$D = \text{duty cycle}$

$V_H = \text{voltage at the high side } (750\ V_{dc})$

$P_c = \text{critical power}$

$f_s = \text{switching frequency}$

$$\therefore L_{min} = \frac{(1-0.596)^2 \times 750^2}{2 \times 26 \times 10^3 \times 100 \times 10^3} = 17.66\ \mu H$$

Again, the capacitor value is obtained using equation 3.13 as (Luta, 2019):

$$C_H = C_L = \frac{D}{R_{H f_s}(\Delta V_H / V_H)} \tag{3.13}$$

Where:

$$R_H = \frac{L_{min} 2 f_s}{D(1-D)^2}$$

$$\therefore R_H = \frac{17.66 \times 10^{-6} \times 2 \times 100 \times 10^3}{0.596(1-0.596)^2} = 36\ \Omega$$

$$\Delta V_H = \frac{V_H D}{R_H C_H f_s}$$

$$\therefore \Delta V_H = \frac{750 \times 0.596}{36 \times 3 \times 10^{-3} \times 100 \times 10^3} = 0.041$$

$$\rightarrow C_H = \frac{0.596}{36 \times 100 \times 10^3 (0.041/750)} = 3\ mF$$

The DC-DC Bi-directional converter links the lithium-ion battery to the boost converter via the DC link as illustrated in Figure 3.10. This specific converter is designed to regulate the lithium-ion battery's charging and discharging. The DC-DC converter operates in the buck mode when charging the lithium-ion battery and the battery current becomes negative. But when the battery is discharging power to the load, the converter operates in the boost mode and the battery current becomes positive.

3.3.3 DC-AC inverter

The purpose of the inverter is to transform the solar PV's DC electricity through a DC-DC boost converter into usable AC power that can be used to meet the load demand at an acceptable frequency and voltage. Additionally, it transforms the battery's DC power into an appropriate AC power suitable for the AC load. This is regulated using the delta modulation index of the PWM as shown in Figure 3.11. But the complete voltage source control (VSC) is shown in Figure 3.12.

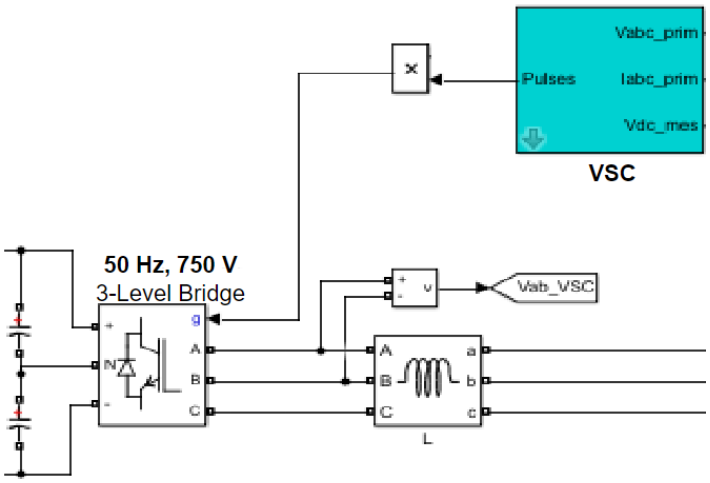

Figure 3.11: DC-AC inverter with VSC

By ensuring that the necessary reference AC currents at the output, the phase angle, and the magnitude are met in accordance with the system requirement, it also controls the voltage at the DC link. To accomplish this, a straightforward PI loop calculates the current's magnitude by equating the reference value to the DC link voltage, and a phase-locked loop provides information on the voltage's phase angle (PLL). Therefore, the DC bus voltage is controlled using the PI controller. For a matching negative error, the PI controller generates a negative reference current and for a positive error, it generates a positive reference current. The excess energy is rather used to charge the battery if the system encounters an increase in the dc bus voltage because this indicates that more energy is available at the dc bus. By imposing extra angle, the bridge's power factor is controlled. The DC link capacitor serves as an input to the inverter and the switching device is an IGBT with a lower switching frequency than a MOSFET. In this study a three phase, two level inverter was used to achieve the power conversion from DC to a corresponding AC.

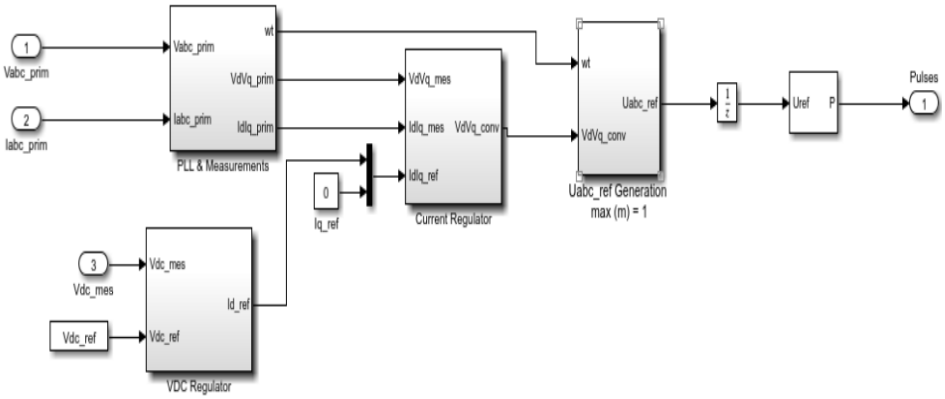

Figure 3.12: The inverter Voltage Source Control

3.4 Lithium-ion battery modelling

The battery is connected through a DC-DC bidirectional converter, which serves as an energy storage system to the output of the DC-DC boost converter so that it can either generate or consume active power. With the use of controllers attached to the converter switches, it is modelled to function as a boost or buck converter. The battery will function as a boost converter when supplying power to the load (discharging) and as a buck converter when consuming power from the solar PV (charging). So, when the battery is charging, the current is negative, and when it is discharging, the current is positive. The ripples in the solar PV output are reduced using a coupling L-filter. Furthermore, connecting a capacitor to the inverter DC link ensures system stability, steady supply of power and appropriate ripple reduction. The Lithium-Ion battery is the most popular form of battery storage in solar PV system applications due to fluctuation and unstable power output from the PV system as well as the presence of a variable load in the system. The Lithium-Ion battery is modelled to discharge up to 20% for both suggested control techniques and charge up to charge 80%.

The battery size and power rating are carefully selected to provide maximum assistance that will improve the power output from the solar PV system when the PV is generating little or no power. In the event that the solar PV is not producing any electricity due to insufficient solar irradiance, the battery is chosen to provide 30 kW for six hours. Hence, the battery is modelled and simulated as a backup system.

Again, due to its high energy density, low self-discharge rate, extended cycle life, and wide operating temperature range, lithium-ion (Li-ion) battery was chosen as the energy storage system for this study (Gao, Jin, Zhang, et al., 2016). It is crucial to understand that a battery does not generate energy on its own; rather, it is an energy storage device that only releases the same amount of energy as was previously stored. Lithium-ions are transferred between the positive and negative electrodes of a Li-ion battery's basic operating principle in order to produce or store energy. Electrons move in the opposite direction to the ions in the electrolyte, which act as a strong barrier for electrons orbiting the outer circuit, under both charging and discharging conditions. The battery pack's charge and discharge dynamics are considered for voltage control. Furthermore, aging effects and temperature are critical in analysing battery performance, but they were both disregarded in this work due to modelling complexity and computational difficulties, as well as the fact that it is not the main focus. The model provided, however, is sufficiently thorough to offer the relationship between current and voltage over a broad state-of-charge that is required for this study (Naqvi et al., 2021; Alkhawaldeh, 2020).

In addition, when compared to other standard batteries such as lead acid battery, alkaline and nickel metal hydride (NIMH) lithium-ion battery is the most suitable for off-grid application. A well modelled high energy lithium-ion battery as a voltage source linked in series with a resistance used to store energy is shown in Figure 3.13.

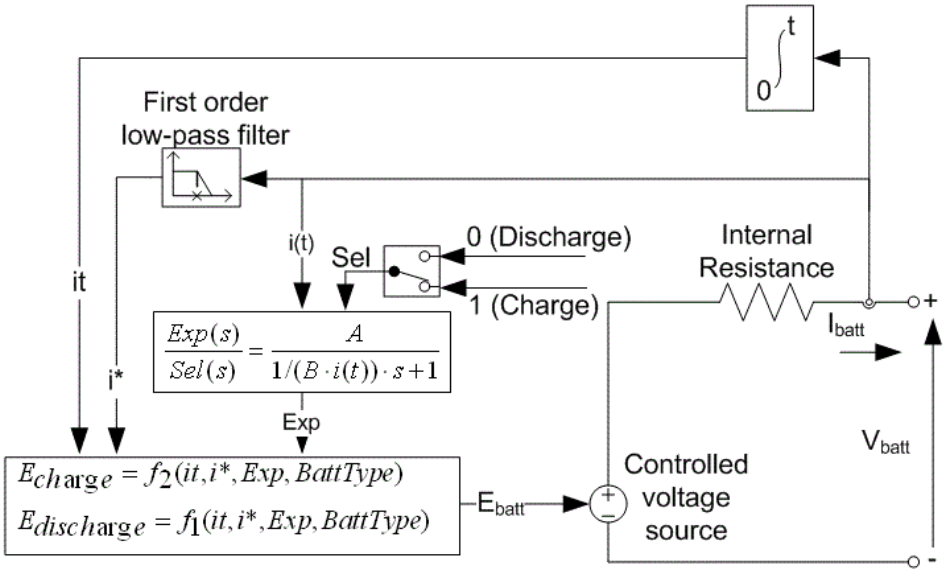

Figure 3.13: Equivalent circuit of the lithium-ion battery

According to Alloui et al. (2013) and Grammatico et al. (2010), equation 3.14 can be used to calculate the battery output voltage (V_{bat}) as follows:

$$V_{Bat} = E_{Bat} - r_{Bat} i_{Batt} \tag{3.14}$$

Where:

E_{Bat} = no load voltage (V)

r_{Bat} = battery internal resistance (Ω)

i_{Batt} = battery current (A)

To avoid complicated calculations, the internal resistance value of the battery is always considered to be constant, even when it fluctuates while charging and discharging or based on the battery current (Wang et al., 2016; George, 2018). Again, neglecting the effects of temperature, the open circuit voltage of the battery is dependent on the state of charge (SoC), battery current, and hysteresis losses of the battery. Therefore, the charge mode model and discharge mode model, which are utilized to establish the operating modes, are the two core components of the characteristics model for this battery (Kyari et al., 2020).

The discharge mode voltage ($i^* > 0$) is given as:

$$f_1(it, i*) = E_o - K.\frac{Q}{Q - it}.i* - K.\frac{Q}{Q - it}.it + A.\exp(-B.it) \quad (3.15)$$

And the voltage during charge mode ($i^* < 0$) is given as:

$$f_2(it, i*) = E_o - K.\frac{Q}{it + 0.1.Q}.i* - K.\frac{Q}{Q - it}.it + A.\exp(-B.it) \quad (3.16)$$

Where:

E_o = constant voltage (V)

K = polarization constant (V/A h)

Q = maximum battery capacity (Ah)

i^* = low frequency current dynamics (A)

B = exponential capacity (Ah^{-1})

A = exponential voltage (V)

it = extracted capacity (Ah)

i = battery current (A)

exp = exponential zone dynamics (V).

Equation 3.16 is used to represent the battery state of charge (SoC) as (Showers, 2019):

$$Q(t) = Q(0) - \int_0^1 i_{Batt} dt \quad (3.16)$$

Furthermore, the C rate is used to characterize and describe the battery's rate of charging and discharging using equation 3.17 as:

$$C_{rate} = \frac{i_{Batt}}{Q/h} \quad (3.17)$$

The battery depletion curve as a function of time (hours) when it is run under standard settings in the MATLAB/Simulink environment is shown in Figure 3.14. The middle area, displayed in

grey colour, shows the area where the battery is running optimally till its nominal voltage, whereas the battery experiences a quick voltage decrease in the charge saturation limits.

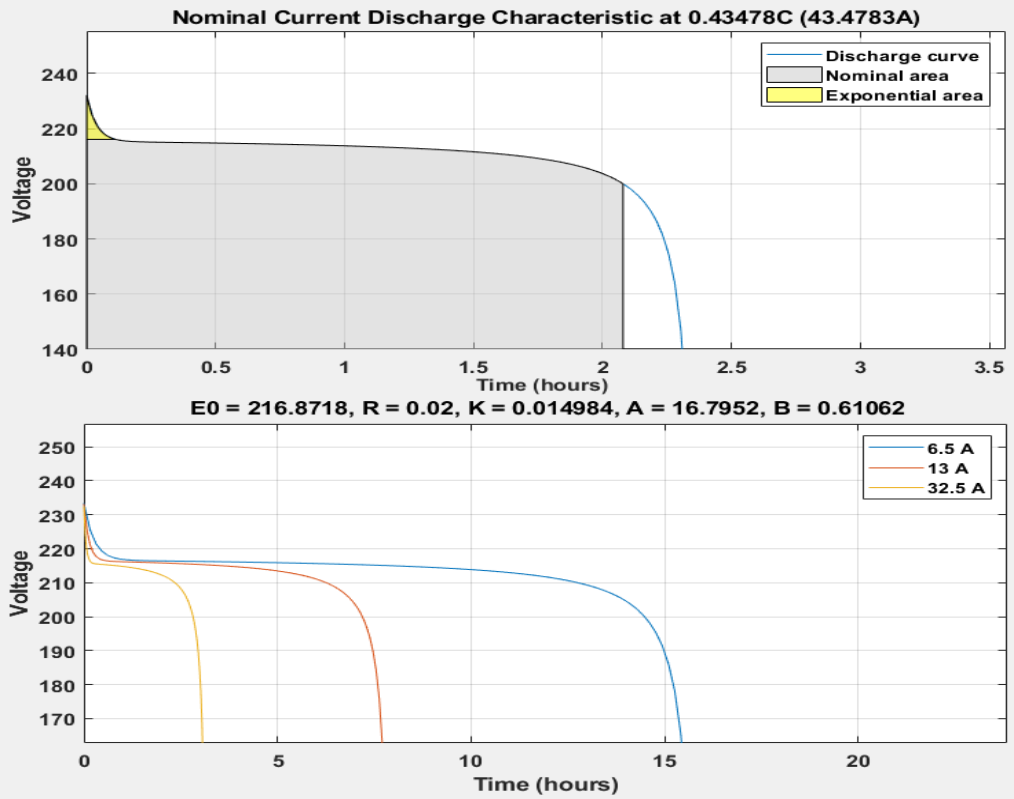

Figure 3.14: Battery discharge characteristics expressed as a function of time

Due to the exponential voltage drop that follows the nominal discharge voltage, the battery completely discharges in this region. Again, heavier loads with higher currents drawn result in a decrease in the battery state-of-charge, as shown in Figure 3.15. However, in the MATLAB/Simulink environment, where the battery state-of-charge (SOC) reflects its initial condition, the battery can be modified to a voltage appropriate for any given operation.

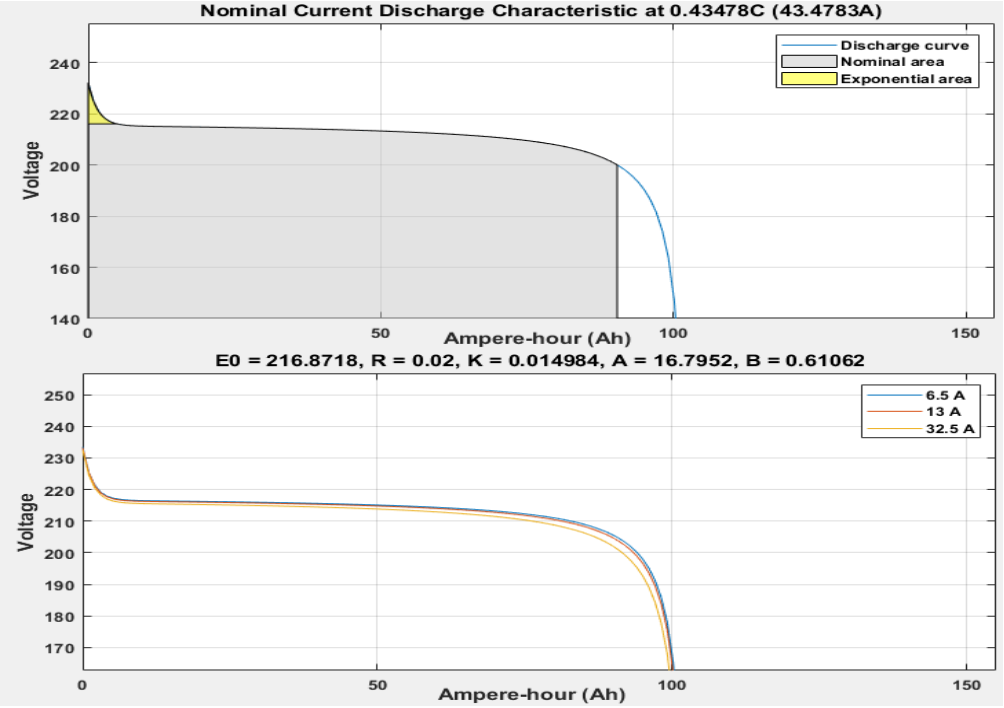

Figure 3.15: Battery discharge characteristics in Amperes-hour

In addition, the battery has a power rating of 30 kW which represents approximately 19% of the solar PV power supply capacity. Once more, the selection of the battery is made to guarantee performance delivery, to provide improved flexibility with a reliable energy source, and to have a wide margin for error. Table 3.1 shows the characteristics of the Li-ion battery.

Table 3.1: Battery specifications

Parameter	**Value**
Chemistry	Li-ion
Nominal Voltage	200 V
Nominal capacity	150 Ah
Nominal Power	30 kW
Initial battery SoC	80 %
Response time	1 s
Nominal temperature	25 ℃

3.5 Load profile

The study modelled an off-grid solar PV system as a resource and lithium-ion battery as a backup for applications in telecommunications base station, farming community and humanitarian aid facility. The variable loads consist of electrical appliances used in telecommunications base station, farming community and humanitarian aid facility as mentioned above as shown in Table 3.2. However, when generating at the maximum power point, the solar PV output power is modelled to meet all existing loads in the system. The solar PV system is connected to the AC load through a boost converter and an inverter at 750 V where the loads are categorised as essential or non-essential loads based on the relevance to the system. As earlier indicated, the lithium-ion battery pack is used as a backup system to supply power during peak demand and when the solar PV output power is less than the load demand. The load profile was carefully chosen to reflect the usual average AC load demand for a farming, telecommunication and humanitarian facility. The farming facility has a total load demand of 1.9 kW, telecommunication base station has a total load demand of 2.706 kW and the humanitarian aid facility has a total load demand of 21.341 kW during peak hour respectively. Therefore, in this study, the total load demand for all three facilities during peak hour is 25.947 kW.

Table 3.2: Details of Variable loads

Telecommunications					
Load	**Power demand (W)**	**Hours/day**	**Quantity**	**Total power (W)**	**Energy demand (kWh/day)**
Rectifier	84	24	1	84	2.016
Alarm system	10	24	8	80	1.92
Router	25	24	2	50	1.2
Switches	25	24	2	50	1.2
Camera system	10	24	8	80	1.92
LED light bulb	6.5	12	4	26	0.312

Transmission node	80	24	1	80	1.92
Switching node	80	24	1	80	1.92
RAN node	80	24	1	80	1.92
Digital multiplexer	15	24	2	30	0.72
Computer/server	160	24	1	160	3.84
Air conditioning	1900	24	1	1900	45.6
Air mux	3	24	2	6	0.14
Total	**2478.5**			**2706**	**64.63**
Farming					
Pumping system	1900	3	1	1900	5.70
Total	**1900**			**1900**	**5.70**
Humanitarian facilities					
Energy efficient solar refrigerator	100	24	5	500	12.00
Kettle	1200	2	5	6000	12.00
Stove	2000	2	5	10000	20.00
Radio	3	8	5	15	0.12
Iron	1000	0.5	5	500	2.50
LED light bulb	6.5	12	4	26	0.312
Geyser	2000	2	1	2000	4.00
Television	150	8	5	750	6.00

Microwave	1300	0.5	5	650	3.25
Computer	150	8	6	900	7.20
Total	**7909.5**			**21341**	**67.38**
Total power of the system	**12288**			**25947**	**137**

In addition, the project location shown in Figure 3.16 also offered helpful information, including solar irradiance and weather conditions, which are crucial in determining the number of hours a certain load required power.

Figure 3.16: Project location (AfriGIS, 2022)

3.6 Summary

This chapter presented the system design and mathematical modelling of individual components that make up the system. These include the solar photovoltaic system, the power electronic converters such as the DC-DC boost converter, the DC-DC bidirectional converter and the DC-AC inverter. Others are the energy storage system (lithium-ion battery) and the load profile which include the farming facility, telecommunication base station and the humanitarian facility. The control systems for the different power electronic converters were also presented.

CHAPTER 4: ENERGY MANAGEMENT SYSTEM ALGORITHM

4.1 Introduction

Conventional power systems are set up with a single power generation, long transmission and distribution networks, and a single direction of power flow. Typically, these power systems are built around generators that run primarily on fossil fuels. However, the usage of renewable generators in off-grid mode has become more common due to the negative environmental impacts of using fossil fuels and the need to increase the reliability of the power networks. As a result, a number of distributed generation units such as solar PV with battery storage system are now essential components of existing off-grid power systems, making the overall system more complex (Chao et al., 2013). The purpose of this new technology is to improve generation, boost system efficiency, and increase demand side flexibility.

Therefore, in this chapter, an advanced energy management system (EMS) for a solar PV and battery storage system supplying power to a farming community, telecommunication base station and a humanitarian facility is implemented using a predefined set of rules and performance criteria. This is implemented under the MATLAB/Simulink environment using the solar PV power output, battery SOC and load demand. The EMS uses the reference current of the solar PV to ensure its optimal operation and at the same time supplying enough power to meet the load demand. The parameters that control system operation mode are modified based on the battery SOC, load demand and the solar PV power output including solar irradiance to improve the energy efficiency of the system. A special set of control functions and energy management algorithm for this system have been created under hierarchical dependence but would not have the capacity to determine the development and operation of the system. This technique is executed in three control levels: energy management, power management and localised controllers as shown in Figure 4.1 (Bevrani & Shokoohi, 2013; Eid et al., 2016; Zsiborács et al., 2019) The energy management algorithm is similar to a decision-making for the effective operation of solar PV off-grid system using specific hours of power demand.

The system uses four control systems developed for optimal operation of the off-grid power system. The control that makes sure that the solar PV voltage is selected according to the bus voltage which is capable of tracking the reference with less error. This is done to make sure that ripples are minimised during transient load under controls with only one degree of freedom, such frequency and duty cycle. In order to optimize the system, a separate control system for lithium-ion battery is developed that regulates the battery system's charge and discharge based on the load requirement and state of charge (SOC). The EM is developed

with a unique control that keeps track of the load demand and available solar PV power output, and a proportional amount of power. Lastly is the primary control, which combines all of the separate controls. The signals from the other three aforementioned controls are used by the central control to make decisions.

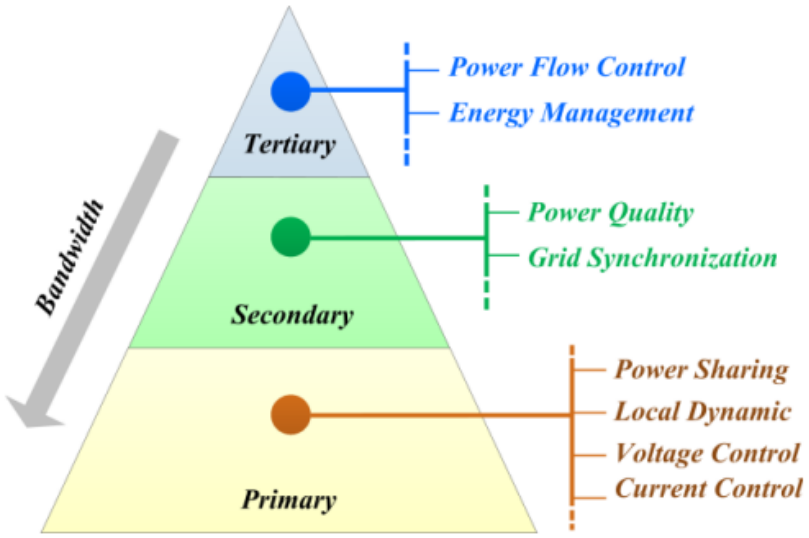

Figure 4.1: A typical hierarchical control scheme (Bevrani & Shokoohi, 2013)

Additionally, the development of a successful EMS for a solar PV and lithium-ion battery off-grid system will lead to the effective power distribution between both sources, which will benefit the system by allowing the solar PV to respond to the load demand more effectively for a given load demand and optimise the system. It will improve the operational performance of individual components and the entire system by ensuring the load is adequately met at all times. It is impossible to overstate the significance of an efficient energy management system (EMS), as it will allow for efficient load distribution between the solar PV and the energy storage system (lithium-ion) (Garcia Torres, 2015).

4.2 Energy management system concepts

According to IEC 61970, an energy management system is a computer unit made up of software that offers essential support services and applications with the functionalities needed for electrical generation and transmission systems to operate profitably and guarantee adequate security of supply at a lower cost (Byeon et al., 2013). In order to provide sustainable, dependable, and clean energy in the best way possible, distributed generation, loads, power electronics converters, energy storage units, and grid components are operated, controlled, and coordinated by energy management systems in the context of grid-connected renewable power systems (Malysz et al., 2014; Fertig & Apt, 2011). Energy management

systems can function to improve self-consumption or participate in the electricity market for grid-connected renewable power systems, whereas they can carry out functions like economic dispatch and load control for 100% renewable power systems (Petinrin & Shaaban, 2015; Khodadoost Arani et al., 2019).

4.3 Problem algorithm

The proposed energy management system is implemented by selecting the operational precedence of the solar PV, battery SOC and the load demand. This is an off-grid system where the availability of adequate power from the solar PV is a crucial factor because it is the only source of energy in the system. The battery depends on the solar PV for its charging. Hence, the following operational parameter restrictions were considered when creating the energy management algorithm:

- Minimum solar PV output power ($P_{PV_{min}}$) = 20 kW
- Maximum solar PV output power ($P_{PV_{max}}$)= 50.34 kW
- Minimum battery SOC ($Batt_{SOC_{min}}$) = 20%
- Maximum battery SOC ($Batt_{SOC_{max}}$) = 80%
- Farming facility load demand (L_{Fam}) = 1.9 kW
- Telecommunication facility load demand (L_{Tel}) = 2.701 kW
- Humanitarian facility load demand (L_{Hum}) = 21.341 kW
- Total load demand (L_{DT}) = 25.947 kW

Therefore, the equation regulating the EMS is as follows:

$$P_{PV_{max}} = L_{Farm} + L_{Tel} + L_{Hum} + P_{Batt} \quad (4.1)$$

Where:

$P_{PV_{max}} = \text{Solar PV maximum output power}$

$L_{Farm} = \text{Farming facility load demand}$

$L_{Tel} = \text{Telecommunication facility load demand}$

$L_{Hum} = \text{Humanitarian facility load demand}$

$P_{Batt} = \text{Battery power}$

Consequently, the energy management system (EMS) control algorithm is designed to ensure effective power supply to the total load demand and power distribution between the solar PV and the lithium-ion battery based on the amount of available power and battery SOC. Hence, the EMS should ensure the following objectives:

- The total load demand is efficiently supplied with adequate power.
- Effective power supply and distribution between the solar PV and energy storage system to prevent battery deep discharge during high load demand.
- Optimal operation of the solar PV and lithium-ion battery pack based on the set minimum and maximum battery SOC.

Again, equations 4.2, 4.3 and 4.4 are used to obtain the proposed energy management system algorithm:

$$P_{PV_{max}} > L_{Farm} + L_{Tel} + L_{Hum} \quad (4.2)$$

$$P_{PV_{min}} < L_{Farm} + L_{Tel} + L_{Hum} \quad (4.3)$$

$$P_{Batt} < L_{Farm} + L_{Tel} + L_{Hum} \quad (4.4)$$

Information like as solar PV power output, battery SOC, and total load demand are used to generate the EMS. These variables are controlled and operated in a variety of ways depending on how much power is available to meet the load demand. Based on equations 4.1 to 4.4, decisions are made using the flowchart in Figure 4.2. and a complete model of the off-grid system and the energy management system is shown in Figure 4.3. The overall purpose of the EMS strategy is to ensure effective power distribution between the solar PV and battery system in a way that ensures sufficient power to meet the load demand at all times, regardless of how complex the EMS algorithm is implemented or how to choose the appropriate resource.

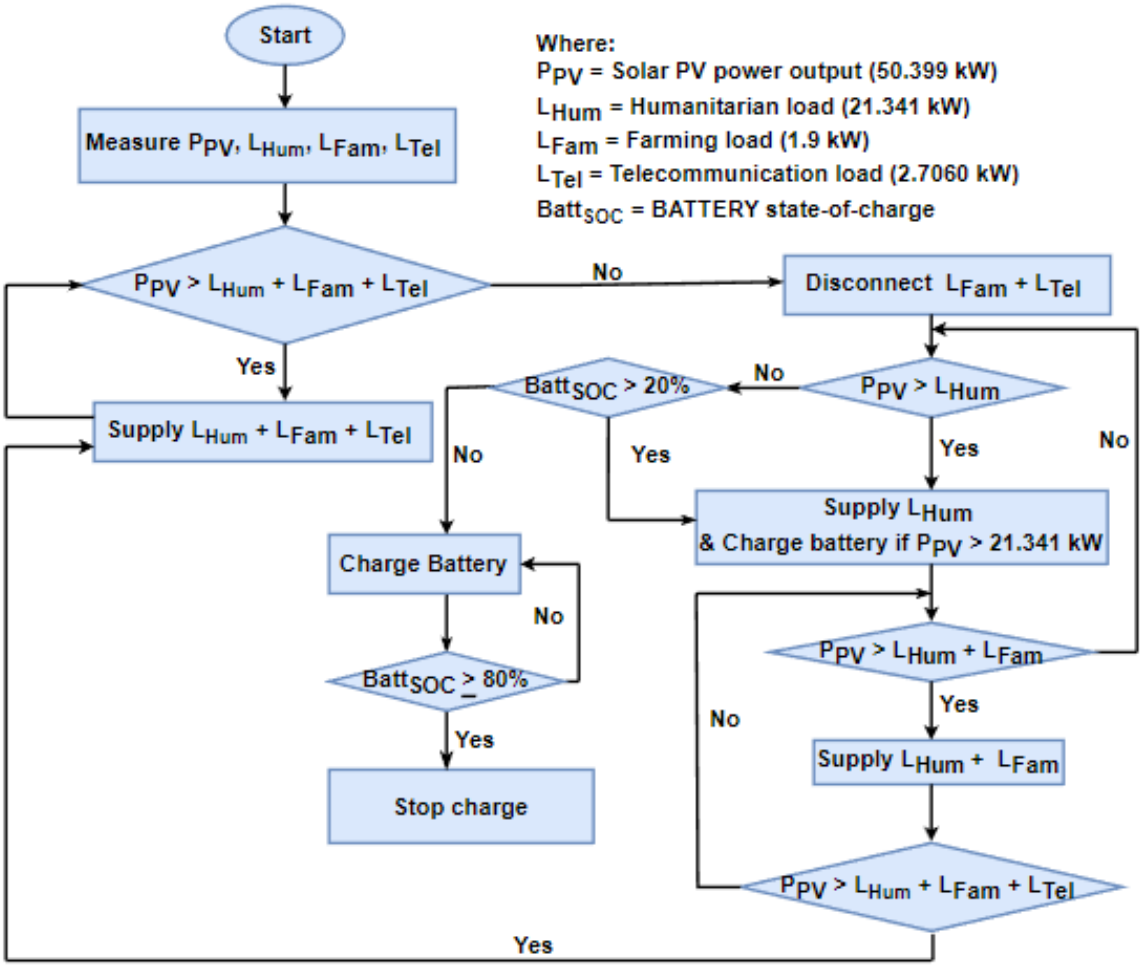

Figure 4.2: System optimization flowchart

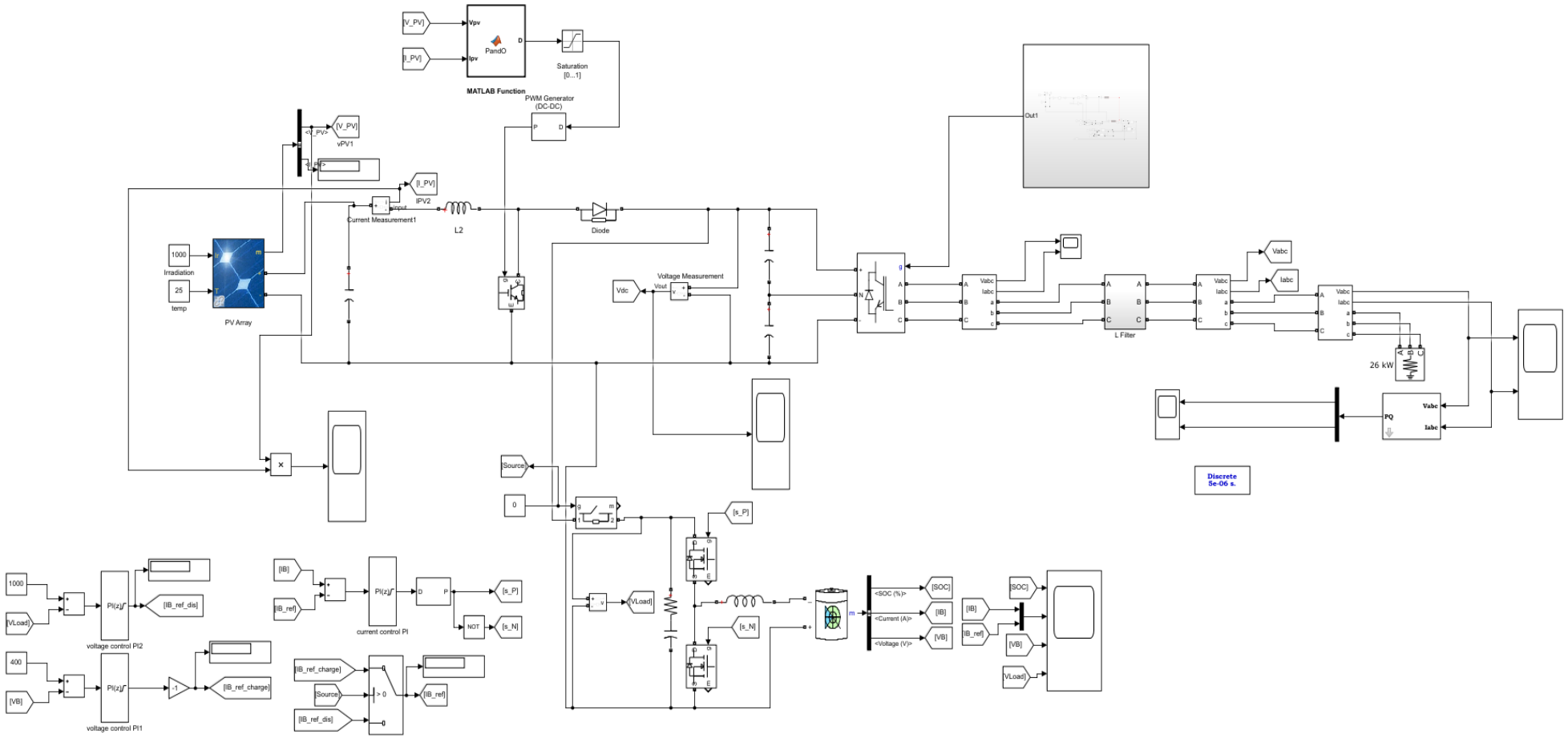

Figure 4.3: MATLAB/Simulink model of the system

4.4 Summary

This chapter presented the energy management system algorithm. The EMS was developed using information such as the solar PV power output, humanitarian facility load, farming facility load, telecommunication base station load and battery SOC. These parameters were systematically selected and controlled to ensure successful implementation of the set objective of efficient power distribution between the solar PV and battery system defined by the total load demand. The chapter also presented a MATLAB/Simulink model of the complete system which includes the solar PV, the DC-DC boost converter, DC-DC bidirectional converter, inverter, control system and the loads.

CHAPTER 5: SIMULATION RESULTS AND DISCUSSION

5.1 Introduction

This chapter presents simulation results of the various components of the off-grid PV system used as a resource in telecommunications, farming and humanitarian aid system with adequate discussions. An off-grid PV system is modelled in the MATLAB/Simulink environment with the primary aim of efficient power distribution and optimisation. This is accomplished using an energy storage system (lithium-ion battery) controlled by the battery SOC, solar PV power output and load demand. The results of the solar PV system simulation are presented in the following sections of this chapter, and section 5.2 discusses the output. Section 5.3 presents the DC-DC boost converter simulation results. To validate the functionality and effectiveness of the boost converter, the voltage before and after the boost converter are properly shown in this section. The simulation results of the battery indicating its SOC, current, voltage and available power is shown in section 5.4. Subsequently, the three different scenarios were presented in section 5.5.

5.2 Solar PV simulation result

The solar PV panel used in this work was modelled and simulated in the MATLAB/Simulink environment using electronic components that are analogous to solar cells, such as resistors, diodes, and current sources as shown in Figures 5.1 and 5.2 respectively.

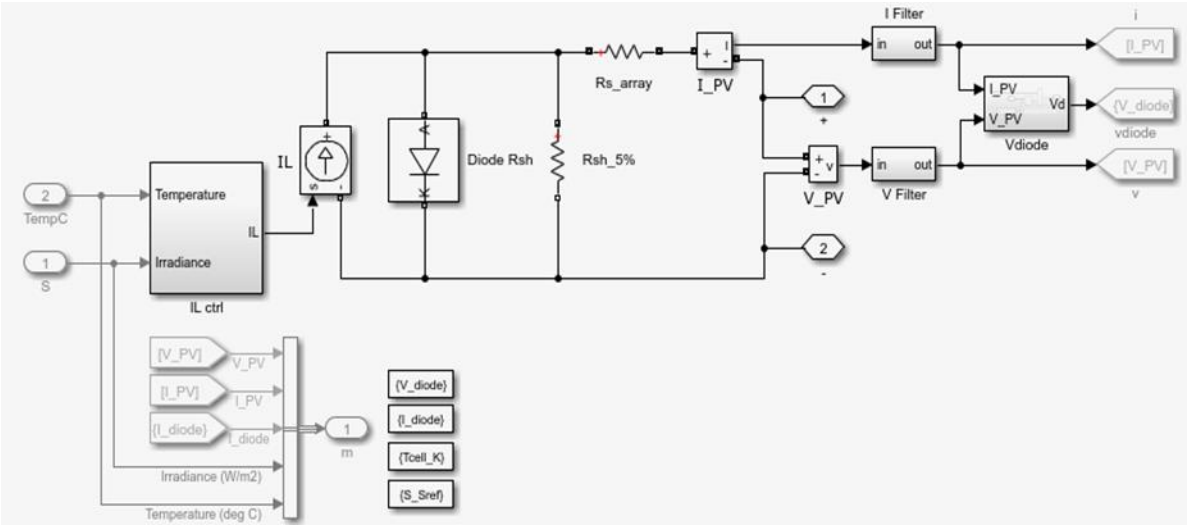

Figure 5.1: A MATLAB/Simulink example of a diode characteristic

Again, as mentioned in the chapters above, the solar cells are connected in series and parallel to create a PV array with a 50 kW total power generating capacity. But, in order to fully

comprehend the effect of temperature on the output power of the solar PV system, the temperature was changed during the simulation from 25°C to 45°C as shown in section 3.2.2.

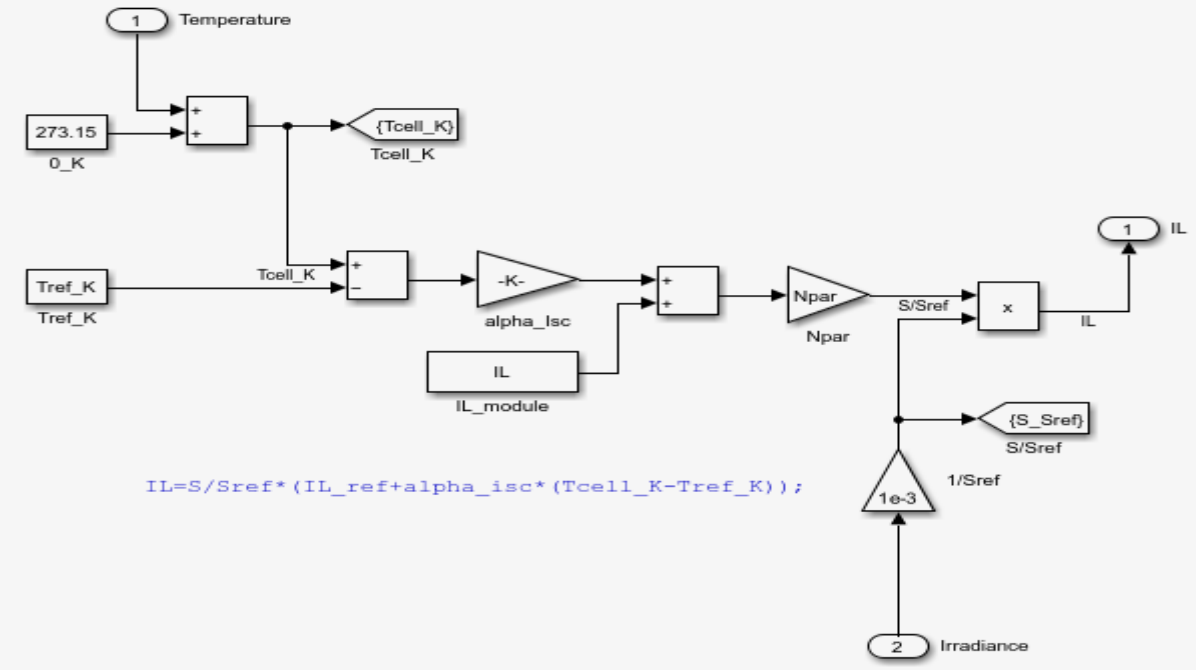

Figure 5.2: Solar cell equivalent circuit in MATLAB/Simulink

The PV system voltage is connected directly to a DC-DC boost converter in order to maintain voltage stability and increase the voltage to the appropriate dc-link voltage. With a duty cycle of 0.6, the PV system's output voltage is stepped up from 303 Vdc to 750 Vdc. Again, in order to control and execute a steady output voltage at 750 Vdc due to the volatility associated with PV system output, the duty cycle is used according to equation 5.1. In order to maintain a constant DC-link voltage, a change in the input voltage determines a change in the duty cycle.

$$D = 1 - \frac{V_{in}}{750} \tag{5.1}$$

Additionally, the chosen and modelled solar PV system was intended to reflect the anticipated output power and voltage. once more, to determine the design efficiency and provide a chance to assess fundamental performance as a result, the solar PV system was modelled with a 50.399 kW power rating, 302.88 Vdc as the output voltage, and 165.082 A as the output current.

The solar PV system output current at a constant solar irradiation of 1000 W/m^2 is shown in Figure 5.3. According to the information in the preceding section, the solar PV system's calculated output current is 165.082 A. However, as shown in Figure 5.3, the simulated value

is 166.082 A, which is 1 A higher than the predicted value because of losses within the system. This simulated outcome shows the accuracy and effectiveness of the model.

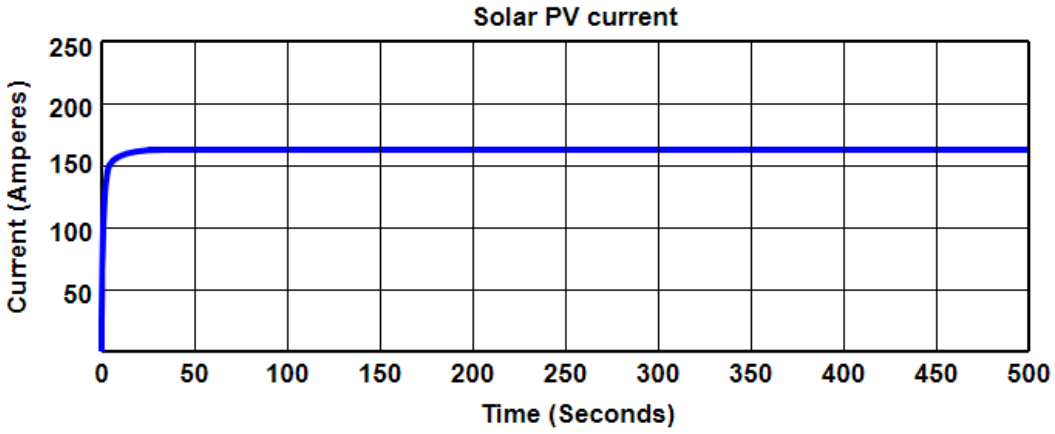

Figure 5.3: Solar PV system output current

The calculated output voltage of the solar PV system is 302.88 Vdc as shown in chapter 3, but the simulated value is 303. 98 Vdc as shown in Figure 5.4. Again, solar PV system output voltage serves as the input to the DC-DC boost converter. Comparing the calculated value with the simulated value indicates a discrepancy of 1.1 Vdc or 0.0036% error between the two. The system's operational losses are the cause of this small value discrepancy, and it is within allowable limit. This result shows a stable output voltage as anticipated but the transient time for the solar PV to reach stability was few microseconds (10 µs) as shown.

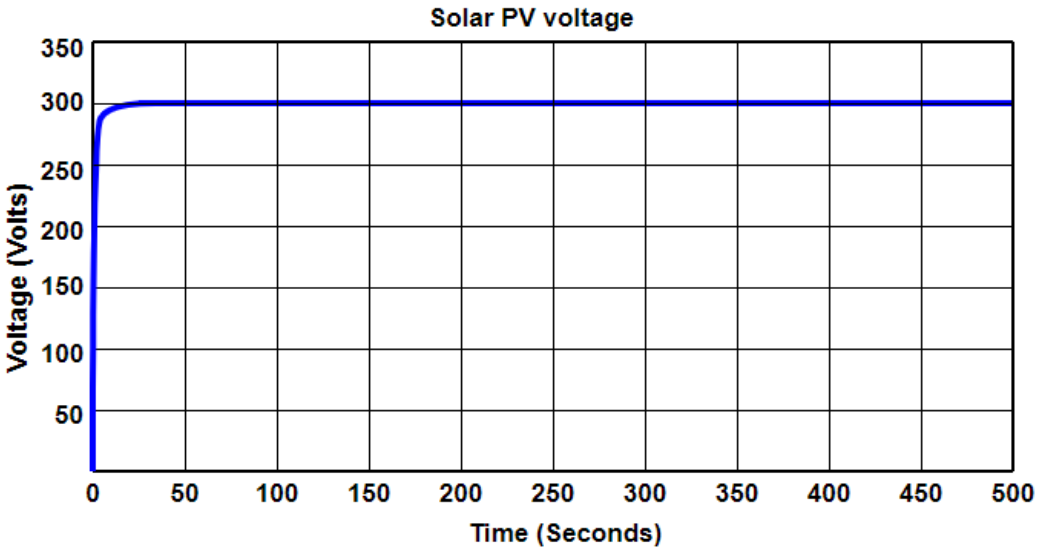

Figure 5.4: Solar PV system output Voltage

Figure 5.5 shows the simulated output power of the solar PV system that is time-dependent. The power generated followed the voltage and current accordingly with adequate reflection of the transient time, but it stabilised after few microseconds (10 µs) throughout the simulation period (500 seconds). In comparison to the calculated value of 50.399 kW, the power generated beginning at the stable state is 50.49 kW. The losses in the system brought on by different system components are responsible for a little variation of 0.18% between the simulated and calculated values. This variation, meanwhile, is minuscule and within the acceptable bounds of such a design. When producing at its highest level, this is the output power that is connected to the DC-DC boost converter.

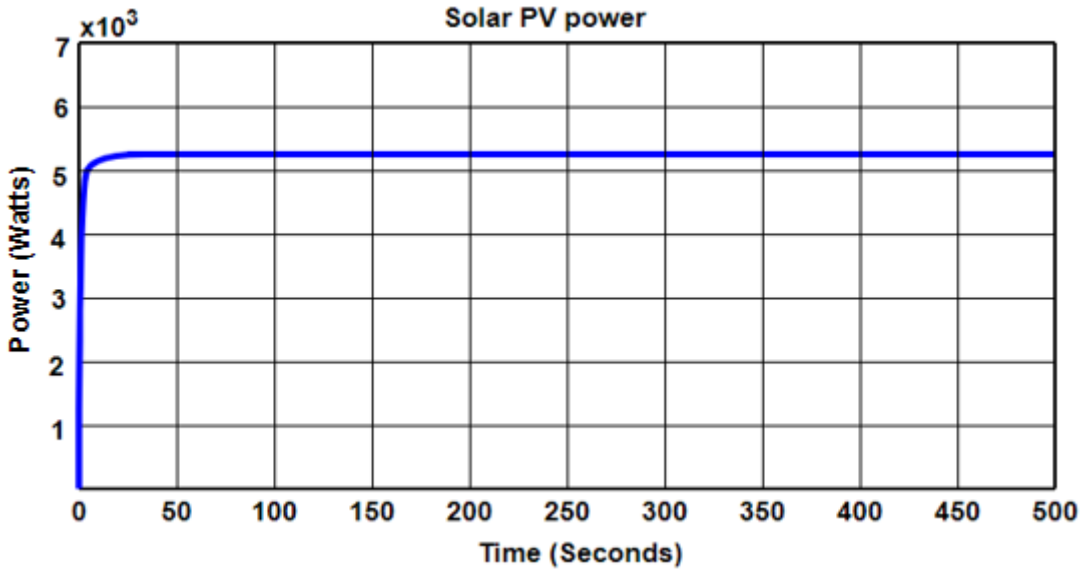

Figure 5.5: Solar PV system power output

However, using an analogous duty cycle of the boost converter, the PV voltage is increased to the necessary voltage of 750 Vdc as demonstrated in the prior section. As illustrated in Figure 5.6, the duty cycle was initially unstable during the input voltage's transient period but stabilized around 0.60.

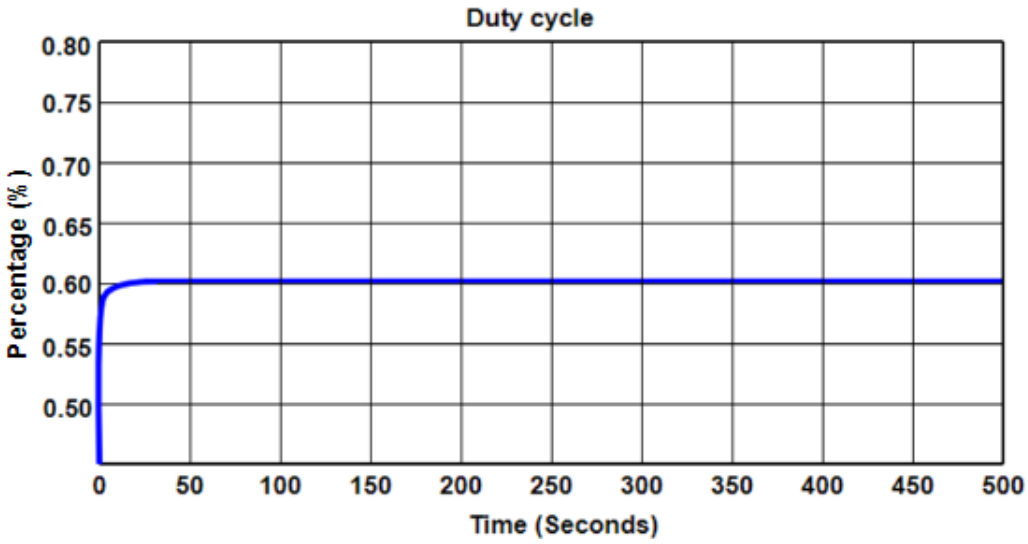

Figure 5.6: Solar PV system original variation duty cycle

The solar PV system temperature and solar irradiance expressed in degrees Celsius and watt/meter square respectively is presented in Figure 5.7. Furthermore, the power output of the solar PV system will increase with an increase in solar irradiation, it will decrease with an increase in temperature. Hence, when designing and modelling PV systems, this relationship is extremely important considering the geographical location of the system.

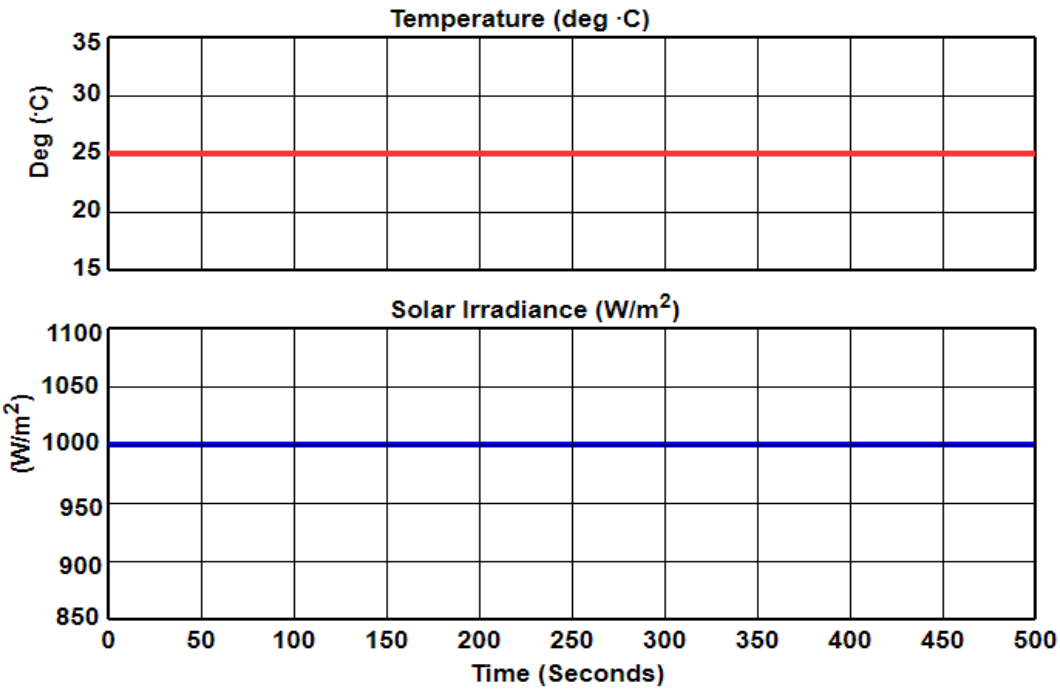

Figure 5.7: Solar irradiance and temperature

5.3 DC-DC boost converter simulation result

Figure 5.8 shows the DC-DC boost converter output voltage in relation to the simulation time, while Figure 5.4 displays the value of the voltage before the boost converter. Over the course of the simulation, the output voltage stays constant at 750 Vdc. The simulated boost voltage matches the calculated boost voltage found in chapter 3 despite the design's 1% standard deviation allowance. This demonstrates the output voltage just after the DC-DC boost converter, which is precise, dependable, and stable.

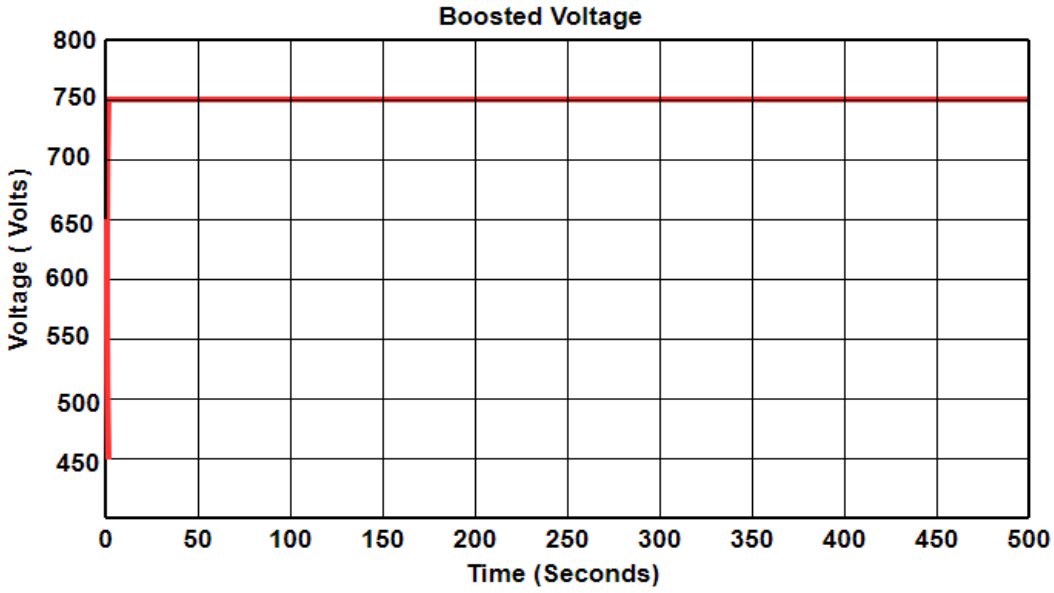

Figure 5.8: Boost converter Output voltage

5.4 Inverter simulation results

Using the procedure described in chapter three, an inverter was utilized to convert the DC to AC in order to achieve the AC component. As illustrated in Figure 5.9, the inverter output voltage waveforms are displayed and labelled as V_{abc}, where V_a is represented by the blue waveform, V_b by the green waveform, and V_c by the red waveform, respectively.

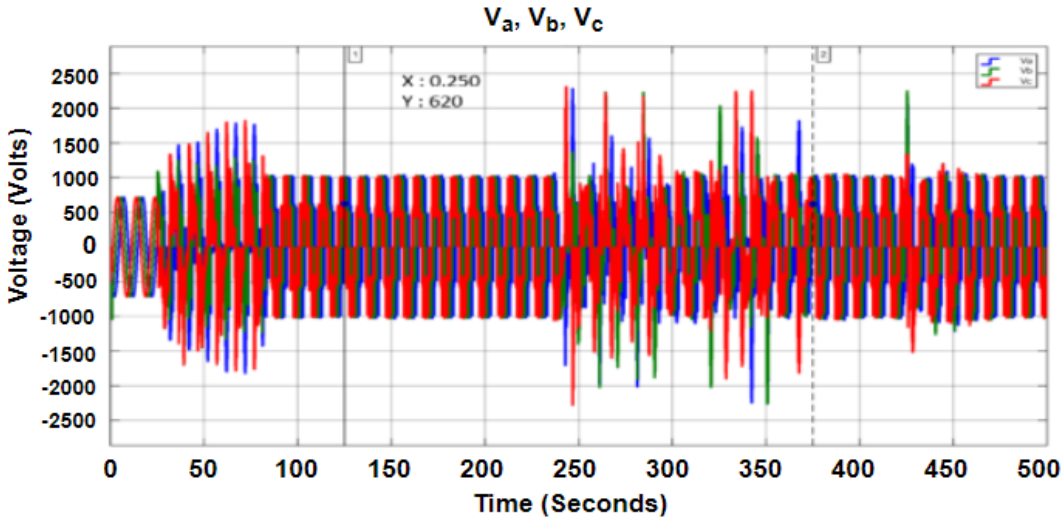

Figure 5.9: The output voltage of the inverter before the LC-filter

In Figure 5.9, the output phase voltages at the inverter output terminal are measured right before the LC filter. These voltages showed that lower and higher harmonic components were present in the output voltage waveforms. However, the harmonic content was caused by the inverter switching result of the inverter switches. Each of these voltages swings between 0 and 620 volts and is known to be 120 degrees out of phase with the other. The switching phase is further illustrated by utilizing just the V_a as shown in Figure 5.10.

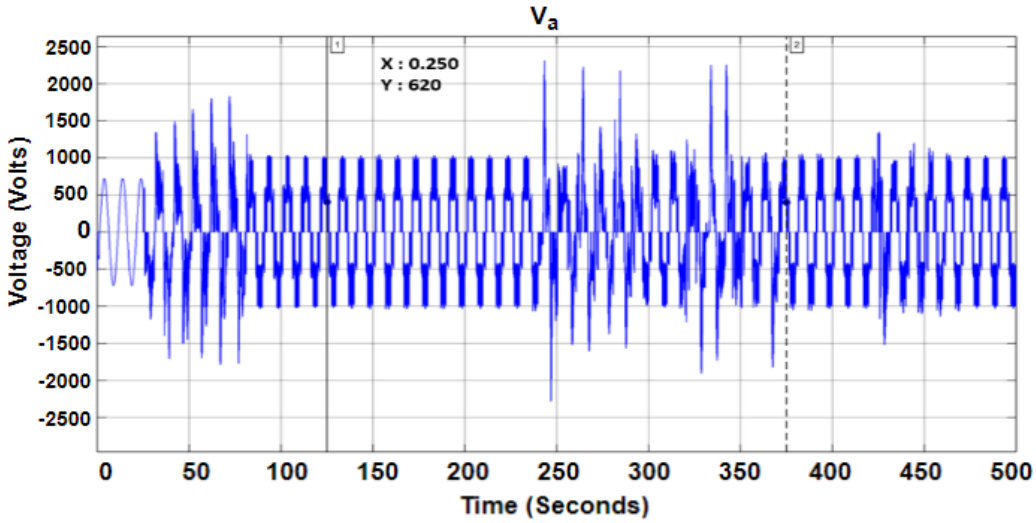

Figure 5.10: V_a phase before the filter to show the switching transition

In Figure 5.10, the inverter voltage for phase a alone is shown, clearly displaying the switching transition duration. It can be seen that the switching effect of the inverter caused a voltage spike (V_a) between 50 and 75 seconds. Additionally, the voltage reverted to its original level of 620 V. This voltage has some ripples as shown, but the LC filter was able to eliminate such

during simulation. Furthermore, the higher order harmonic components that are intended to introduce ripples on the output voltage have been reduced and eliminated by the LC filter following the inverter and the only lower-order harmonics that are left are fundamental and basic in nature. Figure 5.10 shows the line-to-line output voltage waveforms Vab as 620 Vac, while Figure 5.11 shows the line-to-line rms voltage as 484 V at the same nominal frequency of 50 Hz.

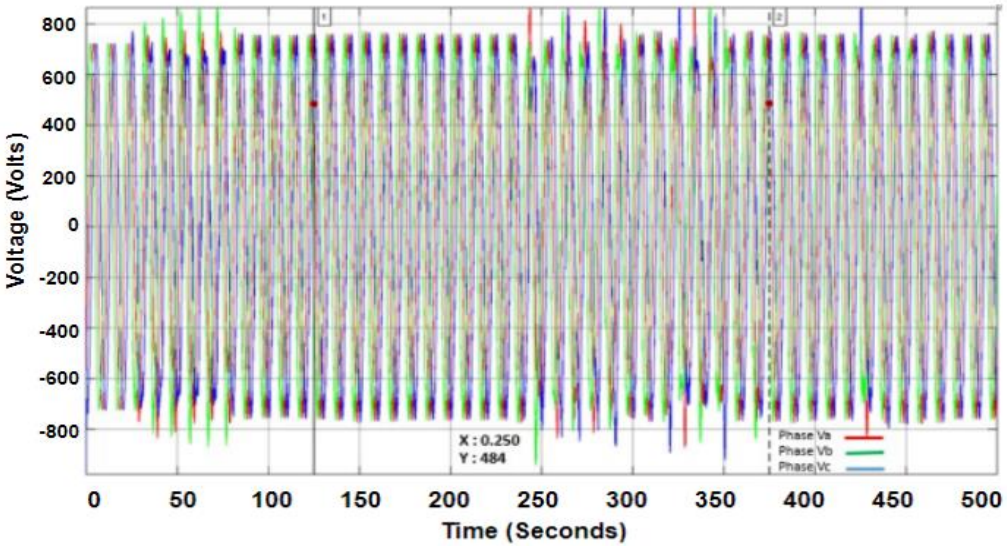

Figure 5.11: Three-phase inverter filtered output voltage

Again, the amplitude modulation index (ma) and inverter input voltage values match the expected values of the output voltage as shown in Figure 5.12. Each phase has a voltage range of 0 to +/620 V, and each phase is 120 degrees out of phase with the others. Figure 5.12 shows the switching transition for only phase a (V_a).

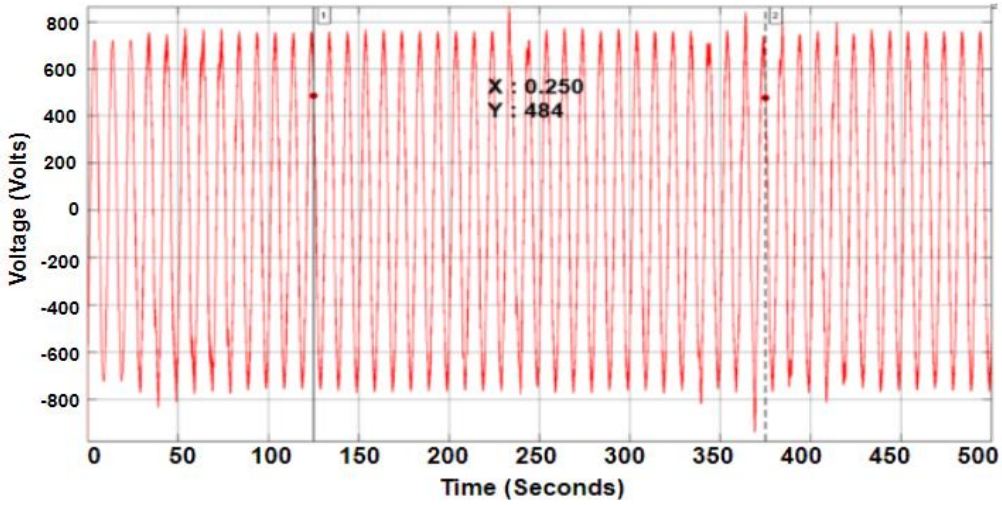

Figure 5.12: Filtered Output voltage after the filter for only phase a

5.5 Off-grid system simulation results

This study uses simulation results to validate the controller performance on the off-grid system in the MATLAB/Simulink environment. Three scenarios are conducted to show how the off-grid system can be operated and controlled effectively based on the amount of solar PV power output, solar irradiance, battery SOC and load demands. These are utilized to validate (assess) the entire off-grid system, as well as the lithium-ion battery system's ability to supply load demand and maintain network stability. The use of scenarios also offers a tried-and-true technique and approach, promotes comprehension while keeping the primary goal in mind, and offers useful suggestions. Hence, Table 5.1 describes the different scenarios and operating modes within established operational constraints.

Table 5.1: Description, scenario and conditions

Description	L_{Hum}	L_{Fam}	L_{Tel}	Battery
Scenario 1 ($P_{PV} > L_{Hum} + L_{Fam} + L_{Tel}$)				
The total power generated by the solar PV is more than the total load demand (L_{Hum} + L_{Fam} + L_{Tel}) hence, the excess power is used to charge the battery because its SOC is less than 80%	ON	ON	ON	Charge
Scenario 2 ($P_{PV} = L_{Hum} + L_{Fam} + L_{Tel}$)				
The total power generated is equal to the total load demand. The battery is disconnected during this period because it is fully charged but supplying L_{Hum}, L_{Fam}, $L_{Tel.}$ Hence, the battery is on standby mode.	ON	ON	ON	OFF
Scenario 3 ($P_{PV} < L_{Hum} + L_{Fam} + L_{Tel}$)				
The battery in discharge mode because the solar PV power output is less than the total load demand and battery SOC > 20%. L_{Tel} is disconnected since the solar PV power output and battery power output can only supply L_{Hum} + L_{Fam}.	ON	ON	OFF	Discharge

5.5.1 Scenario 1 ($P_{PV} > L_{Hum} + L_{Fam} + L_{Tel}$)

When the amount of power produced by the solar PV is greater than the total load (humanitarian aid facility (L_{Hum}), load to the farming facility (L_{Fam}) and load to the telecommunication base station (L_{Tel})) and the battery SOC is less than 80%. Hence, the excess power generated by the solar PV is used to charge the battery which is a fundamental and necessary requirement for effective operation of the off-grid system. The current through the humanitarian aid facility is 44.093 A at 125 seconds and 44.095 A at 375.5 seconds, respectively, as shown in Figure 5.13. The voltage across the humanitarian aid facility and power during scenario 1 are shown in Figures 5.14 and 5.15 respectively as 484 V and 21.34 kW respectively. Due to losses in the system, the total power decreased from 50 kW to 45.8 kW, although it was still within a tolerable range.

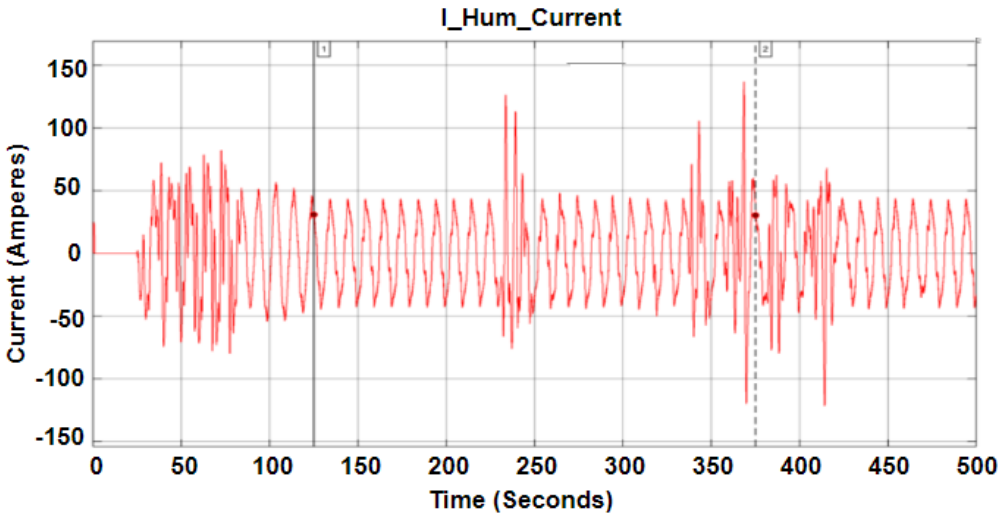

Figure 5.13: Current flowing through the humanitarian aid facility

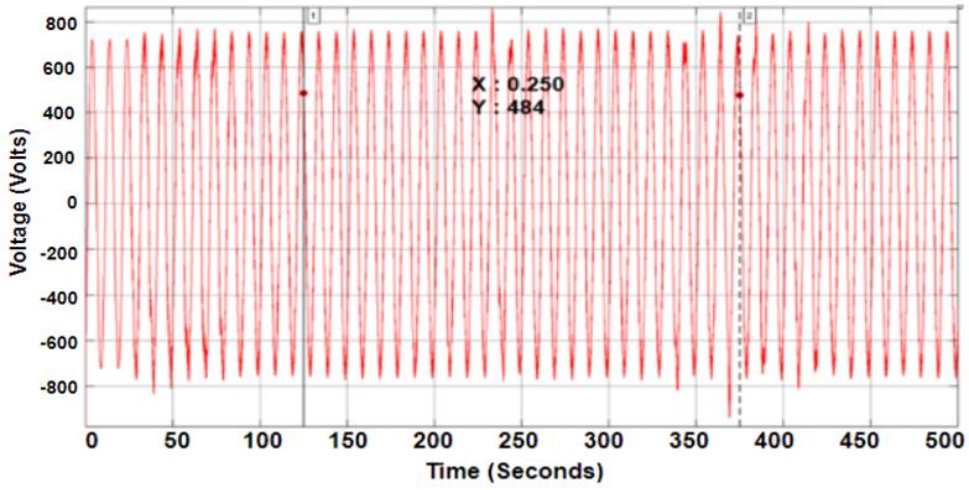

Figure 5.14: Voltage across the humanitarian aid facility

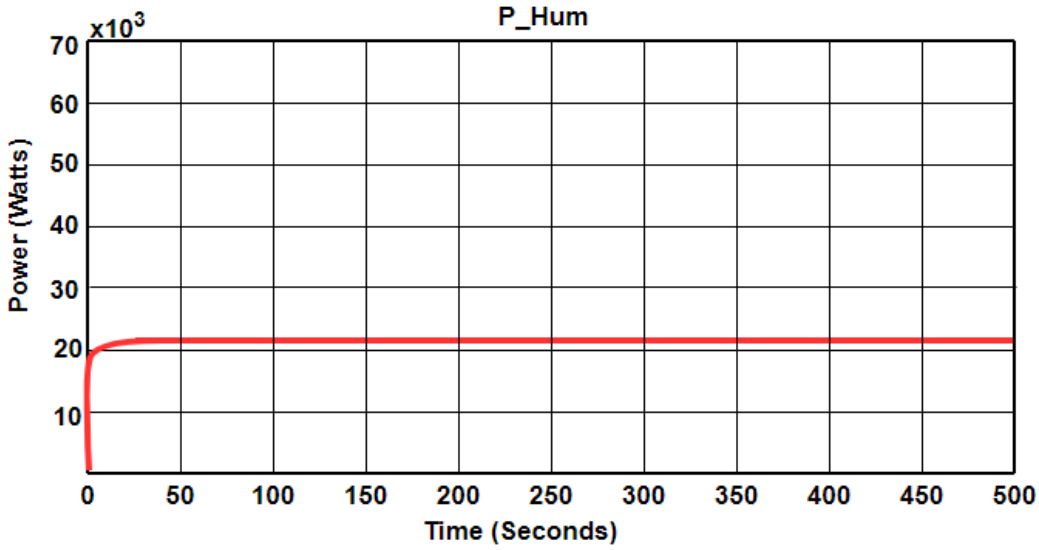

Figure 5.15: Power supply to the humanitarian aid facility

Furthermore, the current through the farming facility is 3.926 A at 125 seconds and 4.1 A at 375.5 seconds respectively as shown in Figure 5.16 (a) while the power supply is 1.9 kW as shown in Figure 5.16 (b). However, the same voltage seats across all three loads because they are connected in parallel. Hence, only the current and power supply to the facility is presented.

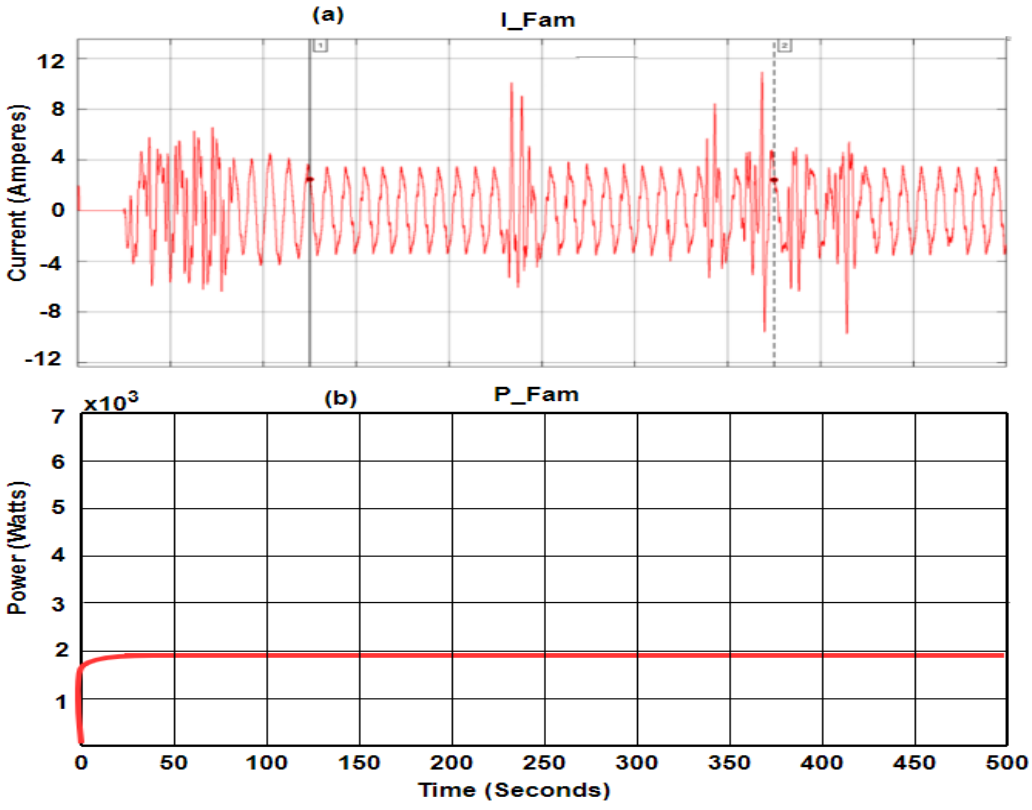

Figure 5.16: Farming facility (a) Current (b) Power

Again, the current through the telecommunication base station is 5.591 A and the power supply is 2.706 kW as shown in Figure 5.17 (a) and (b) respectively. However, the same voltage seats across all three loads because they are connected in parallel. Hence, only the current and power supply to the facility is presented.

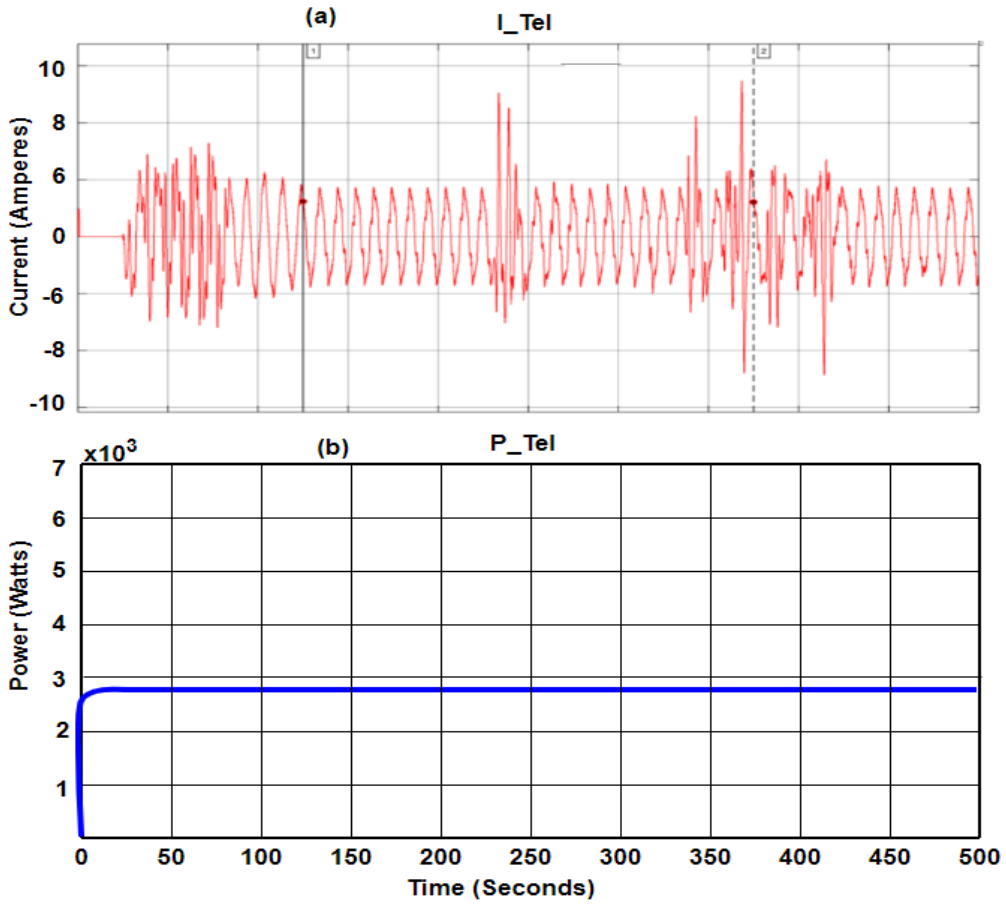

Figure 5.17: Telecommunication base station (a) Current (b) Power

Under constant irradiance of 1000W/m^2, the total power generated by the solar PV system is 45.9 kW which is greater than the total load demand. Hence, the excess power generated is then used to charge the lithium-ion battery. This is shown in Figure 5.18 where the battery SOC increased from 50% which is considered as the initial state of charge to 50.4% within few seconds. The battery charging experienced a spike at the initial stage due to exponential power but slowed down after 25 seconds. This is an indication that that the excess power is used in charging the battery as expected for later use.

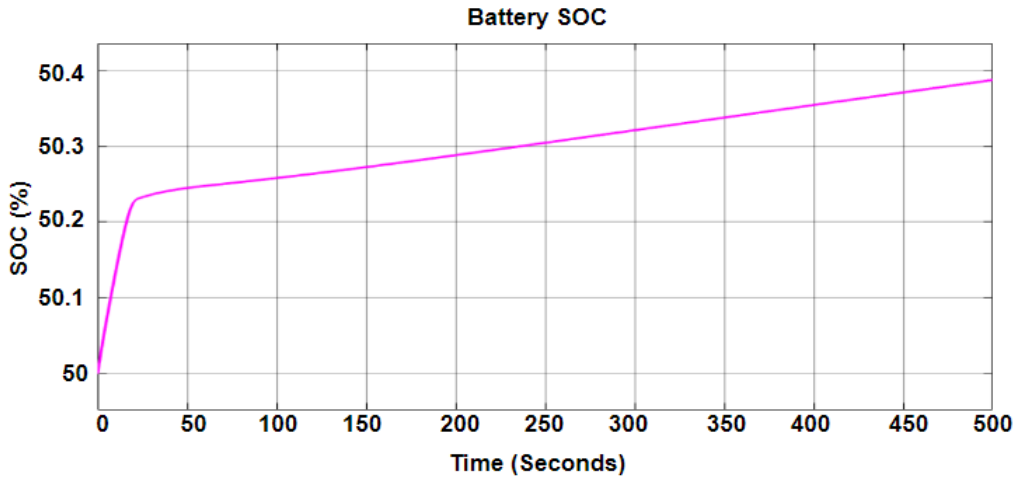

Figure 5.18: Battery charging (SOC increasing)

5.5.2 Scenario 2 ($P_{PV} = L_{Hum} + L_{Fam} + L_{Tel}$)

If the battery SOC is greater than or equal to 80% and the solar PV power output is greater than the humanitarian facility loads demand (L_{Hum}) which is the highest load demand in the system, then supply all three loads ($L_{Hum} + L_{Fam} + L_{Tel}$). Because the battery SOC has reached the maximum permissible level in this instance, it is disconnected, and the excess power produced by the solar PV is used to power the farming facility and the telecommunication base station loads.

Figure 5.19 shows the current flowing through humanitarian facility under scenario 2. Throughout the simulation's 500 seconds running time, the current stays at 44.1 A. Figure 5.20 also shows the power input to humanitarian facility under scenario 2. The result showed that losses in the system caused a power reduction from 21.34 kW to 20.5 kW.

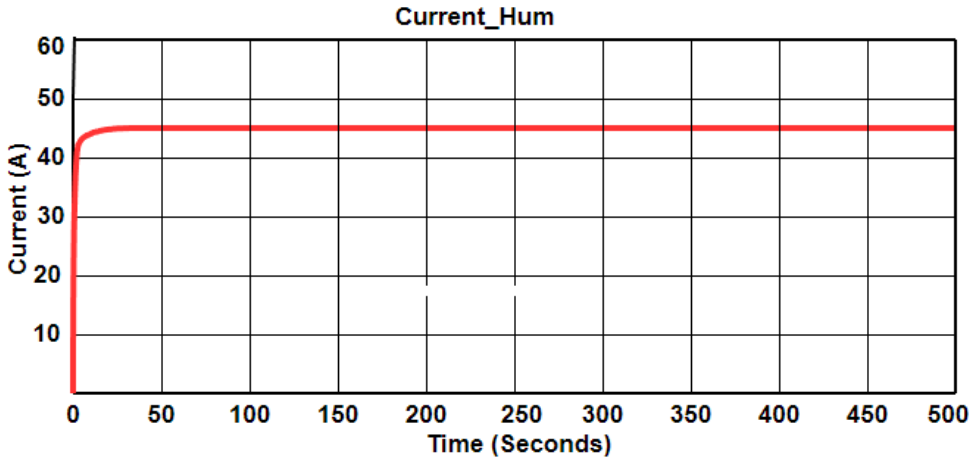

Figure 5.19: Current flowing through the humanitarian facility ($I_{\_Hum}$)

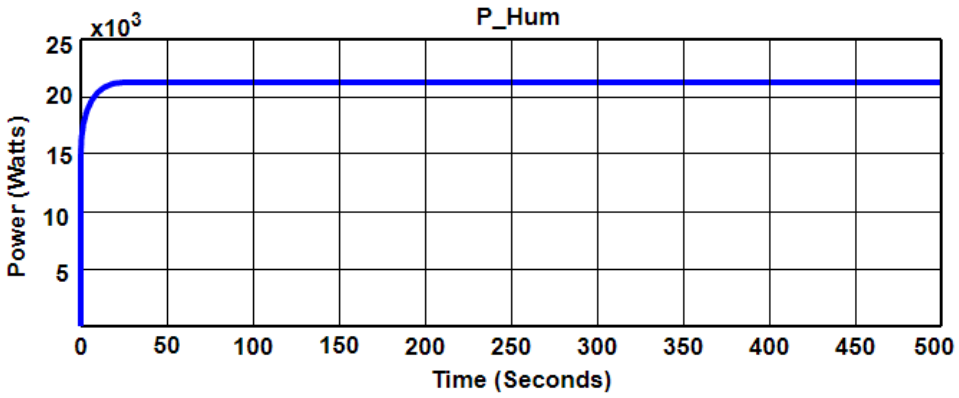

Figure 5.20: Input power to humanitarian facility (L_{Hum})

In scenario 2, the current flowing through the farming community facility is shown in Figure 5.21. The current is kept constant at 3.926 A throughout the simulation time of 500 seconds. The power consumed by the farming community facility under scenario 2 is likewise shown in Figure 5.22. The result showed a drop in the power supply from 1.9 kW to 1.85 kW. This drop in the power supply is caused by the power conversion process implemented by power converters and other factors within the system.

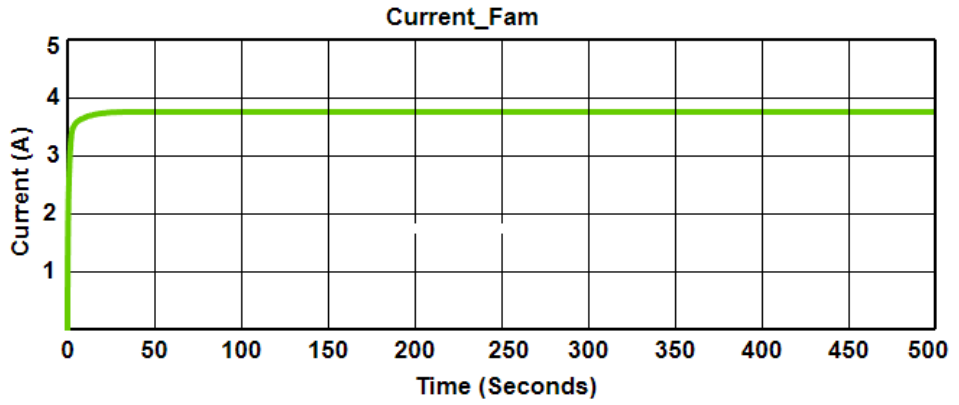

Figure 5.21: Current flowing through the farming community facility ($I_{\_Fam}$)

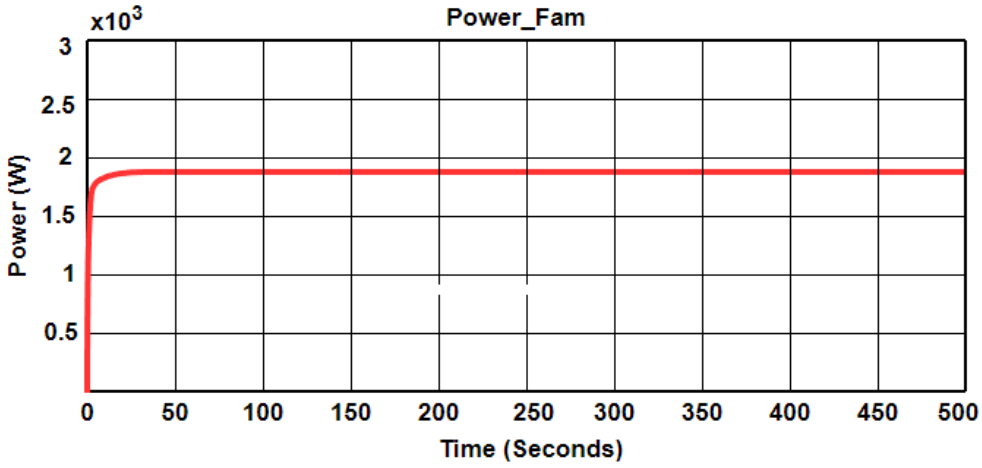

Figure 5.22: Input power to farming community facility (L_{Fam})

The current flowing through the telecommunication base station under scenario 2 is shown in Figure 5.23. The current is maintained at 5.54 A to validate a steady power supply throughout the simulation time of 500 seconds. Again, the power consumed by the telecommunication base station under scenario 2 is shown in Figure 5.24. The result showed a drop in the power supply from 2.706 kW to 2.7 kW. Where, the drop in the power supply is attributed to the power conversion process in the system.

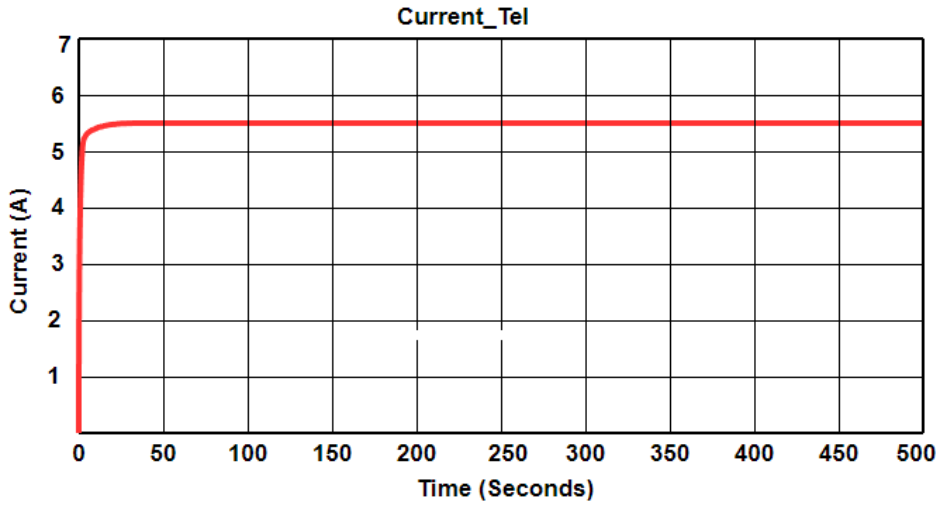

Figure 5.23: Current flowing through the telecommunication base station ($I_{\_Tel}$)

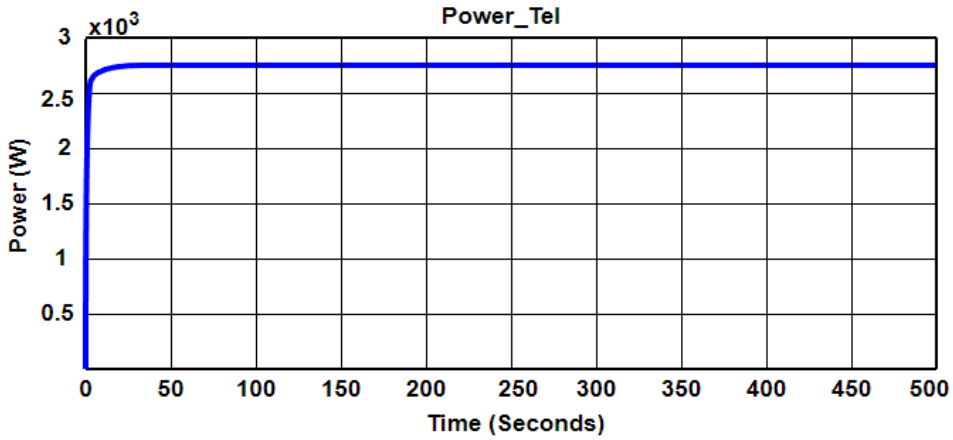

Figure 5.24: Input power to telecommunication base station (L_{Tel})

Furthermore, under scenario 2, the battery SOC is greater than or equal to 80% and the solar PV power output is equal to the total load demand (L_{Hum} + L_{Fam} + L_{Tel}). The battery is disconnected from the system because it has reached the maximum allowable charging. The battery SOC showing its SOC is shown in Figure 2.25. The increase in the battery SOC from 80% to 80.4% is an indication of battery charging which is not necessarily due to the design objective of setting 80% as fully charged hence, it was disconnected.

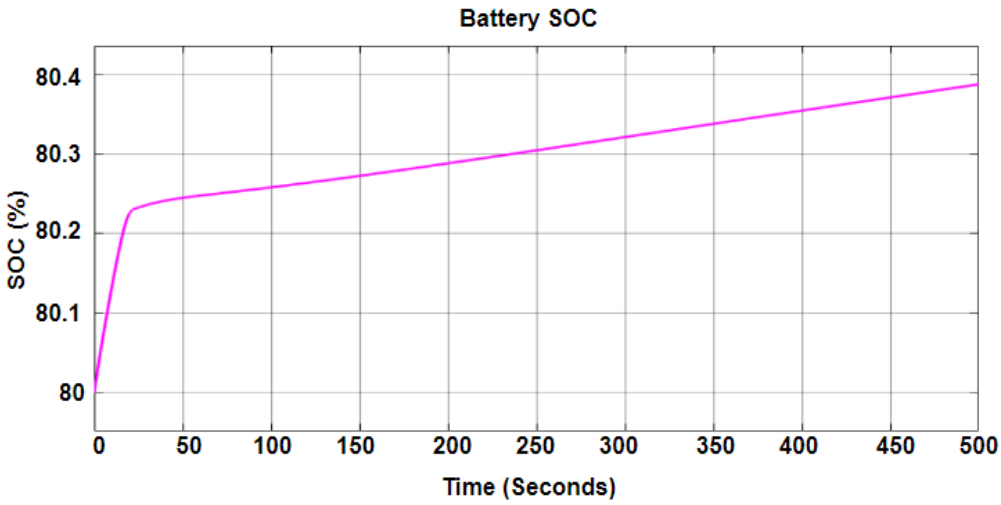

Figure 5.25: Battery SOC under scenario 2

5.5.3 Scenario 3 ($P_{PV} < L_{Hum} + L_{Fam} + L_{Tel}$)

The solar PV power output is less than the humanitarian facility load demand and the battery SOC is greater than or equal to 20%, then discharge the power stored in the battery to supply the humanitarian facility. This means that the battery is on discharge mode. During this period, the telecommunication base station and the farming community facilities are disconnected because the total power generated by the solar PV is less than the humanitarian facility load

demand. Therefore, the humanitarian facility load demand is supplied from a combination of power from both the solar PV and battery at an irradiance of 1000 W/m^2 and temperature of 25 ℃ as shown in figure 5.26.

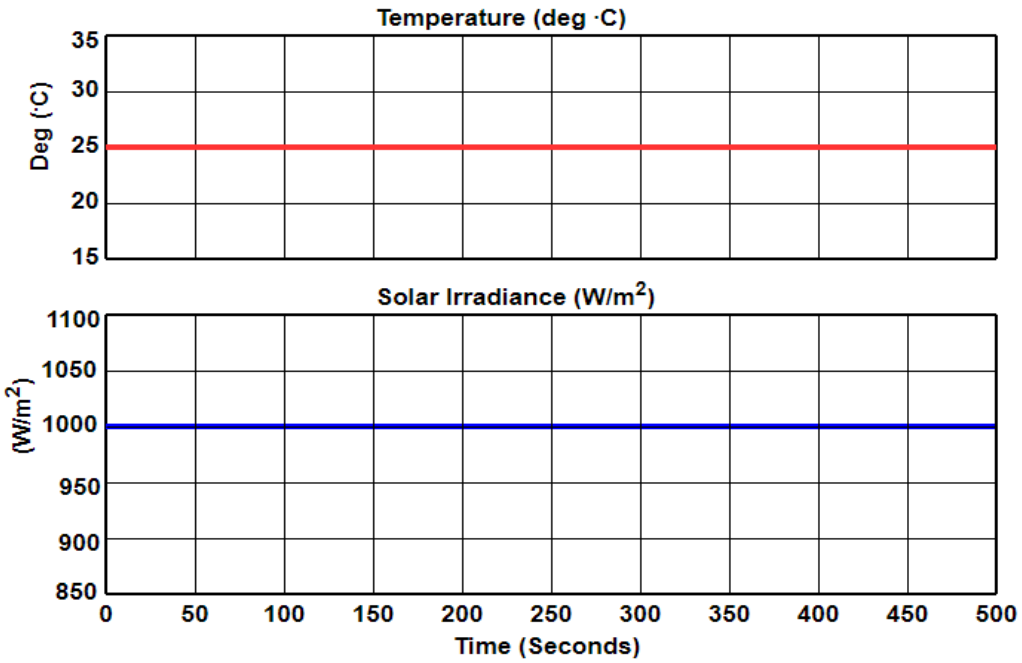

Figure 5.26: Solar PV parameters for scenario 3

Figures 5.27 and 5.28 shows the DC link voltage and current reflecting the amount of power available in scenario 3. Because the power generated by the solar PV is less than the total load demand, the product of these figures represents the total power generated by both the solar PV and the battery in discharge mode.

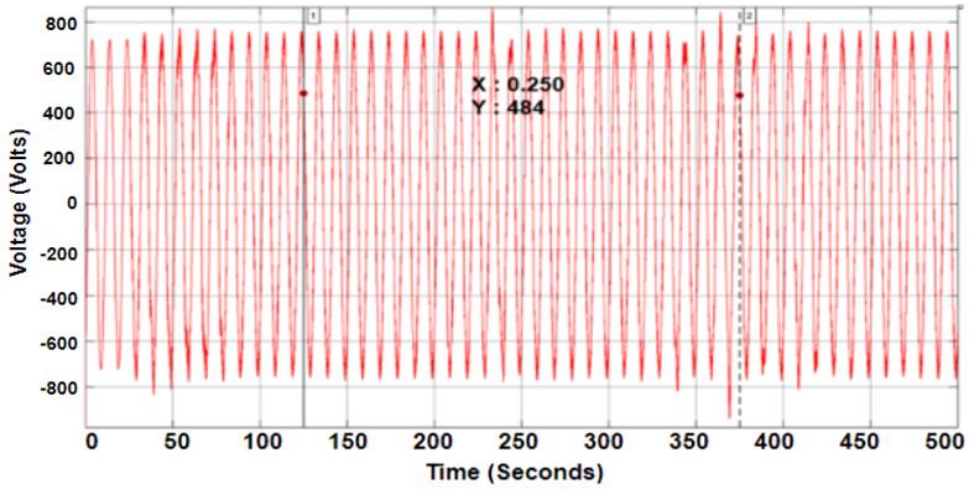

Figure 5.27: Filtered output voltage

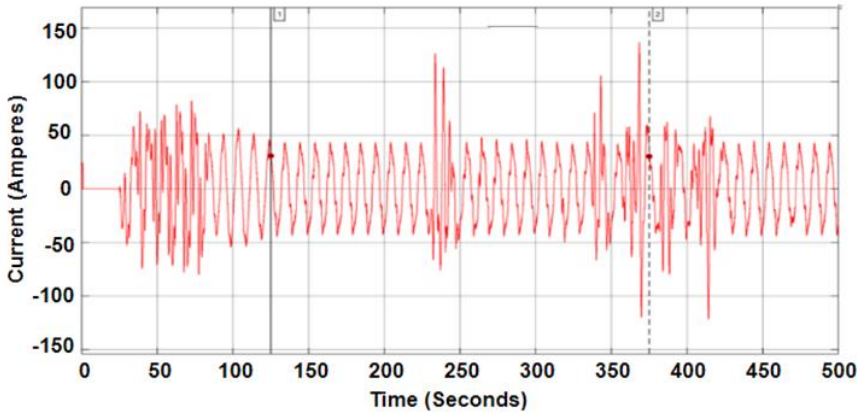

Figure 5.28: Input current into the system

Approximately, a current 44 A flows through the humanitarian aid facility under scenario 3 as shown in Figure 5.29. This indicates that the humanitarian aid facility (primary load) is supplied. In addition, a total power of 21.2 kW is available to humanitarian aid facility as shown in Figure 5.30. This shows an adequate power supply to humanitarian aid facility which is a combination of both power supply from the solar PV and battery storage system.

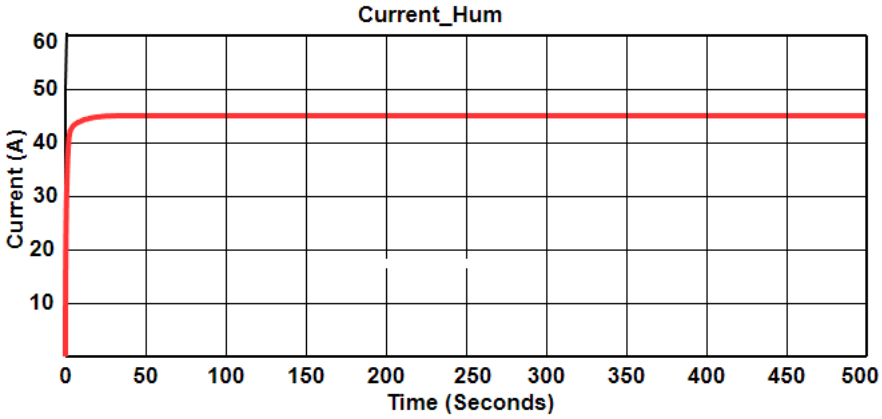

Figure 5.29: Current through humanitarian aid facility under scenario 3

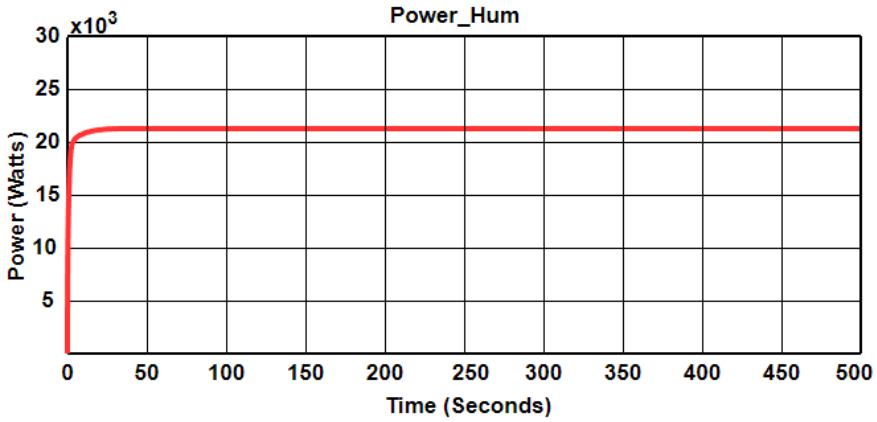

Figure 5.30: Power supply to humanitarian aid facility under scenario 3

Furthermore, the current flowing through the farming facility and telecommunication base station including the available power are both negatives as shown in Figure 5.31 and 5.32 respectively because the available power was only sufficient for the humanitarian aid facility (primary load). Again, this is due to the fact that the farming facility and the telecommunication base station (secondary loads) are disconnected because the power available is not sufficient to supply all three loads in the system.

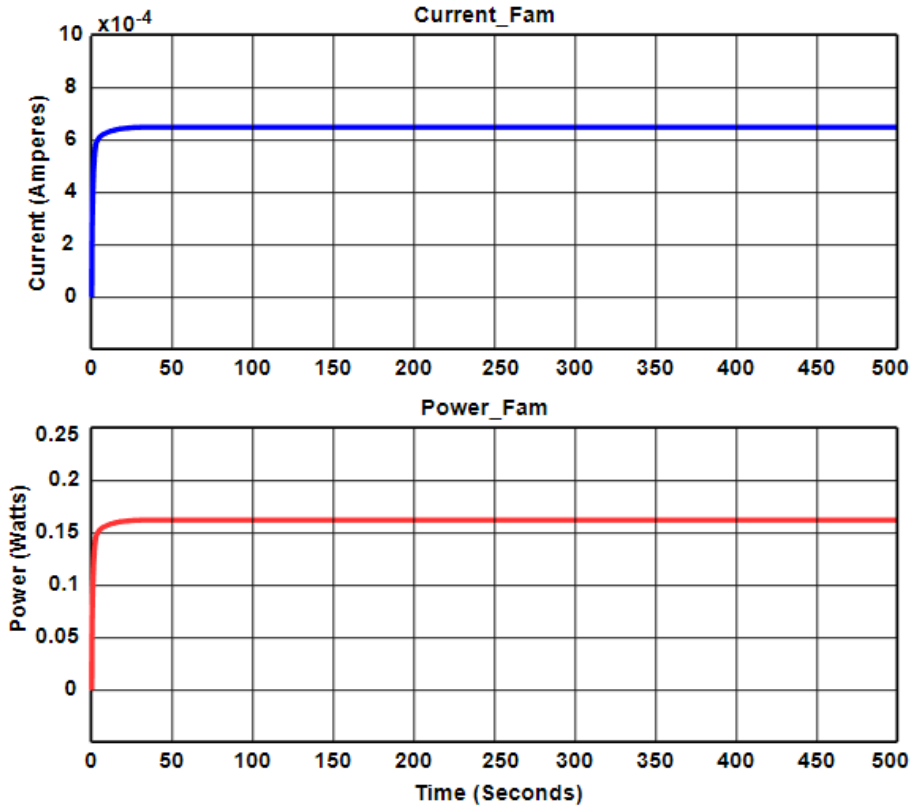

Figure 5.31: Current and power input to the farming facility

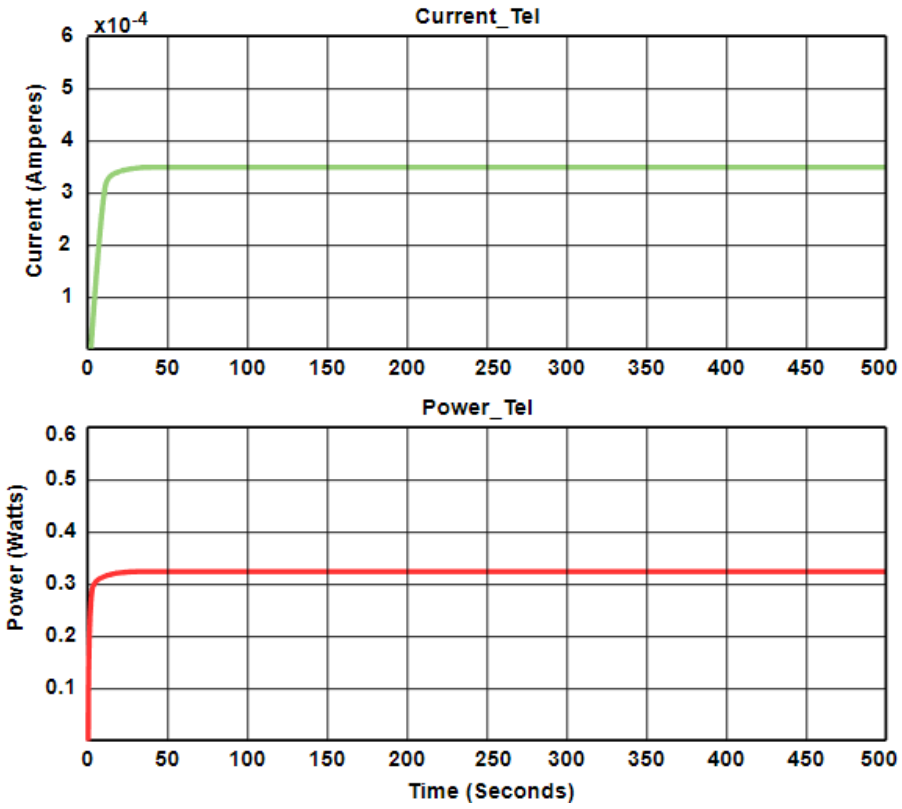

Figure 5.32: Current and power input to the telecommunication base station

5.6 Summary

This chapter presented the simulation results obtained for the off-grid Solar PV system. The model was developed to ensure effective energy management of a Solar PV and lithium-ion battery storage system in an off-grid mode. This was developed in the MATLAB/Simulink environment using PI control system and the simulation results are presented appropriately. The simulation result of the solar PV system was presented in section 5.2 and DC-DC boost converter result was presented in section 5.3, where the voltage before and after the boost converter were presented. Thereafter, the simulation results showing the inverter voltage and current and available power were presented in section 5.4. Furthermore, section 5.5 presented the simulation results of the three scenarios. In scenario 1, the power output from the solar PV is greater than the total load demand and the battery SOC is less than 80% (recharge mode). In scenario 2, the solar PV power output is equal to the total load demand and the battery SOC is greater than or equal to 80%. In scenario 3, the solar PV power output is less than the humanitarian facility load demand (primary load) and the battery SOC is greater than or equal to 20% (discharge mode). Energy management system (EMS) in this study is very crucial to ensure effective power distribution due to the intermittent nature of the renewable energy source (solar PV). Again, the primary aim of the EMS in this study is to maintain efficient power

distribution between the solar PV and the battery system with the aim to optimise both sources by reducing the electrical stress exerted on both sources and other components.

CHAPTER 6: CONCLUSION AND RECOMMENDATION

6.1 Conclusion

The primary aim of this research was to design and model an off-grid solar PV system with lithium-ion battery that is robust and cost efficient for Van Wykslvei farm in the Northern Cape, telecommunication base station and humanitarian facility. This was effectively implemented in the MATLAB/Simulink environment using PI controller. The system is designed for an off-grid application with voltage and power control functionalities. It consists of three main components namely: solar PV system that serves as the primary power supply, lithium-ion battery that serves as the energy storage system and variable loads executed in the MATLAB/Simulink environment. Variable loads were used to analyse the performance over a range of time scales. The load is broadly divided into two categories: the primary load (humanitarian aid facility) and the secondary load (farming facility and telecommunication base station), where the operation depends on the battery SOC and the amount of power produced by the solar PV. A PI controller and switches were used to provide a bi-directional communication between the load, solar PV, and battery storage systems. This ensures efficient power distribution in the system, which is based on the power supply and load demand at any given time. The load was properly supplied utilizing both sources at various periods to demonstrate the effectiveness of the controller.

The second and third objectives were to give a thorough analysis of the literature on standalone Solar PV systems and develop a load profile for a farming community in the MATLAB/Simulink environment using PI controller. According to the literature, PI controllers are suitable for power distribution and control applications in off-grid solar PV systems. Although other methods were investigated, power regulation with PI controllers gave a distinct benefit and flexibility. PI controllers are simple to set up, may be employed in a range of operating scenarios, and can be applied to both small and big non-linear power systems. Additionally, when parameter values are altered, they have no impact. Due to its robustness and simplicity, ability to handle a variety of input variables, and ability to make a precise decision with the aid of a precise function, PI controller is a fantastic answer to challenging issues. It is a synthetic decision-making tool that works in a real-time closed-loop environment.

The modelling of a solar PV and lithium-ion battery system using MATLAB/Simulink software was the fourth objective of this study. The solar PV and battery systems were rigorously simulated in the MATLAB/Simulink environment to achieve this. The principal renewable energy source in the network was accurately calculated and simulated as a solar PV with a power rating of 50 kW. This includes calculating the number of solar PV modules to be

connected in parallel and series in order to produce the desired power rating which were all properly specified. Furthermore, the components in the system such as PV array, inverter and charge controller were all sized properly to meet the system requirement.

The fifth objective was to use PI controllers in the MATLAB/Simulink environment to simulate a control system that could balance the erratic solar power supply and the constantly shifting load demand. By making sure that the load is distributed equally between the solar PV and the energy storage system (lithium-ion battery) based on the demand and availability of power, this objective was accomplished successfully. Using the battery SOC, solar PV power output, and load demand, the MATLAB/Simulink results showed that the power was effectively distributed and the load was properly supplied at all times. When the load on the system was greater than the solar PV output power, the battery responded quickly by discharging energy to meet the load demand. Furthermore, the amount of power available at any given instant was compared against the load demand in order to demonstrate the achievement of this objective. According to the results, the amount of power generated matched the load demand, and any extra power was used to charge the battery. To further guarantee its ability to supply the needed power, this was compared with available literature. The battery SOC was less than 20% and the solar PV generated 50 kW, which is more than the primary load.

The last objective was to use MATLAB/Simulink to model fluctuating solar irradiances that would simulate the unbalanced power supply from solar PV, including a system that would adopt a load-shedding method when the power produced was less than the power required. Three scenarios were explored to accomplish this goal and determine the effectiveness of the controller as well as effective power distribution of the system. This includes to provide results, conclusion and recommendation on the use of solar PV in telecommunication, farming and humanitarian aid facilities.

In the first scenario, the total power produced by the solar PV system exceeded the total load demand (humanitarian aid facility, farming facility and telecommunication base station) and the battery SOC was less than 80%. The total load demand was 25.947 kW while the solar PV system power output was 50 kW, hence, the excess power of 24.053 kW was used to recharge the battery. In the second scenario, the solar PV power output was equal to the total load demand and the battery SOC was greater than or equal to 80% hence, all loads were supplied and the battery was disconnected because it was completely full. Lastly, in the third scenario, solar PV power output was less than the primary load (humanitarian aid facility) and the battery SOC was greater than or equal to 20%. Hence, the battery was used to augment the shortage while the secondary loads (farming and telecommunication base station facilities) were disconnected.

The off-grid solar PV system can be modified utilizing various parameters and component sizes in accordance with design specifications targeted at efficient energy management. Once more, the results showed that lithium-ion battery storage systems can be used in effectively in off-grid systems for efficient energy management. Additionally, the battery storage system can respond quickly and take part in off-grid power stability depending on the required signals, the prevailing power availability, and load requirements. The system did not use complicated control mechanisms, but rather independent, simple-to-implement controls. Various renewable energy sources can be employed to implement the control mechanism, and the system can be scaled up or down depending on the goals of the research. The decision to lithium-ion battery storage system demonstrated a significant advantage in power management since the power from the system may be controlled by giving the user flexibility in accordance with battery size and SOC.

6. 2. Recommendations and future work

A variety of energy storage technologies, including flywheels, supercapacitors, and others should be researched in order to determine the best option from a technical and financial standpoint over a variety of timescales because energy storage systems are essential to the stability of off-grid systems. Again, integrating other sources of renewable energy such as fuel cell and wind turbines will enhance the reliability of the network, improve power quality and provide a more sustainable network. Hence, a study is necessary to understand its technical and economic viability. Finally, given that there are numerous DC loads now in use internationally, research should be done on affordable, commercially feasible DC-DC converters capable of connecting DC loads to distribution lines.

REFERENCES

Acharya, P.S. & Aithal, P.S. 2020. A Comparative Study of MPPT and PWM Solar Charge Controllers and their Integrated System. *Journal of Physics: Conference Series*, 1712(1): 1–6.

Alemshet, A.A. 2010. *Solar PV based rural electrification in REMA rural village*. Royal Institute of Technology (KTH).

Algaddafi, A., Brown, N., Rupert, G. & Al-Shahrani, J. 2016. Modelling a Stand-Alone Inverter and Comparing the Power Quality of the National Grid with Off-Grid System. *IEIE Transactions on Smart Processing and Computing*, 5(1): 35–42.

Alkhawaldeh, L. 2020. *Modeling , Simulation , and Design of Hybrid EV- Battery Charger for Optimum Grid Utilization*. University of Ontario Institute of Technology (Ontario Tech University).

Alsharif, M.H. & Kim, J. 2016. Optimal solar power system for remote telecommunication base stations: A case study based on the characteristics of south Korea's solar radiation exposure. *Sustainability (Switzerland)*, 8(9): 1–21.

Alsharif, M.H., Nordin, R. & Ismail, M. 2015. Energy optimisation of hybrid off-grid system for remote telecommunication base station deployment in Malaysia. EURASIP Journal on Wireless Communications and Networking, 64: 2-15. https://doi.org/10.1186/s13638-015-0284-7.

Aris, A.M. & Shabani, B. 2015. Sustainable power supply solutions for off-grid base stations. *Energies*, 8(10): 10904–10941.

Belkaid, A., Colak, I. & Kayisli, K. 2017. Implementation of a modified P&O-MPPT algorithm adapted for varying solar radiation conditions. *Electrical Engineering*, 99(3): 839–846.

Benavente, F., Lundblad, A., Campana, P.E., Zhang, Y., Cabrera, S. & Lindbergh, G. 2019. Photovoltaic/Battery System Sizing for Rural Electrification in Bolivia: Considering the Suppressed Demand Effect. *Applied Energy*, 235(October 2018): 519–528.

Bevrani, H. & Shokoohi, S. 2013. An intelligent droop control for simultaneous voltage and frequency regulation in Islanded microgrids. *IEEE Transactions on Smart Grid*, 4(3): 1505–1513.

Bokanga, G.M., Raji, A.. & Kahn, M.T.E. 2014. Design of a low voltage DC microgrid system for rural electrification in South Africa. Journal of Energy in Southern Africa, 25(2), 9-14.

Retrieved June 24, 2022, from http://www.scielo.org.za/scielo.php?script=sci_arttext&pid=S1021447X2014000200002&lng=en&tlng=en.

Boutelhig, A. & Bakelli, Y. 2012. Comparative study on Water Max A 64 DC pump performances based Photovoltaic Pumping System design to select the optimum heads in arid area. In *Proceedings of the International Conference on Microelectronics, ICM*.

Byeon, G., Yoon, T., Oh, S. & Jang, G. 2013. Energy management strategy of the DC distribution system in buildings using the EV service model. *IEEE Transactions on Power Electronics*, 28(4): 1544–1554.

Chao, K.-H., Tseng, M.-C., Huang, C.-H., Liu, Y.-G. & Huang, L.-C. 2013. Design and Implementation of a Bidirectional DC-DC Converter for Stand-Alone Photovoltaic Systems. *International Journal of Computer, Consumer and Control (IJ3C)*, 2(3): 44–55. https://pdfs.semanticscholar.org/c8ce/2e345a70c23cd722770bb182cb49cc886b4f.pdf.

Cho, J., Park, S.M., Reum Park, A., Lee, O.C., Nam, G. & Ra, I.H. 2020. Application of photovoltaic systems for agriculture: A study on the relationship between power generation and farming for the improvement of photovoltaic applications in agriculture. *Energies*, 13(18): 1–18.

DOE. 2020. *South Africa"s low-emission developement startegy 2050*. Pretoria. https://www.dffe.gov.za/sites/default/files/docs/2020lowemission_developmentstrategy 30 April 2022.

Eid, B., Rahim, N.A., Selvaraj, J. & El Khateb, A.H. 2016. Control Methods and Objectives for Electronically Coupled Distributed Energy Resources in Microgrids: A Review. *IEEE Systems Journal*, 10(2): 446–458.

Essefi, R.M., Souissi, M. & Abdallah, H.H. 2014. Maximum Power Point Tracking Control Using Neural Networks for Stand-Alone Photovoltaic Systems. *International Journal of Modern Nonlinear Theory and Application*, 03(03): 53–65.

Feron, S. 2016. Sustainability of off-grid photovoltaic systems for rural electrification in developing countries: A review. *Sustainability (Switzerland)*, 8(12).

Fertig, E. & Apt, J. 2011. Economics of compressed air energy storage to integrate wind power: A case study in ERCOT. *Energy Policy*, 39(5): 2330–2342. http://dx.doi.org/10.1016/j.enpol.2011.01.049.

Franceschi, J., Rothkop, J. & Miller, G. 2014. Off-grid solar PV power for humanitarian action: From emergency communications to refugee camp micro-grids. *Procedia Engineering*, 78: 229–235. http://dx.doi.org/10.1016/j.proeng.2014.07.061.

Franklin, E. 2018. *Solar Photovoltaic (PV) System Components*. Tucson.

Garcia Torres, F. 2015. *Advanced Control of Renewable Energy Microgrids with Hybrid Energy Storage System*. Escuela T´ecnica Superior de Ingenieros (Universidad de Sevilla).

Gebreab, E.K. 2013. *Interfacing of Battery with a Medium Voltage DC-DC Converter using MATLAB/Simulink*. Kansas State University.

George, S.S. 2018. *A Modular Multi-Level Converter for Energy Management of Hybrid Storage System in Electric Vehicles*. San Jose State University.

Hesse, H.C., Schimpe, M., Kucevic, D. & Jossen, A. 2017. *Lithium-ion battery storage for the grid - A review of stationary battery storage system design tailored for applications in modern power grids*. Energies, 10: 2107. doi:10.3390/en10122107.

Hossam-Eldin, A.A., Farghly, A., Hossam, A. & Refaey, M. 2015. *A Review on Photovoltaic Solar Energy Technology and its Efficiency Use of Hybrid Renewable Energy in Cathodic Protection View project A Review on Photovoltaic Solar Energy Technology and its Efficiency*. https://www.researchgate.net/publication/287792329.

IEA. 2020. *Global EV Outlook 2020*.

Irena. 2016. *Solar Pv in Africa: Costs and market*.

IRENA. 2019a. *Future of Solar Photovoltaic: Deployment, investment, technology, grid intergration and socio-economic aspects*. Abu Dhabi. www.irena.org/publications.

IRENA. 2018a. *Off-grid renewable energy solutions*.

IRENA. 2019b. Off-grid renewable energy solutions to expand electricity access : An opportunity not to be missed. *International Renewable Energy Agency, Abu Dhabi*: 144. https://www.irena.org/publications/2019/Jan/Off-grid-renewable-energy-solutions-to-expand-electricity-to-access-An-opportunity-not-to-be-missed.

IRENA. 2018b. *Sustainable rural Sub-Saharan Aafrica : A collection of good practices*. Abu Dhabi.

Issi, F. & Kaplan, O. 2018. The determination of load profiles and power consumptions of

home appliances. *Energies*, 11(3).

Jain, S. & Jain, P.K. 2017. The rise of Renewable Energy implementation in South Africa. *Energy Procedia*, 143: 721–726.

Kamran, M., Mudassar, M., Fazal, M.R., Asghar, M.U., Bilal, M. & Asghar, R. 2020. Implementation of improved Perturb & Observe MPPT technique with confined search space for standalone photovoltaic system. *Journal of King Saud University - Engineering Sciences*, 32(7): 432–441. https://doi.org/10.1016/j.jksues.2018.04.006.

Khamisani Advisors, A.A., Ping Liu, P., Cloward, J. & Bai, R. 2018. *Design Methodology of Off-Grid PV Solar Powered System (A Case Study of Solar Powered Bus Shelter)*.

Khodadoost Arani, A.A., B. Gharehpetian, G. & Abedi, M. 2019. Review on Energy Storage Systems Control Methods in Microgrids. *International Journal of Electrical Power and Energy Systems*, 107(November 2018): 745–757. https://doi.org/10.1016/j.ijepes.2018.12.040.

Klepacka, A.M. 2019. Significance of Renewable Energy Sources in Sustainable Development. *Annals of the Polish Association of Agricultural and Agribusiness Economists*, XXI(1): 55–64.

Kyari, İ., Mumammad, J.Y., Abdullahi Gele, M., Waziri, A.B. & Muhammad, A.A. 2020. Design and Sizing of Standalone Solar Power Generation for a Medium Residence in Kano State. *International Journal of Energy and Smart Grid*, 5(1): 44–56.

Li, R., Liang, X., Li, X. & Cai, X. 2014. On/off-grid integrated photovoltaic power generation system. In *Proceedings - 2014 International Power Electronics and Application Conference and Exposition, IEEE PEAC 2014*. Institute of Electrical and Electronics Engineers Inc.: 255–259.

Luo, W., Khoo, Y.S., Hacke, P., Naumann, V., Lausch, D., Harvey, S.P., Singh, J.P., Chai, J., Wang, Y., Aberle, A.G. & Ramakrishna, S. 2017. Potential-induced degradation in photovoltaic modules: A critical review. *Energy and Environmental Science*, 10(43): 43–68.

Luta, D.N. 2019. *An Energy Management System for a Hybrid Reversible Fuel cell / Supercapacitor in a 100 % Renewable Power System*. Cape Peninsula University of Technology.

Malysz, P., Sirouspour, S. & Emadi, A. 2014. An optimal energy storage control strategy for

grid-connected microgrids. *IEEE Transactions on Smart Grid*, 5(4): 1785–1796.

van der Merwe, W. & Brent, A.C. 2020. Evaluating the energy potential of solar PV located on mining properties in the Northern Cape Province of South Africa. *Sustainability (Switzerland)*, 12(14).

Van der Merwe, W. & Brent, A.C. 2020. Evaluating the energy potential of solar PV located on mining properties in the Northern Cape Province of South Africa. *Sustainability*, 12(14).

Mikul, B., Nicolina, A., Ruchi, S., Elisa, P., Elaine R., F., Susan, W., Heather, A. & Carlos, D. 2018. Access to Modern Energy Services for Health Facilities in Resource-Constrained Settings.

Mohanty, P., et al. (eds.), 2016. Solar Photovoltaic System Applications, Green Energy and Technology, DOI 10.1007/978-3-319-14663-8_3.

Mougay, A., Khatir, M., Flitti, M., Zidi, S.A. & Ganoune, A. 2021. Energy management for a new power system configuration of base transceiver station (BTS) destined to remote and isolated areas. *Przeglad Elektrotechniczny*, 97(8): 3–10.

Moumouni, Y. & Gdeisat, M. 2018. Sizing an off-grid photovoltaic system. In *2018 Advances in Science and Engineering Technology International Conferences, ASET 2018*. Institute of Electrical and Electronics Engineers Inc.: 1–4.

Mulaudzi, S.K. & Bull, S. 2016. An assessment of the potential of solar photovoltaic (PV) application in South Africa. In *IREC 2016 - 7th International Renewable Energy Congress*. Institute of Electrical and Electronics Engineers Inc.

Naqvi, A.A., Bin Nadeem, T., Ahmed, A. & Ali Zaidi, A. 2021. Designing of an off-grid Photovoltaic system with battery storage for remote location. *TECCIENCIA*, 16(31): 15–28.

Ntshiba, S. & Krishnamurthy, S. 2022. Digital Implementation of an Auto-Reclose Protection Scheme for a Distribution System. In Institute of Electrical and Electronics Engineers (IEEE): 1–6.

Patel, M.A., Patel, A.R., Vyas, D.R. & Patel, K.M. 2009. *Use of PWM Techniques for Power Quality Improvement Sliding mode control View project Intelligent Physical Compliance View project Use of PWM Techniques for Power Quality Improvement*. https://www.researchgate.net/publication/228891943.

Petinrin, J.O. & Shaaban, M. 2015. Renewable Energy for Continuous Energy Sustainability in Malaysia. *Renewable and Sustainable Energy Reviews*, 50(October 2015): 967–981. http://dx.doi.org/10.1016/j.rser.2015.04.146.

Pougoue Tchintchui, B.P. & Raji, A.K. 2019. *Techno-economic analysis of a renewable energy solution for an off-grid residence; Techno-economic analysis of a renewable energy solution for an off-grid residence*.

Querikiol, E.M. & Taboada, E.B. 2018. Performance Evaluation of a Micro Off-Grid Solar Energy Generator for Islandic Agricultural Farm Operations Using HOMER. *Journal of Renewable Energy*, 2018: 1–9.

Rebeka, R., Velimir, G., Danijel Topi, G.K. & Jurica, P. 2019. 16th International Conference on the European Energy Market (EEM) : 18-20 September 2019, Ljubljana, Slovenia. In *16th International Conference on the European Energy Market (EEM)*. 1–6.

Rousis, A.O., Tzelepis, D., Konstantelos, I., Booth, C. & Strbac, G. 2018. Design of a hybrid ac/dc microgrid using homer pro: Case study on an islanded residential application. *Inventions*, 3(3): 1–14.

Salehi, P. & Solyali, D. 2018. *A review on maximum power point tracker methods and their applications*. www.jser.ut.ac.ir.

Samuels, J.A. 2017. *Design and Implementation of an off-grid PV drive system for small-scale fresh produce cooling*. University of Stellenbosch. https://scholar.sun.ac.za/handle/10019.1/102874.

Showers, S.O. 2019. *Enhanced Frequency Regulation of a Grid-Connected PV System*. Cape Peninsula University of Technology.

Soman Chithra, S.R. 2014. A Literature Review on Soft Switching DC-AC Converters. *2278-0181*, 3(7, July-2014). www.ijert.org.

Swe, W. 2018. Application of Pumped Hydroelectric Energy Storage for Photovoltaic based Application of Pumped Hydroelectric Energy Storage for Photovoltaic based Rural Electrification. , (January).

Tamrakar, V., S.C, G. & Sawle, Y. 2015. Single-Diode PV Cell Modeling And Study Of Characteristics Of Single And Two-Diode Equivalent Circuit. *Electrical and Electronics Engineering: An International Journal*, 4(3): 13–24.

Tan, R.H.G., Chuin, C.B. & Solanki, S.G. 2020. Modeling of single phase off-grid inverter for

small standalone system applications. *International Journal of Power Electronics and Drive Systems*, 11(3): 1398–1405.

Utility, F.E. 2015. Comparative Analysis of Innovative PV Microgrids in Paris and Nice, France. *European Journal of Sustainable Development*, 5(3): 297–310.

Wang, G., Konstantinou, G., Townsend, C.D., Pou, J., Vazquez, S., Demetriades, G.D. & Agelidis, V.G. 2016. A review of power electronics for grid connection of utility-scale battery energy storage systems. *IEEE Transactions on Sustainable Energy*, 7(4): 1778–1790.

Zsiborács, H., Baranyai, N.H., Vincze, A., Zentkó, L., Birkner, Z., Máté, K. & Pintér, G. 2019. Intermittent Renewable Energy Sources: The Role of Energy Storage in the European Power System of 2040. *Electronics*, 8(7): 3–18.